UNIVERSIDAD AUTÓNOMA DE MADRID
Facultad de ciencias
Departamento de Biología Molecular

New insights in p38MAPK function and potential value as therapeutic target for high prevalence diseases

Alejandra Escós López
Madrid, 2019.

UNIVERSIDAD AUTÓNOMA DE MADRID
Facultad de ciencias
Departamento de Biología Molecular

New insights in p38MAPK function and potential value as therapeutic target for high prevalence diseases.

PhD Thesis
Alejandra Escós López

Thesis Director:
Dr. Ana Cuenda

Thesis Tutor:
Dr. Petronila Penela

Departamento de Inmunología y Oncología,
Centro Nacional de Biotecnología (CNB),
Consejo Superior de Investigaciones Científicas (CSIC)

Madrid, 2019.

Agradecimientos

Doy las gracias a Ana Cuenda, mi directora, por darme la oportunidad de realizar esta tesis doctoral y por toda la ayuda y el aprendizje durante este viaje.

Compañeros de laboratorio, del departamente y personal del CNB, por toda la ayuda y apoyo aportado.

Formación Profesional Integral (FPI) 2014 - 2018
ha financiado esta investigaicón.

A mis padres y hermanos

Index

Abstract

Inflammation is a highly regulated process in which macrophages play a fundamental role. These are activated through pattern-recognition receptors that cause the secretion of cytokines by activating the TLR4-Tpl2-ERK1/2 pathway. Our laboratory has shown that the absence of p38γ and p38δ (p38γ/p38δ) caused a decrease in the protein levels of Tpl2 and ABIN2. Consequently, ERK1/2 was not activated, thus blocking the production of cytokines and decreasing the effects in the inflammatory model of septic shock (Risco et al., 2012).

In this thesis we have described for the first time that, in macrophages in response to *Candida albicans* infection, the signaling pathways TAK1-IKK-Tpl2-ERK1/2 and Raf-1-ERK1/2 are activated under Dectin-1. We have also described how the absence of p38γ/p38δ blocks the activation of ERK1/2 by decreasing the protein levels of Tpl2.

Due to the central role of Tpl2 in macrophages, we have studied the molecular mechanism by which p38γ/p38δ regulate Tpl2 proteins levels. We have described that p38γ/p38δ interact with the Tpl2/ABIN2/p105 complex through Tpl2 thus contributing to its stability. In this study we observed that the translation of Tpl2 and ABIN2 decreases in the absence of p38γ/p38δ, and that p38δ could specifically regulate the translation of the *Tpl2* mRNA through its 3'UTR. In turn, p38γ/p38δ could be regulating cap-independent translation of proteins.

Finally, we studied which signaling pathways downstream of the TLR4 receptor were modulated by p38γ/p38δ independently from Tpl2. For this, we generated a new mouse line $p38\gamma^{171A/171A}/p38\delta^{-/-}$, which is deficient in p38δ and expresses inactive p38γ; it also expresses normal levels of Tpl2. By the comparative study of RNA sequencing in $p38\gamma^{171A/171A}/p38\delta^{-/-}$ macrophages stimulated with LPS we have discovered that they induce the overproduction of proteins related to the interferon type I response.

Our results establish that p38γ/p38δ regulate the production of cytokines through gene transcription and translation processes.

Resumen

La inflamación es un proceso altamente regulado en el que los macrófagos juegan un papel fundamental. Estos se activan a través de receptores que reconocen patrones moleculares que causan la secreción de citoquinas mediante la activación de la vía TLR4-Tpl2-ERK1/2. Nuestro laboratorio observó que la ausencia de p38γ y p38δ (p38γ/p38δ) provocaba una bajada de los niveles proteicos de Tpl2 y ABIN2. En consecuencia, ERK1/2 no se activaba, bloqueando así la producción de citoquinas y disminuyendo los efectos en el modelo inflamatorio de choque séptico (Risco et al., 2012).

En esta tesis hemos descrito por primera vez que, en macrófagos en respuesta a infección por *Candida albicans*, las vías de señalización TAK1-IKK-Tpl2-ERK1/2 y Raf-1-ERK1/2 se activan por debajo de Dectin-1. También hemos descrito como la ausencia de p38γ/p38δ bloquea la activación de ERK1/2 al disminuir los niveles proteicos de Tpl2.

Debido al papel central de Tpl2 en macrófagos, hemos estudiado el mecanismo molecular por el que p38γ/p38δ regulan los niveles de Tpl2. Hemos descrito que p38γ/p38δ interaccionan con el complejo Tpl2/ABIN2/p105 a través de Tpl2 contribuyendo así a su estabilidad. En este estudio observamos que la traducción de Tpl2 y ABIN2 disminuye en ausencia de p38γ/p38δ, y que p38δ podría regular específicamente la traducción del mRNA de *Tpl2* a través de su 3'UTR. A su vez, p38γ/p38δ podrían estar regulando la traducción cap-independiente de proteínas.

Finalmente, hemos estudiado qué vías de señalización por debajo del receptor de TLR4 estaban modulando p38γ/p38δ independiente de Tpl2. Para ello generamos una nueva línea de ratón $p38\gamma^{171A/171A}/p38\delta^{-/-}$, que es deficiente en p38δ y expresa la p38γ inactiva; además expresa niveles normales de Tpl2. Mediante el estudio comparativo de la secuenciación de RNA en macrófagos $p38\gamma^{171A/171A}/p38\delta^{-/-}$ estimulados con LPS hemos descubierto que inducen la sobreproducción de proteínas relacionadas con la respuesta de interferón de tipo I.

Nuestros resultados establecen que p38γ/p38δ regulan la producción de citoquinas a través de procesos de traducción y transcripción de genes.

Abbreviations

Abbreviations

3'UTR - 3´untranslated region

5'UTR - 5´untranslated region

ABIN2 - A20-binding inhibitor of NF-κB 2

Camk2b - Calcium/Calmodulin Dependent protein kinase II beta

CLR - C-type lectin receptor

COT - Cancer Osaka thyroid

D-Gal - D-Galactosamine

DAVID - Database of Annotation, Visualization and Integrated Discovery

DEPTOR – Dishevelled, Egl-10 and Pleckstrin domain containing ammalian target of rapamycin complex interacting protein

DMEM – Dulbecco´s Modified Eagle Medium

DMSO - Dimethyl sulfoxide

eEF2 - Eukaryotic elongation factor 2

eEF2K - Eukaryotic elongation factor 2 kinase

ERK - Extracellular signal regulated kinases

FBS - Fetal Bovine Serum

GKAP - Guanylate kinase-associated protein

GO - Gene ontology

hDlg - Human disc large

HSF - Heat shock factor

IFN - Interferon

IKK - Inhibitor of κB kinase

IL - Interleukin

IRAK - Interleukin-1 receptor associated kinase

IRES - Internal ribosomal entry sequences

IRF - Interferon regulatory factors

JNK - C-jun N-terminal kinase

KD - Kinase dead

NFκB – Nuclear factor kappa-light-chain-enhancer of activated B cells
NLR - Nucleotide oligomerization domain-like receptor
NOD - Nucleotide oligomerization domain
NONO - Non-pituitary specific, octamer transcription factor and neural Unc-86 transcription factor domain containing octamer
mTORC - Mammalian target of rapamycin complex
MAPK - Mitogen activated protein kinase
MEF - Mouse embryonic fibroblast
MKK - Mitogen activated protein kinase kinase
MyD88 - Myeloid differentiation primary response 88
LC-MS – Liquid chromatography-mass spectrometry
LPS - Lipopolysaccharide
LRR - Leucine-rich repeat
PABPC1 - Poly(A) Binding Protein Cytoplasmic 1
PAMP - Pathogen-associated molecular pattern
PBS - Phosphate saline buffer
PCA - Principal components analysis
PCR - Polymerase chain reactions
PKD1 - Protein kinase D1
PMA - Phorbol 12-myristate 13-acetate
PRR - Pattern-recognition receptor
PSD - Post-synapse density
PTPH - Protein tyrosine phosphatase-H
qPCR - Quantitative polymerase chain reactions
RBP - Ribonucleic acid binding protein
RIG-I - Retinoid acid-inducible gene I
RLR - Retinoid acid-inducible gene I -like receptor
SAP - Synapse-associated protein
SMOC - SupraMolecular Organizing Centre
TAB - Transforming growth factor β-activated kinase I binding protein
TACE - Tumor necrosis factor α -converting enzyme

TAK1 - Transforming growth factor β-activated kinase I

TdT – Deoxynucleotidyltransferase

TGFβ - Transforming growth factor β

TIR - Cytoplasmatic Toll/interleukin 1 receptor

TIRAP - Cytoplasmatic Toll/IL 1 receptor adaptor protein

TLR - Toll-like receptor

TNF - Tumor necrosis factor

Tpl2 - Tumor progression locus 2

TRAM - Cytoplasmatic Toll/interleukin 1 receptor domain-containing adaptor-inducing related adaptor molecule

TRAF6 - Tumor necrosis factor -receptor-associated factor 6

TRIF - Cytoplasmatic Toll/interleukin 1 receptor domain-containing adaptor-inducing interferon β

TUNEL - Deoxynucleotidyltransferase mediated dUTP nick-end label

uORF - Upstream open reading frame

ZFP36 - Zinc finger protein 36

Introduction

1 Introduction

1.1 Macrophage Immune Response.

The immune system has evolved to protect hosts from invading pathogens, tissue damage and disease, it has a wide variety of cells and molecules that are able to detect an indefinite number of invaders (Kindt, T. et al., 2007). In vertebrate, the immune response has developed into two interlinked subsystems: the innate immunity and the adaptive immunity. The innate immunity is the first line of host defence and is elicited by the activity of phagocytic cells (neutrophils, monocytes and macrophages), cells that release inflammatory mediators (basophils, mast cells and eosinophils), and natural killer. The adaptive immunity is mainly fulfilled by B and T cells (Delves and Roitt, 2000). Tissue damage caused by a wound or an invading pathogen induces the activation of the host defence by triggering the inflammatory response that is classically characterised by four symptoms: redness, swelling, heat and pain. These features correlate with the biological functions of vasodilation, increased capillarity, permeability and influx of phagocytes (Kindt, T. et al., 2007; Takeuchi and Akira, 2010).

The inflammatory process is tightly regulated, involving signals that initiate and maintain inflammation and signals that stops the inflammatory response. Macrophages are a major component of the mononuclear phagocyte system. Monocytes, that are originated in the bone marrow of vertebrates, travel through the blood vessels and migrate to extravasate to specific tissues where they differentiate into macrophages (Murray and Wynn, 2011). These cells are part of the first line of immune system defence and play a critical role in inflammation by having four main functions: antigen presentation, antimicrobial and cytotoxic activities, phagocytosis and immunomodulation through the production of cytokines, chemokines and growth factors (Kindt, T. et al.,

2007).

1.1.1 Candida albicans infection and septic shock.

Fungal pathogens have an enormous impact in plant and animal life. They have been related to species extinction, food security and ecosystem disturbance (Brown et al., 2012). The variety of fungal species is about 3.5-5.1 million but only several hundred are associated with human diseases (Kim, 2016). *Candida* yeast, belong to the fungal species and are classified as opportunistic pathogens, meaning they are only pathogenic under certain circumstances. In normal conditions, overgrowth of *Candida* is inhibited by both specific and non-specific defence systems such as immune system, intestinal flora, peristalsis, intestinal enzymes and defensins (Schulze and Sonnenborn, 2009). Fifteen different *Candida* species can be pathogenic for humans and ~90% of the invasive candidiasis are associated with only five of the them, which include *Candida albicans* (*C. albicans*) (Dadar et al., 2018).

The majority of the studies in host defence against fungus have been performed studying *C. albicans* because is the most abundant in humans. *C. albicans* is part of the human microflora, and is present as a diploid polymorphic yeast in mucosal surfaces such as the human gastrointestinal, respiratory and genitourinary tracts. However, *C. albicans* can cause severe invasive diseases when tissue homeostasis is disrupted. Fungi are then able to colonize and infect the host, which causes sepsis, hypersensitivity disorders or toxic reactions. Septic shock or sepsis leads to acute organ disfunction and it is the most frequent cause of death in intensive care unit´s patients (Angus and van der Poll, 2013; Deutschman and Tracey, 2014). Risk factors for sepsis has not been discovered, the affected hospitalized patients cover a wide range of factors that does not differ between race, geography or health status. The survival of the patient will depend on their capacity to resolve the inflammation process

(Deutschman and Tracey, 2014). *C. albicans* is the predominant pathogen associated with fungal sepsis, being the cause of 15% of the infections of intensive care unit´s patients (Delaloye and Calandra, 2014). This leaves *C. albicans* as the 7 – 10 position of the most common blood stream infections (Kullberg and Arendrup, 2015). Currently, systemic *C. albicans* infections have a mortality rate of ~40% in intensive care unit patients (Dadar et al., 2018; Netea et al., 2015).

1.1.2 Recognition of C. albicans by macrophages: Pattern recognition receptors (PRRs).

The innate immune system is capable of discriminate a large number of potential pathogens from the individual´s own molecules. Innate immune cells have developed a number of pattern-recognition receptors (PRRs) that recognize conserved motifs of pathogens. These conserved motifs are part of essential molecules for pathogens survival and so, they are not subjected to high mutation rates (Aderem and Ulevitch, 2000; Akira et al., 2006). These motifs are called pathogen-associated molecular patterns (PAMPs) and are recognized by the PRRs in cells, that reside in the tissue such as: macrophages, fibroblasts, mast cells and dendritic cells, or in circulating leukocytes like monocytes and neutrophils. Other molecules recognized by PRRs are the ones released from injured cells, which are classified as damage-associated molecular patterns (DAMPs). Four different families have been identified as PRRs: Toll-like receptors (TLRs), C-type lectin receptors (CLRs), retinoid acid-inducible gene I (RIG-I)-like receptors (RLRs) and nucleotide oligomerization domain (NOD)-like receptors (NLRs) (Newton and Dixit, 2012; Takeuchi and Akira, 2010). These receptors activate signalling pathways that induce the production of a wide variety of downstream genes encoding inflammatory cytokines, chemokines, antimicrobial peptides, complement factors and interferons (Liu and Cao, 2016). During *C. albicans* infection, macrophages detect the

fungus through TLR receptors TLR2, TLR4 and TLR6 and CLR receptor Dectin-1 (Netea et al., 2015).

1.1.2.1 Toll-like receptors (TLRs).

TLR receptor family are able to recognize fungal, bacterial and viral PAMPs from the extracellular environment. They are type I transmembrane proteins that contain leucine-rich repeats (LRRs) with a cytoplasmatic domain that contain a signal transductor called cytoplasmatic Toll/interleukin (IL) 1 receptor (TIR). In mice there are 12 TLRs (TLR1 – TLR9 and TLR11 – TLR13), while in humans there are 10 TLRs (TLR1 – TLR10). All TLRs are either at the plasma membrane (TLR1, TLR2, TLR4, TLR5, TLR6 and TLR11) or in endosomes (TLR3, TLR7, TLR8, TRL9 and TLR10). TLR activated pathways such as nuclear factor-κB (NF-κB), mitogen activated protein kinases (MAPKs) and interferon regulatory factors (IRFs), are regulated by phosphorylation and ubiquitination (Liu and Cao, 2016). With the exception of TLR3, all TLRs bind to the adaptor protein myeloid differentiation primary response 88 (MyD88) alone or in combination with the TIR adaptor protein (TIRAP) (Newton and Dixit, 2012; Takeuchi and Akira, 2010) (Fig. I-1). TLR3 binds to the adaptor TIR domain-containing adaptor-inducing IFNβ (TRIF) directly. Additionally, TLR4 is endocytosed after MyD88/TIRAP activation and recruits TRIF indirectly through TRIF-related adaptor molecule (TRAM) from early endosome (Kagan et al., 2008). This makes TLR4 the only TLR that recruits MyD88/TIRAP and TRAM/TRIF and that signals through TRIF- and MyD88-dependent pathways (Ullah et al., 2016) (Fig. I-1).

In the TLR family, one of the most studied receptors is the TLR4, which interacts with lipopolysaccharide (LPS), a PAMP found in the external membrane of Gram (–) (Fig. I-1). LPS interacts with TLR4 and the co-receptor MD2 triggering the assembly of a supramolecular organizing

centre (SMOC) known as Myddosome. The Myddosome is composed by MyD88, TIRAP and proteins from the interleukin-1 receptor associated kinase (IRAK) family (Lin et al., 2010; Motshwene et al., 2009). The E3 ubiquitin protein ligase, tumor necrosis factor (TNF)-Receptor-Associated Factor 6 (TRAF6), interacts with the IRAK proteins and catalyses the formation of Lys63 linked polyubiquitination chains that recruits the TGFβ-activated kinase I (TAK1) complex (Lomaga et al., 1999; Wang et al., 2001). TAK1 can be found in two different complexes in the cell, one with TAK1 binding protein 1 (TAB1) and TAB2, the other with TAB1 and TAB3 (Cheung et al., 2004). TAK1 is essential for the activation of the canonical complex protein kinase inhibitor of κB (IκB) kinase (IKK) (Sato et al., 2005; Shim et al., 2005). IKK complex is compose of two catalytic subunits, IKKα and IKKβ, that induces the activation of the NFκB (DiDonato et al., 1997; Mercurio et al., 1997; Zandi et al., 1997). IKK complex also has an essential component (IKKγ) that modulates the complex (Rothwarf et al., 1998; Yamaoka et al., 1998). TAK1 phosphorylates mitogen-activated protein kinase kinase 4/6 (MKK4/6) and activates the IKK complex by catalysing a priming phosphorylation of IKKβ that permits its autophosphorylation and its own activation (Li et al., 2003; Wang et al., 2001; Zhang et al., 2014). IKK complex and MKKs activation will lead to NFκB and MAPK signalling pathway activation and transcription of pro-inflammatory cytokine (Akira et al., 2006; Cohen, 2014; Newton and Dixit, 2012). As mentioned before, TLR4-MD2-LPS complex is internalized into endosomes where it binds to TRAM, which induces the SMOC Triffosome formation (Kagan et al., 2008). The Triffosome is assembled by the recruitment of TRIF to TLR4/TRAM and activates TRAF3/6 to promote IRF3-dependent type-I interferon (IFN) production (Fitzgerald et al., 2003; Hoebe et al., 2003; Kieser and Kagan, 2017; Verstak et al., 2014; Yamamoto et al., 2003) (Fig. I-1).

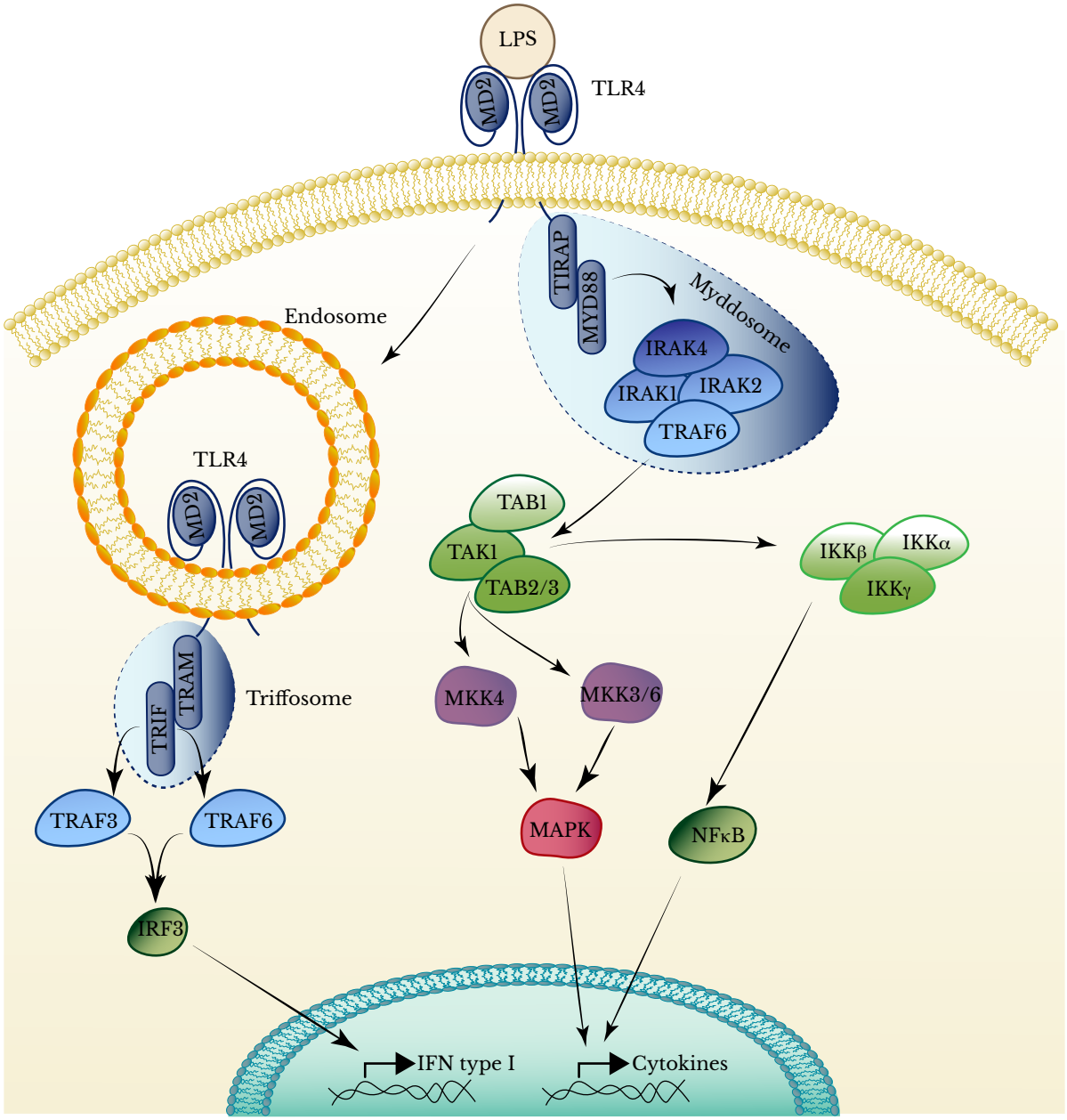

Figure I-1. TLR4 signalling pathway. LPS triggers TLR4 signalling by the recruitment of MyD88 and IRAK family to the receptor for Myddosome formation. Mydossome assembly recruits and activates TAK1 complexes, which in turn activate the canonical IKK complex and MKK4/3/6. IKK complex activates the transcription factor NFκB inducting, together with MAPKs, the transcription of cytokines. Internalized TLR4-MD2-LPS complex recruits TRAM and TRIF, which form the Triffosome that induces IRF3-dependent IFN type I transcription.

1.1.2.2 Dectin 1 receptor signalling.

Different families of PRRs such TLRs and CLRs recognise mannan-containing structures and β-glucans, respectively, present in *C. albicans* cell wall (Netea et al., 2015).

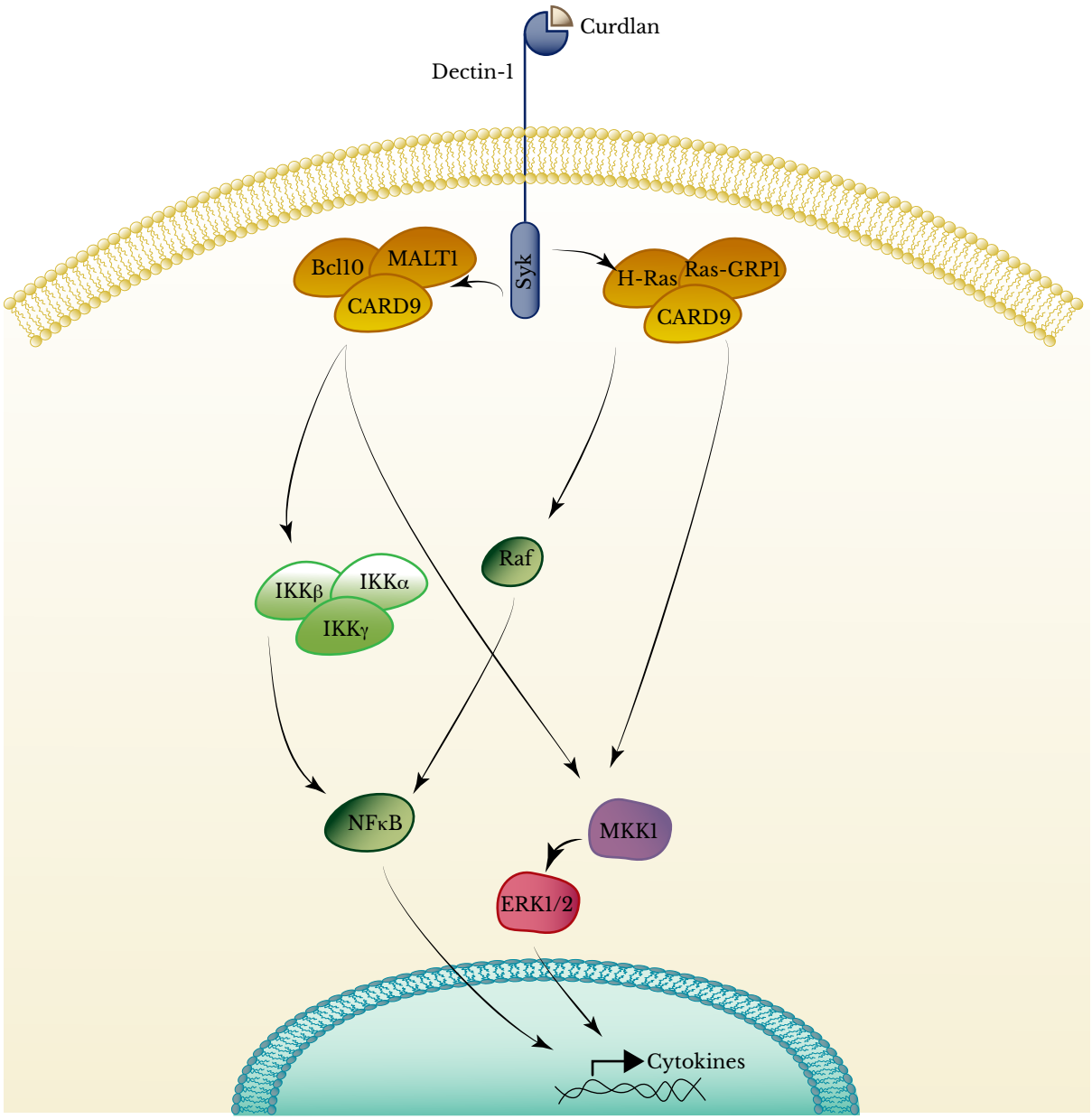

Figure I-2. Activation of Dectin-1 receptor signalling pathways. The adaptor protein spleen associated tyrosin kinase (Syk) binds to Dectin-1 after stimulation by β-glucans such us Curdlan. Syk activates two different complexes; caspase recruitment domain family member 9 (CARD9)/B cell CLL/Lymphoma 10 (Bcl10)/Mucosa-associated

Lymphoid tissue lymphoma translocation (MALT1) and CARD9/Ras protein specific guanine nucleotide releasing factor (RasGRF1)/Harvey rat sarcoma viral oncogene homolog (H-Ras). CARD9/Bcl10/MALT1 activates MKK1/2-ERK1/2 and IKKs-NFκB pathway. On the other hand, CARD9/RasGRF1/H-Ras activates MKK1-extracelular signal regulated kinase (ERK1/2) and the non-canonical NFκB pathway through rapidly accelerated fibrosarcoma (Raf). ERK1/2 and NFκB activation leads to cytokine transcription.

In macrophages, the TLRs that are involved in *C. albicans* recognition are TLR2, TLR4 and TLR6. Dectin-1, which is the main CLR in macrophages, is also implicated in *C. albicans* recognition. It is well known that upon PAMPs detection PRRs trigger the activation of MAPK cascade, particularly the ERK1/2 pathway. The molecules implicated in the ERK1/2 activation downstream of TLR are well described, however, little is known about the ones involved in Dectin-1 signalling (Geijtenbeek and Gringhuis, 2009; Lee and Kim, 2007; Netea et al., 2015). Dectin-1 stimulation activates the adaptor protein Syk, which induces the recruitment and formation of the scaffold complex CARD9/BCL10/MALT1 that leads to both IKKs-NF-κB and MKK1-ERK1/2 activation (Gross et al., 2006; Rogers et al., 2005; Underhill et al., 2005). Another signalling pathway that is activated in response to *C. albicans* infection is the non-canonical NF-κB pathway that is activated through Raf-1 (Gringhuis et al., 2009). This suggested that multiple signalling pathways induced NFκB activation. It was described that after Dectin-1-Syk signalling activation, the protein CARD9 forms another complex with RasGRF1 and H-Ras mediating ERK1/2 activation (Geijtenbeek and Gringhuis, 2009; Hoving et al., 2014; Jia et al., 2014) (Fig. I-2).

1.1.3 MAPK signalling.

MAPK family compromise a group of proteins evolutionary conserved that are ubiquitously expressed. The activation of MAPK pathways activation has major effects in cell physiology and is triggered by different

stimuli such as alterations in nutrient concentration, growth factors, cytokines, environmental stress, alteration in nutrient concentration, DAMPs and PAMPs. All MAPKs are activated by a dual phosphorylation on Tyr and Thr in the conserved sequence Tyr-X-Thr that is located in the activation loop of the kinase subdomain VIII.

MAPKs are activated by MKKs (also known as MAP2Ks, mitogen associated protein 2 kinase), MKKs N-terminal region acts as a docking site for the activation loop of the MAPKs. The structure of the MKK region makes phosphorylation of MAPKs very selective. The MKK are also selectively activated by MAP3Ks (MKKK) such as Tpl2, Raf or TAK1 (Cuenda and Rousseau, 2007; Kyriakis and Avruch, 2012).

MAPKs are Pro directed kinases that phosphorylate Ser/Thr residues followed by Pro. The MAPKs family include ERK 1, 2 and 5, the c-jun N-terminal kinases (JNKs) and p38 MAPKs (Fig. I-3). These proteins have been broadly studied in the innate immune response (Arthur and Ley, 2013; Kyriakis and Avruch, 2012).

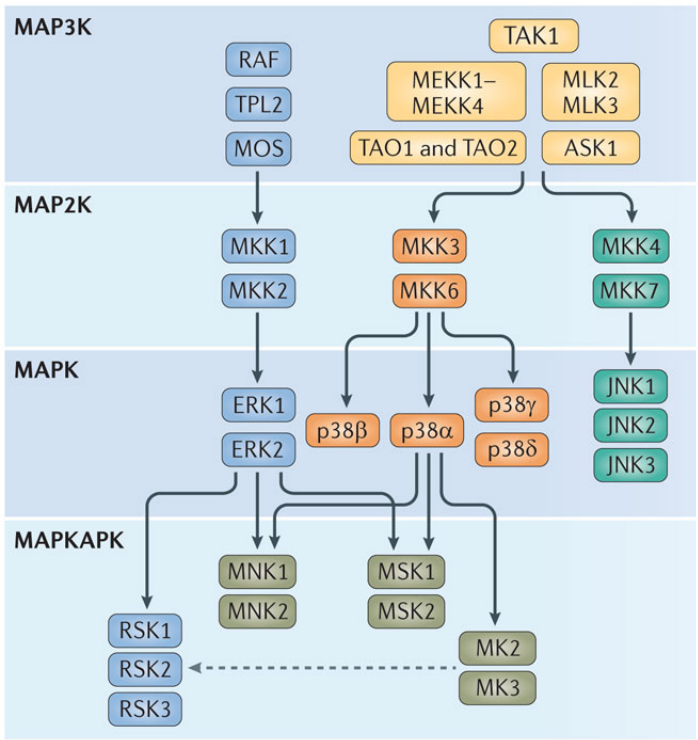

Figure I-3. MAPK signalling in innate immunology. MAP3K protein family selectively phosphorylate MKKs, which selectively phosphorylate their MAPK and finally their substrates. ASK1 (apoptosis signal-regulating kinase-1), MEKK (MAPK/ERK kinase kinases), c-jun N-terminal kinase (JNK), MK (MAPK-activated protein kinase), MLKs (mixed-lineage kinases), MNK (MAPK-interacting protein kinase), MOS (proto-oncogene Ser/Thr-protein kinase), MSK (mitogen and stress-activated kinase), TAO (thousand-and-one amino acid). Figure from (Arthur and Ley, 2013).

1.1.3.1 ERK1/2 signalling pathway: Tpl2/ABIN2/p105 complex.

ERK1 and ERK2 are MAPKs that are ubiquitously expressed and involved in the Ras-Raf-MKK1/2-ERK1/2 pathway. This pathway regulates many physiological process, such as cell adhesion, cell cycle progression, cell migration, cell survival, differentiation, metabolism, proliferation and transcription (Roskoski, 2012). Ras-Raf-MKK1/2-ERK1/2 pathway has also been thoroughly studied because it is involved in the development of one-third of all human cancers (Roskoski, 2012). Ras protein family has three gene products, H-Ras, K-Ras and N-Ras, that change from Ras-GDP to Ras-GTP that activates the MAP3K Raf-1 (Roskoski, 2012). In the immune system, especially in macrophages and dendritic cells, ERK1/2 is also activated by the MAP3K tumor progression locus 2 (Tpl2) (Gantke et al., 2011).

Tpl2 is a Ser/Thr kinase also known as 'cancer Osaka thyroid' (COT) (Miyoshi et al., 1991). The gene is known as *MAP3K8*, is widely expressed and is found as a 58 and 52 kDa protein isoforms due to alternative translational initiation at Met 1 (M1) or Met 30 (M30) (Aoki et al., 1993). Both isoforms M1-Tpl2 and M30-Tpl2 are predominantly localized in the cytoplasm (Miyoshi et al., 1991) and forms a ternary complex with two other proteins, NF-κB1 (p105) and A20-binding inhibitor of NF-κB2 (ABIN2) (Belich et al., 1999; Lang et al., 2004). Tpl2-MKK1/2-ERK1/2 is activated by TLRs, tumor necrosis factor receptor

(TNFR), CD40 or IL1 receptor (Fig. I-4) (Gantke et al., 2011; Xu et al., 2018).

The formation of Tpl2/ABIN2/p105 ternary complex has two important functions for Tpl2. One is to prevent the activation of Tpl2, by the interaction of the death domain of p105 with Tpl2 kinase domain (Beinke et al., 2003), and the other, is to maintain the stability of Tpl2, by interacting with ABIN2, although Tpl2/ABIN2 interaction is not necessary for the phosphorylation of MKK1/2 by Tpl2 (Lang et al., 2004; Papoutsopoulou et al., 2006). Recent findings indicate that Tpl2 is necessary for the stability of ABIN2 (Fig. I-4) (Sriskantharajah et al., 2014; Ventura et al., 2018).

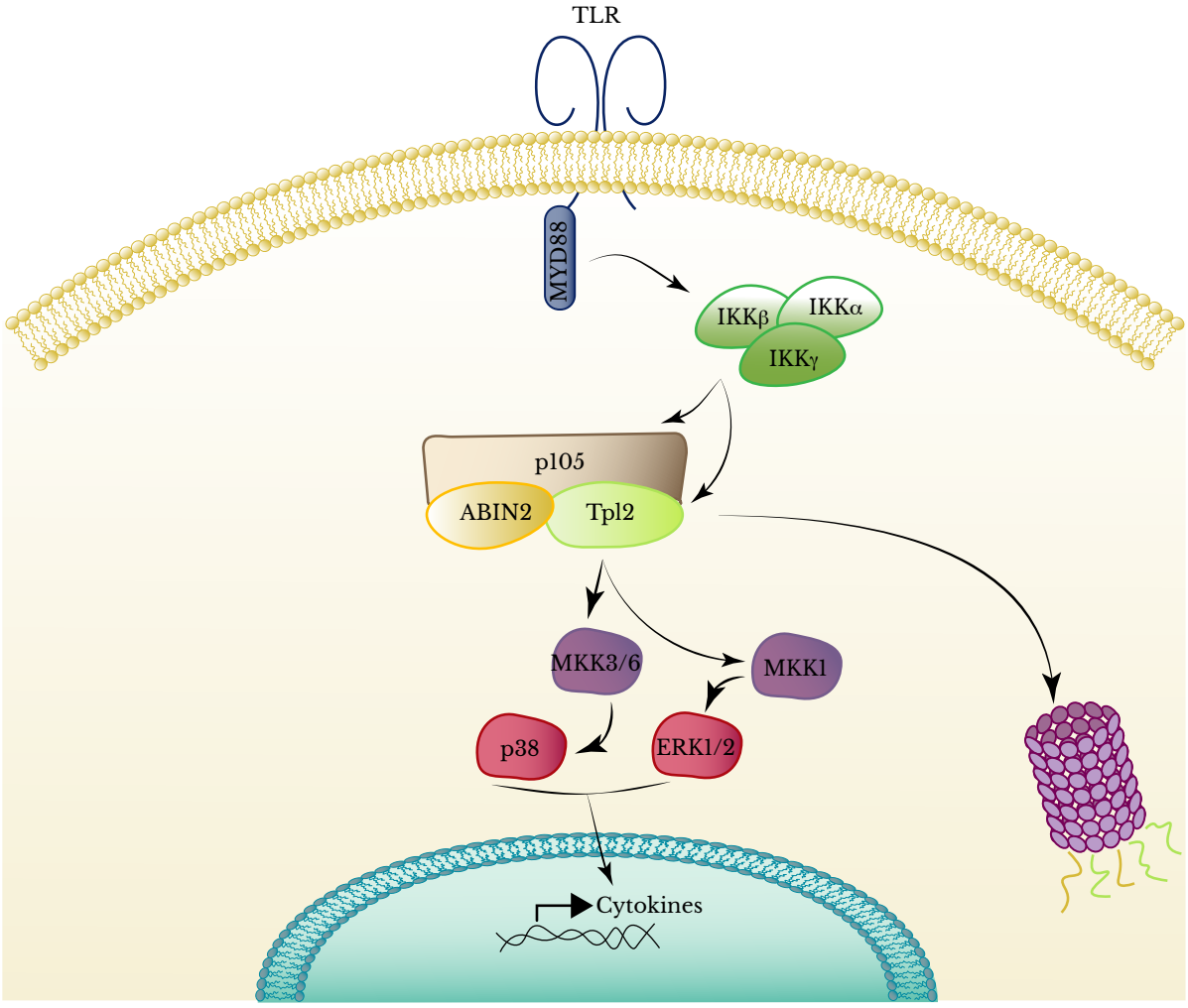

Figure I-4. Tpl2/ABIN2/p105 complex. TLRs signalling activates IKK complex by phosphorylating IKKβ that in turn phosphorylates p105 and Tpl2 in the Tpl2/ABIN2/p105 complex. Tpl2 will phosphorylate MKK1/2 and MKK3/6. All components of the Tpl2/ABIN2/p105 complex are then degraded then by the

proteasome. MKKs phosphorylate p38MAPK and ERK1/2 that induce the transcription of cytokines.

IKKβ phosphorylates p105 and Tpl2, which activates Tpl2 that phosphorylates MKK1/2. The phosphorylation of p105 promotes the release of Tpl2 from the complex (Beinke et al., 2004; Waterfield et al., 2003). The phosphorylation of Tpl2 by IKKβ in Ser400 induces the autophosphorylation of Tpl2 in Ser443. The autophosphorylation of Tpl2 promotes its interaction with 14-3-3, that is key for the phosphorylation of MKK1/2 and ERK1/2 activation (Ben-Addi et al., 2014). It has been recently demonstrated that Tpl2 phosphorylates MKK3/6 and therefore activate p38MAPKs in macrophages stimulated with Gram-negative bacteria, *Mycobacterium tuberculosis* and *Listeria monocytogenes* (Pattison et al., 2016; Xu et al., 2018). Once the Tpl2/ABIN2/p105 ternary complex separates, all components are degraded by the proteasome to stop the induction of pro-inflammatory cytokines and the proteins that forms the Tpl2/ABIN2/p105 complex is synthetized *de novo* (Fig. I-4) (Lang et al., 2004; Papoutsopoulou et al., 2006).

1.1.3.2 p38 MAPK pathway.

p38 MAPK family is a group of proteins composed of four isoforms called p38α , p38β, p38γ and p38δ encoded by different genes *MAPK14*, *MAPK11*, *MAPK12* and *MAPK13*, respectively. They are widely expressed although with different tissue expression patterns. p38MAPK are phosphorylated by different MKKs (MKK3, MKK6 and MKK4) (Fig. I-5). p38α is phosphorylated mainly by MKK3/6 but under ultraviolet stimulation can be phosphorylated by MKK4 (Brancho et al., 2003; Kang et al., 2006). p38β and p38γ are both phosphorylated by MKK6 and MKK3, whereas p38δ was found to be primarily phosphorylated by MKK3 (Remy et al., 2010).

p38α was the first p38MAPKs discovered (Han et al., 1994; Lee et al., 1994; Rouse et al., 1994), it is widely expressed and is the isoform most

studied by the scientific community. p38α$^{-/-}$ mouse has been demonstrated to induces embryonic lethality (Adams et al., 2000), whereas p38β deletion are viable, fertile and have no apparent phenotype (Beardmore et al., 2005). Although, p38β expression is decreased in most tissues, it has been shown that p38α and p38β complement each other during embryonic heart development (Barrantes et al., 2011). p38γ and p38δ are not as widely expressed. p38γ is predominantly expressed in skeletal muscle, while p38δ is found mainly in the kidney, testis, pancreas and small intestine (Goedert et al., 1997; Kumar et al., 1997; Lechner et al., 1996; Li et al., 1996; Wang et al., 1997). Our group has generated p38γ$^{-/-}$ and/or p38δ$^{-/-}$ mice. These mice are viable and fertile and without apparent phenotype (Sabio et al., 2005). We have found that p38γ and p38δ are not as widely expressed as p38α, however, they still have a big impact in health and disease as recently demonstrated using different pathology animal models (Cuenda and Sanz-Ezquerro, 2017; Escós et al., 2016).

The p38 MAPK family is subdivided in two groups, on one hand p38α and p38β and on the other, p38γ and p38δ. This subdivision is based on their homology in sequence, p38α and p38β have 75% identical sequence and p38γ and p38δ are ~70% (Kumar et al., 1997; Wang et al., 1997); their susceptibility to different inhibitors, p38α and p38β isoforms are inhibited by SB203580 and other pyridinyl imidazoles (Bain et al., 2007; Goedert et al., 1997) and by the diaryl urea compound BIRB796, which at much higher concentrations can also inhibit p38γ and p38δ (Bain et al., 2007; Kuma et al., 2005). Finally, the two p38MAPK subgroups have different specificity against different substrates. Many substrates have been described for p38α and p38β, from transcription factors to protein kinases, while the number of known p38γ and p38δ targets is still small in part because of the absence of specific inhibitors for these two kinases (Fig. I-5) (Escós et al., 2016; Risco and Cuenda, 2012).

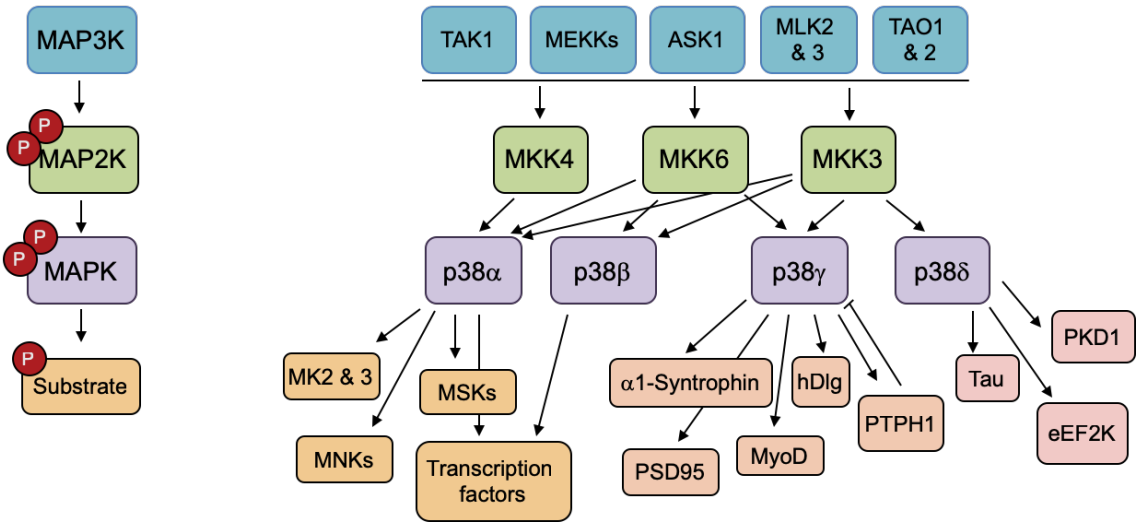

Figure I-5. p38MAPK. These pathways can be activated by growth factors, inflammatory cytokines, and a wide range of cellular stresses. Stimuli activate MAP3K that phosphorylate MAP2K who phosphorylate MAPK. The p38MAPKs are phosphorylated by MKKs to then phosphorylate different substrates, including protein kinases, cytosolic substrates and transcription factors. eEF2K (eukaryotic elongation factor 2 kinase), hDlg (human disc large), PKD1 (protein kinase D1), PSD95 (post-synapse density 95), PTPH1 (protein tyrosine phosphatase H1). Figure from (Escós et al., 2016).

1.1.3.3 *p38γ* and *p38δ MAPK: The alternative p38MAPK.*

p38γ and p38δ MAPK substrates and their biological function have been discovered in recent years (Cuenda and Sanz-Ezquerro, 2017). In the case of p38δ, this kinase phosphorylates the neuronal microtubule-associated protein Tau in the same residue that are found phosphorylated in Alzheimer´s disease patients (Feijoo et al., 2005); the eEF2K, which has been claimed to regulate TNFα translation in liver (González-Terán et al., 2013; Knebel et al., 2001, 2002); the PKD1, that control chemotaxis of neutrophils and regulates insulin secretion and cell death in pancreatic β cells (Ittner et al., 2012; Sumara et al., 2009); and the signal adaptor p62 that controls mammalian target of rapamycin complex 1 (mTORC1) activation, autophagy and tumour growth (Fig. I-5) (Linares et al., 2015).

Several physiological substrates of p38γ have been described with

the help of a unique feature found in its C-terminal sequence (-KETXL), which is able to interact with proteins that contain PDZ domains. Thus, p38γ interacts and phosphorylates α1-syntrophin, synapse-associated protein (SAP) 90/PSD95, hDlg, also known as SAP97 and PTPH (Hasegawa et al., 1999; Hou et al., 2010; Sabio et al., 2004, 2005). PTPH phosphorylation by p38γ has been shown to leads to oncogenic transformation of fibroblasts expressing K-Ras (Hou et al., 2010). p38γ$^{-/-}$ mice was found to increase seizure severity during neuronal excitotoxicity stimuli. The molecular mechanism responsible was the interaction of p38γ with PSD95/Fyn/Tau complex through PSD95 PDZ domain, that induces the phosphorylation of PSD95 and Tau by p38γ in a different site found in Tau phosphorylated by p38δ. This phosphorylation induces Tau dissociation from the PSD95/Fyn/Tau complex and inhibits amyloid-β toxicity (Ittner et al., 2016). Another substrate of p38γ dependent on PDZ domain interaction is hDlg. Phosphorylation of hDlg by p38γ negatively regulates hDlg interaction with cytoskeletal guanylate kinase-associated protein (GKAP) and Kif13b (Noseda et al., 2016; Sabio et al., 2005). Although p38γ phosphorylates Ser158, Thr209 and Ser442 residues of hDlg, Thr209 was still phosphorylated in p38γ$^{-/-}$ cells by p38δ and only decreased in p38γ/δ$^{-/-}$ cells, demonstrating a redundancy in the activity between p38γ and p38δ (Sabio et al., 2005). In previous studies it has been demonstrated that p38γ has a physiological role independent from its kinase activity. In fibroblasts under osmotic stress p38γ accumulates in the nucleus where, p38γ-hDlg association displaces hDlg from the hDlg/protein-associated splicing factor (PSF)/p54nrb/RNAs complex (Sabio et al., 2010). Proteins that are phosphorylated by p38γ that do not have a PDZ domain are; the transcription factor MyoD, which phosphorylation by p38γ decreases its transcription factor capacity (Gillespie et al., 2009); and the heat shock factor 1 (HSF1) that its phosphorylation induces trimerization and nuclear translocation of HSF1,

which controls heat shock response (Fig. I-5) (Dayalan Naidu et al., 2016).

The biological functions of p38γ and p38δ (p38γ/p38δ) have been studied using different mouse models, in both single knock out mice for p38γ and p38δ, and double knock out mice for p38γ/p38δ. The absence of both p38γ/p38δ increases the phenotype of the mouse models eliminating the redundancy between both kinases (Cuenda and Sanz-Ezquerro, 2017). p38γ/p38δ are implicated in inflammatory disease like arthritis, where they regulate T cell activation, cytokine and antibody production and bone destruction (Criado et al., 2013); and the development of different cancers associated to inflammation, such as colon cancer associated to colitis or skin epithelial papilloma, where they are involved in cytokine production, immune cell recruitment and cell transformation (Reino et al., 2014; Zur et al., 2015). p38γ/p38δ are also involved in regulating protein synthesis in heart muscle, by phosphorylating the protein DEP domain containing MTOR interacting protein (DEPTOR), which is an inhibitor of mTOR (González-Terán et al., 2016).

The role of p38γ/p38δ in the regulation of cytokine production has been thoroughly studied in recent years. Our laboratory found that when inducing septic shock in mouse model by injecting LPS/D-Galactosamine (D-Gal), the survival of p38γ/δ$^{-/-}$ mice was significantly increased compared to wild type (WT) mice survival. This effect was due to a lower production of proinflammatory cytokines such as IL1β or TNFα by p38γ/δ$^{-/-}$ mice (Risco et al., 2012). p38γ/δ$^{-/-}$ macrophages, which were the primarily producers of cytokines in the septic shock mouse model secreted less IL1β and IL10 and higher levels of IFNβ and IL12 (Risco et al., 2012). The signalling pathway affected in these cells was the TLR4-Tpl2-ERK1/2 that is activated by LPS (Fig. I-6). The molecular mechanism by which p38γ/p38δ regulated the cytokine production was by modulating Tpl2 and ABIN2 proteins levels and in consequence disrupting ERK1/2 activation and TNFα (and other cytokines) production (Risco et al., 2012).

ERK1/2 phosphorylates metalloproteinase TNFα-converting enzyme (TACE) needed for TNFα protein maturation and secretion (Rousseau et al., 2008). p38γ/p38δ have been demonstrated to also regulate translation of TNFα in the liver by the pathway p38γ/δ-eEF2k-eEF2, although the complete mechanism by which this specificity might occur has not been described yet (González-Terán et al., 2013; Knebel et al., 2001; Proud, 2015). p38δ was described to mediate IL1β secretion by activating NLRP3 inflammasome that is found upregulated in atherosclerosis that induces inflammation and accumulation of lipids in the arterial wall (Fig. I-6) (Rajamäki Kristiina et al., 2016).

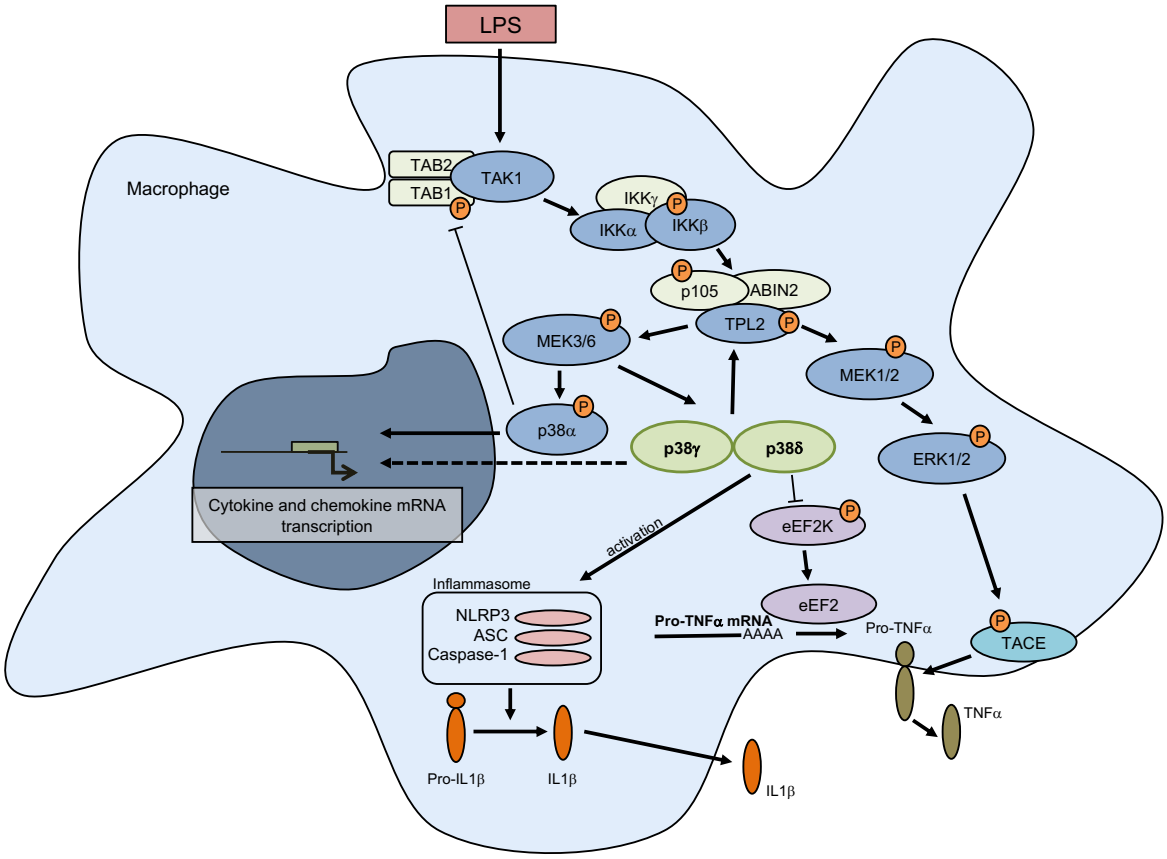

Figure I-6. Alternative p38MAPK in macrophages. LPS activates TAK1 complex. TAK1 activates IKK complex that activates the MAP3K Tpl2. Tpl2 activates MKK1/2/3/6 that activates ERK1/2 and p38MAPK to induce cytokine and chemokine transcription. p38α phosphorylates TAB1 blocking TLR4 signalling. ERK1/2 phosphorylates TACE, that is needed for TNFα processing and release. p38δ activates the inflammasome for IL1β

processing. eEF2K is phosphorylated by p38δ to promote *TNFα* mRNA translation elongation. Figure from (Cuenda and Sanz-Ezquerro, 2017).

1.2 **Translation.**

Recent data showed that the protein abundance in the cell is mainly controlled at translational level. Only ~40% of the protein levels changes are explained by the shift in the mRNA levels, which are mainly due to their transcription rate. It has been shown that mRNA and protein stability are minor contributors to mRNA and proteins total levels respectively due to the energy waste (Schwanhäusser et al., 2011). Protein synthesis is a highly conserved process that uses ribosomes to decode mRNA templates to produce specific amino acid chains. There are many signalling pathways involved in the regulation of translation, MAPKs pathways are among the best understood (Roux and Topisirovic, 2018).

mRNAs translation can be regulated by both general or specific mechanism base of mRNA modifications and sequences. The canonical modifications of mRNA ends are, the cap structure (*5´*m^7GpppN) at the *5'* end and the poly(A) tail at the 3' end, both are the promoters of translation initiation and are highly regulated (Gebauer and Hentze, 2004). Other structure and regulatory mRNA sequences are: the internal ribosomal entry sequences (IRES), which are found in the *5´*untranslated region (*5'*UTR) mediating cap-independent translation initiation; the upstream open reading frames (uORFs), that normally inhibit translation from the main ORF; secondary and ternary RNA structures (hairpins), which can be part of the IRES element, also regulates cap-independent translation; and finally specific binding sites for regulatory complexes that include RNA binding proteins (RBPs) and microRNAs (Fig. I-7) (Gebauer and Hentze, 2004).

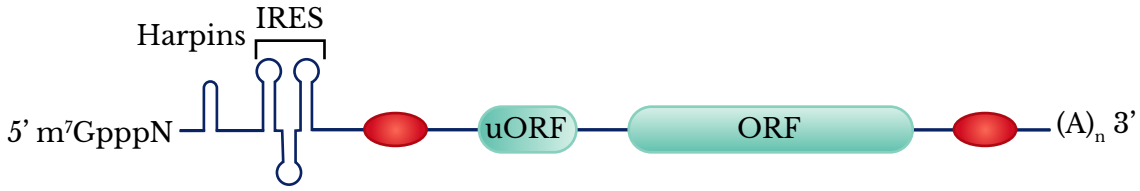

Figure I-7. Elements that influence translation of mRNAs. The 7-methilguanosine connected to the mRNA via *5*' to *5*' triphosphate linkage (m^7GpppN) forms the cap structure at the *5*'end of the mRNA. Hairpin (that acts as secondary/ternary structure), IRES elements mediate cap-independent translation, upstream open reading frame (uORF) followed by ORF and finally Poly(A) tail are indicated at the 3' end. Red ovals represent regulatory mRNA sequences where RBP or microRNAs bind specifically. Figure adapted from (Gebauer and Hentze, 2004).

The translation process has four phases: initiation, elongation, termination and ribosome recycling. Initiation phase is the most regulated in translation, the AUG start codon is identified by the first tRNA, methionyl tRNA initiation (Met-tRNAi), that is recruited to the ribosome (Hershey et al., 2012; Sonenberg and Hinnebusch, 2009). The initiation phase, canonical cap-dependent translation, starts with the assembly of the eIF4F complex at the *5*' end of the mRNA. This complex is composed by the *5*'m^7GpppN (cap) binding factor eIF4E, which interacts with the scaffold protein eIF4G, and the DEAD-box helicase protein eIF4A (Sonenberg and Hinnebusch, 2009). Poly(A) binding protein (PABP) on the 3' poly(A) end interacts with eIF4G at the cap, where this circularization of the mRNA creates a closed loop and promotes translation initiation. 40S small ribosomal subunit is preassembled forming the 43S pre-initiation complex (43SPIC) that contains Met-tRNAi and eukaryotic initiation factor (eIFs) 1, 1A, 2, 3 and *5* (Sonenberg and Hinnebusch, 2009). 43S PIC is recruited to *5*' end of the mRNA facilitated by the cap structure, eIF4F complex, and scans for AUG initiation codon (Fig. I-8) (Leppek et al., 2018; Sonenberg and Hinnebusch, 2009). This complex is highly regulated and the different components can be post-translationally modified inducing the association with other factors regulating mRNAs translation (Roux and

Topisirovic, 2018).

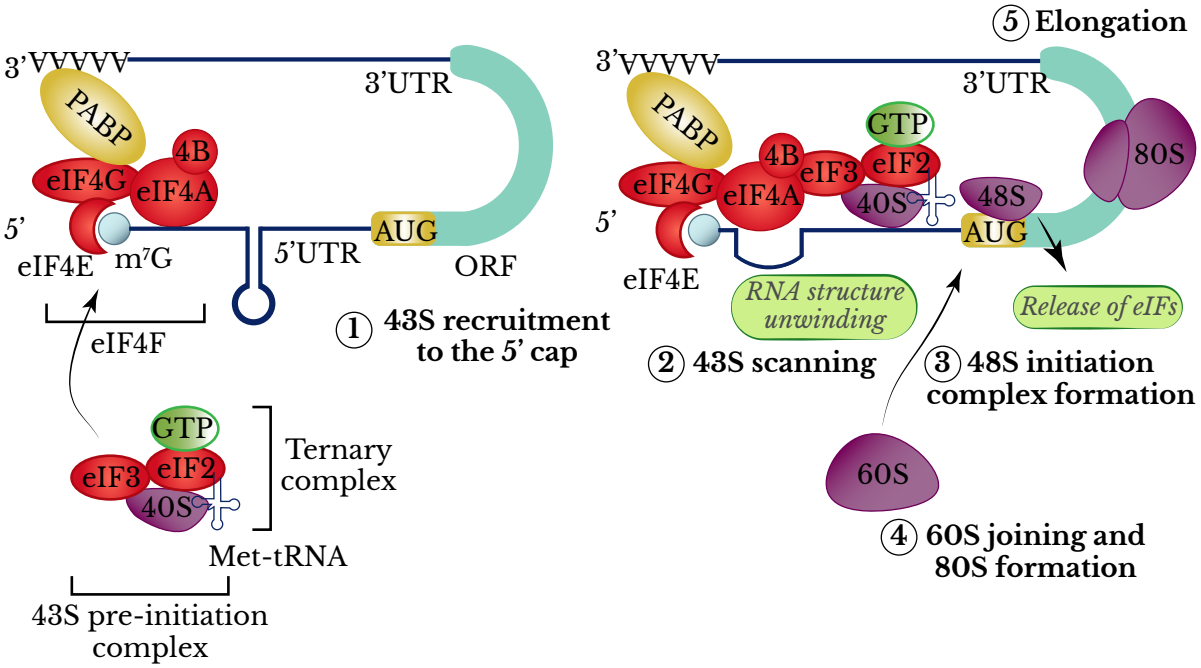

Figure I-8. Elements that influence cap-dependent translation. eIF4E binds to the Cap-structure with scaffold protein eIF4G and Dead-box helix eIF4A. Poly(A) binding protein (PABP) binds to the 3'UTR and eIF4G, creating a closed loop. **1)** 43SPIC contains 40S ribosomal subunit, eIF2 ternary complex (GTP-eIF2-Met-tRNAi) and eIF3 with eIF1, 1A and 5 not shown. **2)** 43PIC is recruited to the eIF4E complex and scans for AUG initiation codon binding to eIF4A that unwinds 3' end of the mRNA. **3)** 43S PIC bound to AUG in a stable manner generated the 48S complex. **4)** 60S ribosomal subunit binds to the 48S complex and finally **5)** 80S formation releases eIFs for the elongation phase. Figure adapted from (Leppek et al., 2018).

Virus have evolved IRESs to evade host translation regulation by evading cap-dependent initiation. IRES form secondary and ternary structures to evade the need of some or all eIFs. These structures have been used in research to study step mRNA translation (Chio et al., 2016). For translation initiation of Hepatitis C virus (HCV) mRNAs, their IRES requires eIF2 ternary complex (GTP-bound eIF2 and Met-tRNAi) and eIF3 to bind 40S forming the 48S complex, while cricket paralysis virus (CrPV) does not require any eIFs. CrPV-IRES directly binds to 80S ribosome and starts from the elongation phase using eEF2 and eEF1A (Leppek et al., 2018; Petrov et al., 2016).

Objectives

2 Objectives

The global objective of this doctoral thesis is to study the molecular mechanism by which p38γ and p38δ regulate the innate immunity response in macrophages.

To fulfil this aim, we established the following specific objectives:

1. To determine the role of p38γ and p38δ in *C. albicans* signalling in macrophages.

2. To study the molecular mechanism by which p38γ and p38δ regulate Tpl2 protein levels.

3. To determine the role of p38γ and p38δ in TLR4 signalling independently of the Tpl2/ABIN2/p105 complex.

Material & Methods

3 Materials and Methods

3.1 General buffers.

Lysis Buffer: 1% Triton X-100, 50 mM Tris-HCl pH 7.5, 1 mM EDTA, 1 mM EGTA, 50 mM NaF, 10 mM sodium glicerophosphate, 5 mM sodium pyrophosphate, 1 mM sodium orthovanadate, 270 mM sucrose and 0.1% β-mercaptoethanol, supplemented with a mixture of protease inhibitors: 1 mM benzamidine and 0.2 mM phenylmethylsulfonyl fluoride (PMSF).

Orthovanadate, $[VO_4]^{-3}$, is an inhibitor of protein tyrosine phosphatases. To prepare sodium orthovanadate solution, salt was dissolved in MilliQ water forming decavanadate, $[V_{10}O_{26}]^{-6}$. This solution was heated until boiling, cooled at room temperature and then pH was adjusted to pH 10. This process was performed up to five times to stabilize the solution that changes from orange (decavanadate) to clear (orthovanadate), and then the solution was aliquoted and stored at -20°C until use.

PBS (phosphate saline solution): 137 mM NaCl, 2.7 mM KCl, 4.3 mM Na_3PO_4 and 1.4 mM K_2HPO_4.
Protein Loading buffer: 50 mM Tris-HCl pH 6.8, 6% (v/v) Glycerol, 2% (w/v) SDS, 1% (v/v) β-mercaptoethanol, 0.004% (w/v) Bromophenol blue.
SDS-PAGE Running buffer: 192 mM Glycine, 25 mM Tris base, 0.1 (w/v) SDS.
TBS/TBS-T: 50 mM Tris/HCl pH 7.4 and 100 mM NaCl. The TBS-T contains 0.05% (v/v) Tween20.
Transfer buffer: 39 mM Glycine, 48 mM Tris base, 0.04% (w/v) sodium dodecyl sulphate (SDS), 20% (v/v) Methanol.
trypsin-EDTA: 0.05% (w/v) trypsin and 0.02% (w/v) EDTA in PBS.

3.2 Mouse manipulation.

Mice lacking p38γ (p38$\gamma^{-/-}$), p38δ (p38$\delta^{-/-}$), and p38γ/δ (p38$\gamma/\delta^{-/-}$) or expressing p38$\gamma^{(171A/171A)}$ or WT have been described previously (Sabio et al., 2005, 2010). All mice were backcrossed onto the C57BL/6 strain for at least nine generations. Mice were housed in specific pathogen-free conditions, and all animal procedures were performed in accordance with national and EU guidelines, with the approval of the National Centre of Biotechnology Animal Ethics Committee, CSIC and the Community of Madrid (Reference: CAM PROEX 316/15).

3.2.1 Generation of p38$\gamma^{171A/171A}$/p38$\delta^{-/-}$ mouse.

The new *p38$\gamma^{171A/17A}$/p38$\delta^{-/-}$* mouse line was generated by crossing p38$\gamma^{171A/171A}$ mice with p38$\delta^{-/-}$ mice. The genotyping of the new mouse line, *p38$\gamma^{171A/17A}$/p38$\delta^{-/-}$*, was performed by two polymerase chain reactions (PCR) as is described in (Sabio et al., 2005) for p38$\delta^{-/-}$ and (Sabio et al., 2010) for p38$\gamma^{171A/171A}$. All genotyping of the mice from our group is performed by Ruth Gómez-Caro Gil.

Briefly, genomic DNA was extracted from 3 – 5 mm of the end of the mouse´s tail. The tissue was lysed adding 500 μl of tail lysis buffer (100 mM TRIS/HCl pH 8.5, 5 mM EDTA pH 8, 0.2% (w/v) SDS, 200 mM NaCl 0.2 mg/ml proteinase K) and digested for 3 h at 1,400 rpm and 56°C and shaking in Thermomixer compact, Eppendorf. To obtain the solubilized DNA, samples were centrifuged for 5 min at 12,000 rpm and 4°C (Mikron 200R, Hettich Zentrifugen centrifuge) and the pellet was then discarded. DNA was precipitated from the supernatant by adding 500 μl of 2-propanol (isopropanol alcohol) and centrifuged for 5 min at 12,000 rpm and 4°C (Mikron 200R, Hettich Zentrifugen centrifuge). The pellet was washed (genomic DNA) with 500 μl of 70% (v/v) ethanol in distilled water, then re-suspended in 100 – 200 μl of distilled water, and 1 – 2 μl of the solution was used for the PCR with master mix (5Prime MasterMix).

Amplification of the gene sequence was achieved by PCR reaction using the primers (Table M-1). The PCR reaction was performed in a My cycler thermal cycler (Bio-rad) and resolved in a 1% (w/v) agarose gels (Conda). DNA marker ladder 100bp (BioLabs) was used for the identification of the bands (Sabio et al., 2005, 2010).

Table M-1. PCR primers for PCR genotyping $p38\gamma^{171A/17A}/p38\delta^{-/-}$.

Gene	Primers
$p38\gamma^{171A/171A}$	CAGACCAGACTGGCCTTGAATCCATAGAGATC
	CTCTGCAGGCACCGAGTACACAGGTGGTGT
p38δ	CCCTTGAGCCATAGATCCTGGACTTTGG
	CATGAGCTTGAGATGCTCTCTGGGACAC
	GGCGATGCCTGCTTGCCGAATATCATGG

3.2.2 Septic shock model: LPS/D-Gal.

LPS/D-Gal Septic shock mouse model is a classical model of inflammation that mirrors septic shock in humans that occurs after there is a bacterial invasion. In consequence, an overproduction of cytokines is secreted into the blood stream promoting multiorgan failure. The LPS/D-Gal mouse model consists of an intraperitoneal injection with 25G needle syringe, of a solution containing LPS 50 µg/kg and D-Gal 1 g/kg. LPS will mimic the bacterial response by stimulating TLR4. D-Gal, which is an amino saccharide, will sensitize hepatocytes to the effect of the cytokines permitting a shortening of the LPS reaction. The major contributors to the cytokine production in this model are macrophage (Deutschman and Tracey, 2014; Risco et al., 2012). The LPS/D-Gal injection was performed in the peritoneal cavity of 12-weeks-old *WT*, $p38\gamma^{171A/17A}$, $p38\gamma^{-/-}$, $p38\gamma^{171A/17A}/p38\delta^{-/-}$ and $p38\gamma/\delta^{-/-}$ male and female mice. Mouse survival was monitored and 36 h post-injection the survivor mice were sacrificed. Additionally, blood samples were collected 2 h post-injection for cytokine production analysis; and mouse liver was extracted at 0 or 6 h post-injection for apoptosis (with TUNEL staining) and haemorrhage (with

haematoxylin-eosin staining) evaluation.

3.2.2.1 Serum preparation.

Blood samples were extracted from the maxillofacial vein at 2 h post-injection of LPS/D-Gal. Samples were incubated at 37°C for 1 – 2 h for the formation of the sanguine clot, then centrifuged for 15 min at 13,000 rpm and 4°C (Mikron 200R, Hettich Zentrifugen centrifuge) and supernatant (serum) was stored at -20°C.

3.2.2.2 TUNEL staining.

Mouse liver was extracted at 0 or 6 h post-injection of LPS/D-Gal, then imbedded into paraffin blocks and cut into thin sections for TUNEL and haematoxylin and eosin staining.

The evaluation of apoptotic cells in the liver sections was performed with terminal deoxynucleotidyltransferase (TdT) mediated dUTP nick-end label (TUNEL) staining. Briefly, paraffin-embedded kidney sections were deparaffinised and rehydrated by using xylene for 20 min and rehydrated with 3-min incubations in ethanol at decreased concentrations (2 x 100%, 1 x 90% and 1 x 70%). The sections were washed with PBS and cell membrane permeabilized in PBS containing 0.5% (v/v) Triton X-100. Next, the sections were preincubated for 15 min at room temperature (RT) in freshly prepared TdT 1x buffer (25 mM Tris/HCl pH 8.8, 0.025% (w/v) bovine serum albumin (BSA), 0.025 and 0.2 M sodium cacodylate trihydrate) containing 1 mM cobalt (II) chloride to avoid unspecific signals. The TdT-based reaction were carried out in a humid chamber at 37°C for 1 h in the same buffer, containing also 3% (v/v) TdT (Roche, 03333574001) and 2% (v/v) biotin-16-dUTP (Roche, 11093070910). After this the sections were washed twice with PBS containing 0.01% (v/v) Tween 20. Sections were then incubated with streptavidin conjugated with a cyanine fluorochrome (Cy5). Nuclei were stained with Hoechst33342.

The slides were observed by fluorescent microscopy.

3.3 Cell culture.

Cell culture manipulation was always performed under laminar flow hood type II and with sterile material. Cell culture were maintained in an incubator with a humidified atmosphere, 5% of CO_2 at 37°C. All culture media and reagents were stored at 4°C and were preheated at 37°C before use. Tissue culture dish used were p100 (100 x 20 mm), p60 (60 x 20 mm), 6 well dish or 96 well dish.

3.3.1 Cell culture methods.

3.3.1.1 Freezing and unfreezing cells.

Freezing cells for liquid nitrogen storage:

Confluent cells in tissue culture dish p100, were washed with 5 ml of Phosphate saline buffer (PBS), incubated for 3 – 5 min with 1 ml of trypsin-EDTA, then 1 ml of freezing medium (20% (v/v) Dimethyl sulfoxide (DMSO) and in Fetal Bovine Serum (FBS)) was added and collected in cryovials. For gradual freezing, cryovials were enveloped in paper towel and maintained at -80°C for three days. Afterwards cryovials were stored liquid nitrogen.

Unfreezing cells:

Cryovials were quickly unfrozen at 37°C. The cells were seeded on p100 culture dish with 10 ml of cell culture medium and after 8 – 16 h the medium containing DMSO was replaced with fresh medium. The composition of the cell media depends on the cell type and will be indicated below.

3.3.1.2 Subculture of cells.

When cells reached confluency, culture dishes were washed with PBS at RT and then incubated with trypsin-EDTA at 37°C for ~5 min to separate cells from the dish. Cell suspension was diluted in fresh cells culture medium and split into fresh dishes.

3.3.2 Primary cell culture.

3.3.2.1 Mouse embryonic fibroblast (MEF).

MEF were obtained from 12.5 days old mouse embryos. Isolation conditions were kept as sterile condition working under laminar flow hood. Once the embryos were extracted, we removed the head and internal organs. The rest of the tissues were disaggregated with scalpel and digested with 2 ml every 3 embryos of 0.5 mg/ml trypsin-EDTA for 10 min at RT, and then centrifuged for 5 min at 800 rpm (centrifuge Megafuge 2.0 r, Heraeus). Pellet was digested again as before, and the new pellet was re-suspended in MEF medium (DMEM supplemented with 10% (v/v) FBS, 2 mM glutamine, 100 U/ml penicillin, 0.1 mg/ml streptomycin, 1% (v/v) sodium pyruvate, 1% (v/v) essential amino acid solution and 0.001% (v/v) β-mercaptoethanol), passed through a 100 µm filter and left to sediment for 1 min. Cell suspension in the supernatant was seeded at 1 embryo per p100 dish in MEF medium. When MEF cultures reach confluency, cells were sub-cultured 1 in 5 in p100 dish. The medium was changed to fresh one every 3 days. Experiments were performed with cells from passage 1 to 5.

3.3.2.2 Bone marrow derived macrophages from mice (BMDM).

Bone marrow was isolated from the hind legs of the mouse (tibial, femur and innominate bones). The extraction was performed in sterile conditions under a laminar flow hood and rinsing all dissecting

instruments in ethanol. Bones were placed in medium A (RPMI 1640 medium supplemented with 10% (v/v) FBS, 10 mM HEPES, 1 mM Sodium pyruvate, 50 μM β-mercaptoethanol, 2 mM glutamine, 100 U/ml penicillin and 100 μg/ml streptomycin) that was kept at 4°C, then washed for 1 min with 70% (v/v) ethanol and placed in a new dish with fresh medium A. Bone marrow was flushed using medium A with a syringe (20 ml with 25G needle) and collected. Bone marrow cells were seeded at 5 x 10^6 cells/p100 culture dish with 10 ml of medium B (RPMI 1640 medium supplemented with 10% (v/v) FBS, 10 mM HEPES, 1 mM Sodium pyruvate, 10% (v/v) L929 medium, 50 μM β-mercaptoethanol, 2 mM glutamine, 100 U/ml penicillin and 100 μg/ml streptomycin). At day 4 another 10 ml were added of fresh medium B/p100 culture dish and by day 7, cells were differentiated to Macrophages. To seed the macrophages at the same density, they were dislodged with 5 ml of PBS containing 5% (v/v) FBS and 2.5 mM EDTA for 10 min at 4°C. Macrophages were collected and centrifuge for 5 min at 1,500 rpm and 4°C (centrifuge Megafuge 2.0 r, Heraeus). They were then re-suspended in medium A with 0.1% (v/v) FBS to reduce basal phosphorylation and seeded at 3 x 10^6 cell/p60 mm dish. At day 8, cells were ready for experiments.

3.3.2.3 Peritoneal macrophages.

Mice were injected intraperitoneally with 2 ml of 3% (w/v) thioglycolate for macrophage recruitment. It is important to prepare the thioglycolate solution 6 months protected from light before use. After 3 days, mice were killed and then their peritoneal cavity was washed with sterile and cold PBS. Cells were centrifuged for 5 min at 1,200 rpm and 4°C (centrifuge Megafuge 2.0 r, Heraeus) and pelleted cells were re-suspended in peritoneal macrophage medium (RPMI 1640 medium supplemented with 10% (v/v) FBS, 2 mM glutamine, 100 U/ml penicillin and 100 μg/ml streptomycin). Cells were then seeded at 7 x 10^6 cells/p100 mm dish. After

5 h, macrophages have adhered and the rest of the cells are found in suspension. Cell culture dish were washed with PBS to remove non-macrophage cells and then fresh medium was added. The following day two washes with PBS were performed. To reduce basal phosphorylation, medium was changed to fresh peritoneal macrophage medium with 2.5% (v/v) of FBS for 2 - 4 h before the experiment.

3.3.3 Cell lines.

3.3.3.1 Human embryonic kidney 293 cells (HEK293).

HEK293, HEK293T or Flp-In T-REx HEK293 were used for protein overexpression experiment in which protein-protein interaction was studied. HEK293 cells were cultured in DMEM supplemented with 10% (v/v) FBS, 2 mM glutamine, 100 U/ml penicillin and 100 μg/ml streptomycin. When confluent, cells were split 1 in 10.

3.3.3.2 Murine macrophages cells (RAW264.7).

Cells were used to isolate endogenous protein complexes by gel filtration. Cells were cultured in DMEM supplemented with 10% (v/v) FBS, 2 mM glutamine, 100 U/ml penicillin and 100 μg/ml streptomycin. When confluent, cells were split 1 in 6.

3.3.3.3 Immortalized Mouse Embryonic Fibroblast (MEF).

Cells were cultured in MEF medium (DMEM supplemented with 10% (v/v) FBS, 2 mM glutamine, 100 U/ml penicillin, 0.1 mg/ml streptomycin, 1% (v/v) sodium pyruvate, 1% (v/v) essential amino acid solution and 0.001% (v/v) β-mercaptoethanol). When confluent, cells were split 1 in 5.

3.3.3.4 L929 cells.

L929 cells were used to obtain supernatant for the differentiation to macrophages from bone marrow. L929 supernatant supplies macrophage colony-stimulating factor (CSF-1), that is required among other unknown factors for BMDM differentiation. These cells were cultured in DMEM supplemented with 10% (v/v) of FBS, 2 mM glutamine, 100 U/ml penicillin and 100 μg/ml streptomycin. Cells were split by a sequence of passes from T25 flasks to T75 flask and finally to T150 flasks. When T150 flasks had 90 – 100% confluency, fresh medium was added up to 100 ml/T150 flasks and left for 3 days. 1 L of supernatant was collected from 10 T150 flasks, filtrated in "kitasato" with a bottleneck "büchner" and aliquoted for storage at -80°C. Supernatant was always tested negative for mycoplasm before storage.

3.3.4 Cell transfection.

Cell transfection was performed using both JetPei and Lipofectamine reagents. In all cases, when cells reached 50 - 70% confluency, cell medium was changed before cells transfection.

JetPei stock solution was prepared at 1 mg/ml of PEI (Polysciences, Warrington, PA) in 20 mM HEPES pH 8. The solution was neutralized (pH 7) with HCl and then filtered through 0.22 μm filter under laminar flow hood. Aliquots were stored at -80°C until usage. Once aliquots were unfrozen they were never used again.

When using JetPei, two separate solutions were prepared before cell transfection. Solution A containing the plasmid(s) in 150 mM NaCl and solution B containing 5% (v/v) of transfection reagent JetPei diluted in 150 mM NaCl. Solutions A and B were incubated for 5 min at RT. Then solution B was added over solution A and the mix incubated for 20 min at RT. Then, the mix was added drop-wisely onto the medium, trying to cover as much of the cell dish as possible, for transient transfection.

When using lipofectamine as transfection reagent same protocol was applied but plasmid and lipofectamine 2000 were diluted in OPTI-Mem instead of NaCl.

In experiments in which proteins were silenced in cells, the siRNA SMART pool Dharmacon reagent was used and the transfection was performed using the lipofectamine protocol (Table M-2). In this case, cells were incubated in an incubator (section 3.3) with transfection mix alone, without cell culture medium, for 5 h. Then the transfection mix was removed and fresh medium was added, and left for 3 days prior lysing of the cell.

Table M-2. siRNAs.

Gene	Specie	Company	Reference
NONO	mouse	Dharmacon	M-048587-00-0005
PABPC1	mouse	Dharmacon	M-060385-00-0005
TTP	mouse	Dharmacon	M-041045-01-0005

3.3.5 Cell lentiviral infection.

3er generation lentiviral vectors with pLX_TCR317 backbone were purchased from "Broad Genetics Perturbation Platform". These were used in p38$\gamma/\delta^{-/-}$ MEF to induce stable expression of empty vector (EV), p38γ or p38δ proteins (Table M-3). This protocol was performed in Dr. Sonnenberg's laboratory with Dr. Mehdi Jafarnejad from Goodman Cancer Research Centre in Montreal, Canada.

Virus generation was performed in HEK293T transfecting lentiviral constructs with lipofectamine transfection protocol for 24 h with 3.75 µg of psPAX2 (2nd generation lentiviral packaging plasmid), 1.75 µg of pMDG2 (encoding VSV-G envelope expressing plasmid) and finally, the plasmids of interest with 5 µg of pLX_TCR317 (containing EV, p38γ or p38δ, (Table M-3)). At day 2, HEK293T medium was changed to fresh medium for virus collection, while, MEF were seeded at 80% in 6 well

dishes with 1 ml of MEF medium in preparation for lentiviral infection. The day after (day 3), HEK293T medium with virus particles was collected, filtered through 0.20 µm filter and then 2 ml/well were added to MEF seeded in 6 well dish for infection. HEK293T medium with virus particles that were not used were aliquoted at 1ml/cryovial and frozen at -80°C. At day 4, infected MEF were sub-cultured to a p100 mm dish with MEF medium for recovery. At day 5, to select infected MEF expressing pLX_TCR317 plasmids, their medium was changed to conditional medium (MEF medium containing 5 µg/ml of puromycin). Selection was considered done when non-infected control cells were cleared, after 3 – 5 days. Cells were then tested for the expression of the protein of interest and from there on, selected MEF were grown always in selective medium.

Table M-3. Lentiviral infection plasmids.

Gene	Code	Vector	Bacteria	Selection
human MAPK12	TRCN0000469459	pLX_TRC317	Ampicillin	Puromycin
human MAPK13	TRCN0000479890	pLX_TRC317	Ampicillin	Puromycin

3.3.6 CRISPR-Cas9 for gene editing.

Flp-In T-REx HEK293 were genetically edited with CRISPR-Cas9 system to eliminate p38γ, p38δ and p38γ/δ expression for translation studies.

Flp-In T-REx HEK293 cells were supplied by Dr. Sonenberg´s laboratory from Goodman Cancer Research Centre in Montreal, Canada. CRISPR-Cas9 system and reagents were bought from "Dharmacon". This system uses single guide RNA (sgRNA) and Cas9 endonuclease. sgRNA is composed of: 1) trans-activating CRISPR RNA (tracRNA), that provides a constant sequence to hybridize to CRSPR RNA (crRNA) and binds to Cas9. This RNA was bought containing ATTO™ 550 nm fluorophore, which we will use for single cell sorting. 2) crRNA, is specifically designed for the gene target and has 19 to 20 nucleotides that binds to the targeted genomic DNA. sgRNA was designed in collaboration with Dr. Luis Montoliu´s

laboratory from the National Centre of Biotechnology in Madrid, Spain (Oliveros et al., 2016).

Flp-In T-REx HEK293 were seeded at 2.5 x 10^6/p60 mm to have 50% confluency the next day. Before transfecting, to generate the sgRNA, we annealed tracRNA conjugated with ATTO™ 550 nm and crRNA at 1:1 ratio (Table M-4). Annealing was performed with PCR (5 min at 95°C and 5°C/min ramp until 25°C) and then used or froze at -80°C protecting from light. For transfection, we generated sgRNA/Cas9 complex by incubating 2,500 ng of sgRNA with 10 µg/µl of Cas9 protein for 10 min in ice and then followed lipofectamine 2000 transfection protocol treating sgRNA/Cas9 complex as plasmid. The transfection of Flp-In T-REx HEK293 was left for 72 h to provide time to the sgRNA/Cas9 complex to be transfected and then edit the genomic DNA. To improve clone growth, we prepared medium that was left for 24 h with Flp-In T-REx HEK293 control in p150 mm dish. This medium was filtered with 0.22 µm filter and added 100 µl/well of a 96 well dish, where clones were seeded during the single cell sorting. Transfected cells were then prepared for single cell sorting by first, lifting them with trypsin-EDTA and centrifuging for 5 min at 1,200 rpm and 4°C. Secondly, cells were re-suspended in filtered (0.22 µm) sorting solution (PBS containing 1% (v/v) FBS and 1mM EDTA) and then filtered again through 0.40 µM filter to remove aggregated cells. Transfected cells were single cell sorted by ATTO™ 550 nm fluorophore seeding them into the prepared 96 well dish and left for 5 days for colony formation. Medium was changed every 3-5 days and split to 6 well dishes when reaching 60% confluency. Edition was then tested by immunoblot.

Table M-4. Human sgRNAs for CRISPR-Cas9 gene edition.

Gene	sgRNA
h-MAPK12-sgRNA	ATTCACTCCTGATGAGACCC
h-MAPK13-sgRNA	ACGGATCTGCAGAAGATCAT

3.4 DNA manipulation.

3.4.1 E. coli transformation and culture.

Bacteria transformation was achieved by adding 10 ng of plasmid to 50 µl of competent *E. coli* DH5α cells, that were supplied by the Department of Immunology and Oncology kitchen service. Bacteria were mixed gently with DNA and then left at 4°C for 30 min. For DNA transformation by heat shock, mix was incubated at 42°C for 30 seconds and immediately transferred to ice for 5 minutes. Bacteria were incubated in Luria-Bertani (LB) broth for 1h at 37°C in a shaking platform and then spread in LB selective agar p100 mm bacterial dish (100 µg/ml ampicillin or 50 µg/ml of kanamycin depending on the resistance of the plasmid). Cells were incubated for 37°C overnight for colony formation. One colony was picked for starter culture and incubated by shaking at 37°C for 8 – 10 h in 5 ml of selective LB. Starter culture was inoculated into 0.5 – 1 ml in selective LB and incubated by shaking at 37°C overnight.

3.4.2 DNA plasmid purification and quantification.

For DNA plasmid purification of the of transformed cells, bacteria were harvested by centrifugation for 30 min at 8,000 x g. We used Geneaid Maxi Plasmid Kit Quick (Quiagen) with the supplied protocol from the company. DNA plasmid was dissolved in MilliQ water and then quantified using nanodrop spectrophotometer.

3.4.3 Cloning psiCHECK2 mouse Tpl2-3'UTR and psiCHEK2 mouse ABIN2-3'UTR.

Bicistronic plasmid psiCHEK-2 (Promega) was used for luciferase assay studies where *Tpl2* and *ABIN2* 3'UTR were cloned to control *Renilla* mRNA translation while using *firefly* as transfection control (Fig. M-1). Assays were performed following Dual-luciferase Reporter Assay system (Promega).

Tpl2 and *ABIN2* 3'UTR template originated from *Tpl2* and *ABIN2* mRNA in MEF. This protocol was performed in Dr. Sonnenberg's laboratory with Dr. Mehdi Jafarnejad from Goodman Cancer Research Centre in Montreal, Canada.

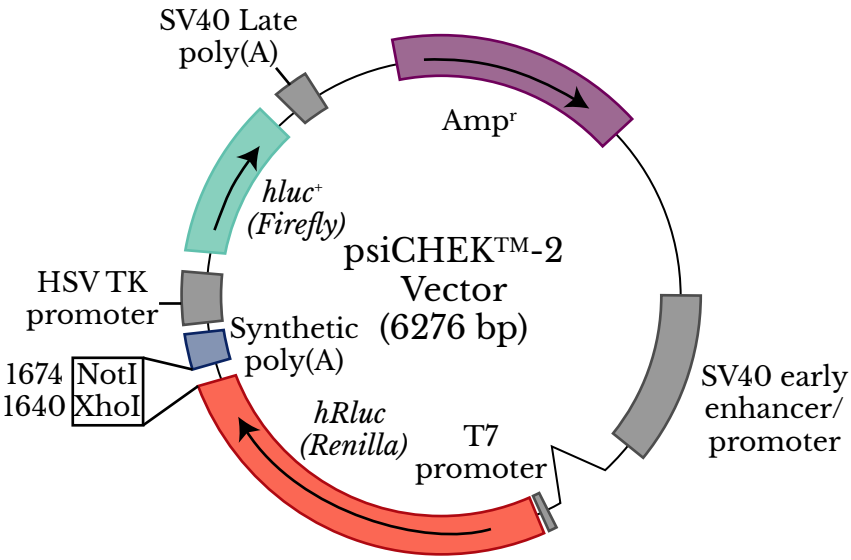

Figure M-1. Diagram of psiCHEK-2 (Promega). Bicistronic plasmid with *Renilla* and *Firefly* luciferase genes. *Tpl2* or *ABIN2* 3'UTR were cloned in psiCHEK-2 plasmid to study the effect of *Tpl2* or *ABIN2* 3'UTR on *Renilla* mRNA translation. *Firefly* was used as a transfection control to use to normalize luciferase quantification.

Total mRNA was extracted and cDNA was generated. *Tpl2 (MAP3K8)* and *ABIN2 (Tnip2)* 3'UTR was amplified by PCR protocol with designed primers from Table M-7. For Tpl2, PCR program was: **1)** 1 min at 95°C, **2)** 35 cycles of denaturalization for 30 sec at 95°C, annealing for 1 min at 54°C and extension for 1:30 min at 68°C and **3)** 3 min at 68°C. For ABIN2, PCR program was: **1)** 1 min at 95°C, **2)** 35 cycles of denaturalization for 30 sec at 95°C, annealing for 1 min at 53°C and extension for 1:30 min at 68°C and **3)** 3 min at 68°C. DNA amplification was isolated running a 1% (w/v) agarose gel and extracted with QIAquick Gel Extraction kit (Quiagen). 1 µg of psiCHECK2 plasmid (Promega) and 0.2 µg of insert (amplified PCR products) were digested for 15 min at 37°C with XhoI and NotI fast digest enzymes (Thermos scientific). Digested plasmid was run in 1% (w/v) agarose gel in parallel with un-cut plasmid as control and then extracted

with QIAquick Gel extraction kit (Quiagen) to isolate cut plasmid. Inserts were purified using QIAquick Gel extraction kit (Quiagen) to eliminate molecules from the digestion reaction. Ligation was performed with 1 µl of T4 DNA ligase from (Thermo scientific), 25 ng of cut and purified plasmid and 75 ng of insert (or no insert as control) for 1 h at RT. Ligations were transformed into DH5α cells following bacteria transformation protocol. 5 – 6 colonies from each transformation were sub-cultures for Presto Mini Plasmid Kit Quick (Quiagen). Finally, plasmids were sequenced with Sanger sequencing services.

Table M-7. PCR primers for cloning in psiCHEK2 plasmid.

Gene	Primer Forward	Primer Reverse
Tnip2	ATTTCTCGAGGCCAGACATTGCCCGTGTGA	ATTTGCGGCCGCAGGAAATAAAGGTGCTTTCCCTTTTGG
MAP3K8	ATTTCTCGAGGGCTTTGTTGGCAACAAAACAGG	ATTTGCGGCCGCACAACGGAGGCATTACCAAGA

3.5 Protein manipulation.

3.5.1 Cell stimulation and lysis.

When indicated, cells were incubated with inhibitors or with the solvent as control for the required period of time before stimulation or lysis. Stimulation was performed by adding the indicated agonists for the times showed in the figures. For cell lysate, medium was removed from the dishes and lysis buffer was added in volumes of 500 µl/p100 mm dish or 250 µl/60 mm dish. Samples were centrifuged for 15 min at 13,000 and 4°C rpm (centrifuge Mikron 200R, Hettich Zentrifugen). Supernatant was collected, the pellet discarded and stored at -80°C. Proteins lysates were quantified by the Bradford method, using Coomassie Plus Protein reagent (Thermo Scientific).

3.5.2 Protein immunoprecipitation and GST pull-down assay.

Protein immunoprecipitation (IP) and GST pull-down (PD) assay, were performed to obtained enriched samples of the protein of interest. For

protein immunoprecipitation assay we used protein G-sepharose beads (GE Heathecare) and for GST pull-down assays we used protein GSH-sepharose beads (GE Heathecare). Both beads were stored at 4°C as slurry in 20% ethanol.

3.5.2.1 Immunoprecipitation (IP).

Ethanol was eliminated from the protein G-sepharose beads by washing them 3 times with cold PBS. To couple antibody to the protein G-sepharose bead, 10 µl of beads per assay were incubated with 0.5 - 2 µg of antibody for 30 min at 4°C in a shaking platform. Antibody coupled-beads were washed twice with cold lysis buffer to remove unbound antibody and then incubated with cell lysates for 2 h at 4°C in a shaking platform. Proteins bound to the beads were centrifuged 1 min at 13,000 rpm (centifuge Minispin, Eppendorf) and the supernatant discarded.

3.5.2.2 GST-pull-down assay (PD).

GSH-sepharose beads were equilibrated in cold lysis buffer by washing 3 times. 10 µl of beads per assay were incubated with GST-protein or cell lysates for 1 h at 4°C in a shaking platform. Proteins bound to the beads were centrifuged 1 min at 13,000 rpm (centifuge Minispin, Eppendorf) and the supernatant discarded.

Proteins bound to the beads (GSH-sepharose or protein G-sepharose) were washed twice with cold lysis buffer containing 0.5 M of NaCl to minimise non-specific binding and twice with cold lysis buffer alone. When isolating complexes, the pellets were washed four times with cold lysis buffer containing 0.1 M of NaCl.

3.5.3 Western Blot.

3.5.3.1 Electrophoresis.

Sodium dodecyl sulphate-polyacrilamide gel electrophoresis (SDS-PAGE) was performed in BIO-RAD equipment. 30 – 50 µg of protein sample were denatured in loading buffer and heated for 5 min at 90°C. SDS-PAGE gels were used at 4% bis-acrilamide for stacking and 10% or 12% bis-acrilamide to resolve proteins. We used Electrophoresis buffer to run the samples at a constant voltage of 120 v for 2 h.

3.5.3.2 Semi-Dry Transfer Cell and immunodetection.

Protein samples resolved by SDS-PAGE were transferred by Semi-Dry Transfer Cell to nitrocellulose membranes (BIO-RAD) and transfer buffer. Semi-Dry Transfer Cell (BIO-RAD) was used, as indicated by the provider and the conditions were set at a constant voltage of 20 v for 20 min. Nitrocellulose membranes were tested for transference efficiency with Red Ponceau solution (Pierce).

Membranes were blocked in TBS-T with 5% (w/v) dried skimmed milk. Blocking solution was discarded and primary antibodies were diluted in blocking solution by incubating 2 h at RT or overnight at 4°C (Table M-5). When ABIN2 antibody was used, the blocking solution changed to PBS instead of TBS. The membranes were washed 3 times with TBS-T for 10 min/wash. Secondary antibodies, conjugated with a fluorochrome, were also diluted in blocking solution. After the incubation for 1 h at RT, membranes were washed 3 times for 10 min with TBS-T. Signal of the secondary antibody was detected with "Odyssey Licor System" equipment.

Table M-5. Antibodies. (WB) Western blot, (IP) immunoprecipitation, (DSTT*) Division of Signal Transduction Therapy, Dundee, UK.

Antibody	Company	Reference	Dilution	IgG
α1-tubulin	Santa Cruz	134237	1µg/ml (WB)	mouse
ABIN2	Steve Ley	--	2µg/ml (WB)	mouse
Alexa Fluor 680 Anti-Rabbit	Molecular Probes	A-21109	1/5000 (WB)	goat
Alexa Fluor 680 Anti-Sheep	Molecular Probes	A-21102	1/5000 (WB)	donkey
Alexa Fluor 700 Anti-Mouse	Molecular Probes	A-21036	1/5000 (WB)	goat
β-actin	Santa Cruz	sc-47778	1/1000 (WB)	mouse
ERK1/2	Cell Signaling	9102	1/1000 (WB)	rabbit
ERK5	DSTT*	--	1µg/ml (WB)	sheep
GST	Cusabio	CSB-MA000031M0m	1µg/ml (WB)	mouse
hDlg/SAP97	DSTT*	--	1µg/IP	sheep
hDlg/SAP97	DSTT*	--	1µg/ml (WB)	sheep
JNK	Cell Signaling	9252	1/1000 (WB)	rabbit
lamin-β1	Santa Cruz	sc-374015	1µg/ml (WB)	mouse
NONO	Santa Cruz	sc-166702	1/1000 (WB)	mouse
p-ERK1/2 (Thr202/Tyr204)	Cell Signaling	9101	1/1000 (WB)	rabbit
p-JNK (Thr183/Tyr185)	Cell Signaling	44682	1/1000 (WB)	rabbit
p-p105 (Ser 933)	Cell Signaling	4806	1/1000 (WB)	rabbit
p-p38 (Thr180/Tyr182)	Cell Signaling	9211	1/1000 (WB)	rabbit
p-Ser158-hDlg/SAP97	DSTT*	--	1µg/ml (WB)	sheep
p105	Cell Signaling	4717	1/1000 (WB)	rabbit
p38!	Santa Cruz	sc-535	1/1000 (WB)	rabbit
p38" C-terminal	DSTT*	--	1µg/IP	sheep
p38"	DSTT*	--	1µg/ml (WB)	sheep
p38#	DSTT*	--	1µg/ml (WB)	sheep
PABPC1	Abcam	ab-21060	1/1000 (WB)	rabbit
Tpl2	Santa Cruz	204351	1µg/ml (WB)	rabbit
TTP (Zfp36)	Santa Cruz	sc-376162	1µg/ml (WB)	mouse

3.5.4 Gel filtration chromatography.

Gel filtration chromatography separate protein complexes by their molecular size. Raw264.7 cell lysates were prepared and quantified as indicated previously (section 3.5.1). Triton X-100 from the lysates was removed by dialyzing the samples in lysis buffer without the detergent. These experiments were performed in collaboration with Dr. César Santiago from the protein X-ray crystallography unit in the National Centre of Biotechnology in Madrid, Spain.

The column used was Superdex 200 10/300 GL from GE Healthcare and was equilibrated with lysis buffer without Triton X-100 that has been previously degassed. Samples were filtered through a 0.22 µm filter to eliminate protein aggregates before loaded into the column.

0.5 ml fractions were collected from the gel filtration chromatography till 25 ml and 50 µl were used for western blot for proteins analysis as indicated.

3.5.5 Pulse chase and ^{35}S-Methionine and Cysteine labelling.

To measure protein stability, plasmids expressing GST tagged proteins were transfected in MEF cells for 24 h and then used for pulse chase assay.

Cell were starved of Met/Cys for 45 min and then incubated in the same medium without Met/Cys, but supplemented with S^{35} Met/Cys at 100 µCi/ml, to radioactive label proteins, and incubated for 30 min. During this time cell will use the radiolabelled Met and Cys in protein translation. At different time points cells were washed twice with cold PBS and then lysate. Protein lysates were quantified by Bradford method and pulled by GST pull-down assay. Samples were loaded into SDS-PAGE electrophoresis and gels were dehydrated for signal amplification. Signal was visualized by incubating the dehydrated gel with film at -80°C overnight.

3.5.6 Luciferase assay

To measure the translation activity of *Tpl2* and *ABIN2* 3'UTR or SV40-CAP, HCR-IRES and CrPV-IRES we used Dual-luciferase Reporter Assay system kit (Promega). Buffers were provided by the company and all the plasmids used were bicistronic. This protocol was performed in Dr. Sonnenberg's laboratory with Dr. Mehdi Jafarnejad from Goodman Cancer Research Centre in Montreal, Canada.

We seeded MEFs in 24 well dish at 25,000 MEF/well and 24 h later, we transfected 500 ng of bicistronic plasmid/well with lipofectamine protocol. The next day, MEFs were washed once with cold PBS and then lysed with 50 µl of "passive lysis buffer" (provided by the kit) for 20 min at RT in a shaking platform. The lysates were either used immediately

after lysis or saved at -80°C for later use. Luciferase measurements were performed by adding in a 1.5 ml eppendorf: 50 µl of "luciferase assay reagent II" (which measures firefly luciferase reporter) and 2 µl of lysate (pipetting several times for mixture), and then measuring firefly luciferase with luminometer, which remains constant up to 1 min. Afterwards, 50 µl of "Stop & Glo reagent" was added to block firefly luciferase and activate Renilla luciferase, and measured again for Renilla luciferase with luminometer. Depending on the plasmid, one luciferase was used as transfection control to normalize the studied luciferase, that had their translation controlled by 3'UTRs or IRES features.

3.5.7 Mass spectrometry experiment.

To study the interactome of p38γ and p38δ in macrophages we performed a mass spectrometry experiment from isolated complexes from p38γ or p38δ pull-down assay in BMDM.

We generated and lysed WT BMDM in basal conditions and 4.5 mg of protein lysates were incubated with different GST-tagged proteins. These proteins were mutated inactive versions of p38γ and p38δ, kinase dead (KD), GST-p38γKD and GST-p38δKD, while GST alone was used as control. A total of 18 mg of WT BMDM lysates were first pre-cleared for 1 h in a shaking platform at 4°C with 20 µl of GSH-sepharose beads bound to 20 µg of GST. Then aliquots of 4.5 mg of pre-cleared protein lysates were incubated for 1 h in a shaking platform at 4°C with either 10 µl of GSH-sepharose beads bound to 10 µg of GST, as control, or to 10 µg of GST-tagged protein. Pull-down was performed and then washed twice with lysis buffer. The preparation and identification of the proteins pulled-down with GST, GST-p38γKD and GST-p38δKD, was performed in collaboration with the Proteomic unit in the National Centre of Biotechnology in Madrid, Spain. Pull-downs were loaded in 12% SDS-PAGE and run only for 1 cm in the resolving gel and then dye with

colloidal coomassie. Bands from the different pull-down assays were cut, digested with trypsin, and quantified by fluorimetry. 1 µg of each digestion was run through reverse phase C-18 liquid chromatography for peptide separation by polarity and eluted peptides were then fragmented in TRIPLE-TOF mass spectrometry (LC-MS/MS). The collected data from the mass spectrometry results were used to identify peptides using mouse UNIPROT database and raw data was analysed with MASCOT software that calculated false discovery rates (FDR) for each of the identified proteins.

3.5.8 Phospho-proteomic experiment.

To identify possible targets of p38γ and p38δ that could be involved in the specific regulation of *Tpl2* and *ABIN2* mRNA, we performed a phospho-proteomic analysis, using peritoneal macrophages from WT, p38$\gamma^{-/-}$, p38$\delta^{-/-}$ and p38$\gamma/\delta^{-/-}$ mice.

Peritoneal macrophages were lysed at basal conditions and then 1 – 0.25 mg of proteins were precipitated (samples were in triplicate). Protein precipitation was performed adding four times the sample volume of cold (-20°C) of acetone (high quality, for HPLC, SIGMA ≥ 99.9 %). Proteins with acetone were mixed by vortex for 10 seconds and incubated overnight at -20°C. Precipitated mix was centrifuge for 10 min at 15,000 x g and 4°C. Supernatant was removed and acetone left evaporated by leaving uncapped tubes for 30 min at RT without over-drying the pellet. Precipitated protein was then sent to Dr. Eric Bonneil from the Proteomic Platform in the Institute for research in immunology and cancer in Montreal, Canada. The phospho-proteomic procedure was performed by enrichment of phospho-peptides with TiO_2 and then separating the multi-phosphorylated peptides from mono-phosphorylated peptides with (SIMAC). The raw data obtained was analysed bioinformatically only keeping those that: at least two observation out of the three replicates for

at least one condition, had a p-value under 0.05 and also had a $-1<\log_2(\text{fold change})<1$ (FC).

3.6 RNA manipulation.

3.6.1 RNA extraction and quantification.

TRI Reagent (Sigma Aldrich) was applied for the RNA purification. Nuclease-free aerosol-resistant tips (Thermo Scientific) were used to prevent RNA degradation during RNA purification. TRI Reagent was added to the samples and then mixed by vortex with isopropanol, then samples were left at -20°C overnight for RNA precipitation. RNA was washed twice with 70% (v/v) ethanol and re-suspended in RNAse free water. RNA was quantified with Nano Drop equipment by adding 1.5 µl of purified RNA in the machine pedestal. The concentration was determined by the software using Beer-Lambert formula and samples were saved at -80°C.

3.6.2 RNA reverse transcription.

cDNA was generated from RNA by reverse transcription polymerase chain reaction. 500 ng of RNA/sample were converted to cDNA with High Capacity cDNA Reverse Transcription kit (Applied Biosystems). Thermo cycler conditions were 10 min at 25°C, 120 min at 37°C and 5 min at 85°C. cDNA samples were stored at -20°C.

3.6.3 qPCR analysis.

Quantitative PCR (qPCR) reaction was performed in 384-well plates (Bio-Rad) with reactions in triplicate and using 5 µl of cDNA/sample and 3 µl of Master Mix. Master mix includes Eva Green buffer and the primers of interest, all diluted in RNAse free water (Table M-6).

For qPCR analysis SDS v2 program was used. This programme

considers the threshold of the samples, making sure it was adjusted at the slope and the noise was eliminated. Ct values were checked to be below 35 cycles from the standard curve and all melting curves had the same peak. The samples were quantified using comparative Ct method relative to a house keeping gene (*actin* or *GAPDH*) and relativized to unstimulated control samples from the same experiment.

Table M-6. Table of qPCR primers.

Gene	Primer Forward	Primer Reverse
ABIN2	TTCAGGTCCTTGGTGTAGGC	GACGCTGGGGAGAAAAGC
β-actin	AAGGAGATTACTTGCTCTGGCTCCTA	ACTCATCGTACTCCTGCTTGCTGAT
Camk2b	AGCAGGCATGGTTTGGTTT	TGTACAGGATCACCCCACAT
GAPDH	CCCATCACCATCTTCCAGGA	CGACATACTCAGCACCGGC
IFNβ	TCAGAATGAGTGGTGGTTGC	GACCTTTCAAATGCAGTAGATTCA
IL10	CAGGACTTTAAGGGTTACTTG	ATTTTCACAGGGGAGAAATC
IL1β	TGGTGTGTGACGTTCCCATT	CAGCACGAGGCTTTTTTGTTG
nos2	CAGCTGGGCTGTACAAACCTT	CATTGGAAGTGAAGCGTTTCG
Sik1	ACAGCACCACTCTTCTACCGC	TCACAGGGAGCAAGCACATAGG
TNFα	CTGTAGCCCACGTCGTAGC	TTGAGATCCATGCCGTTG
Tpl2	ACGAAACCAGAGCCGATGTT	CTCTGTTTGCTGAGCCTGGA

3.7 Cytosol/Nucleus separation.

Cells were incubated with PBS, 5% (v/v) FBS and 2.5 mM EDTA, for 10 min at 4°C and then scraped from the dish. They were collected and centrifuged for 5 min at 1,200 rpm and 4°C (centrifuge Mikron 200R, Hettich Zentrifugen) and washed with cold PBS. Nuclease-free aerosol-resistant tips and eppendorfs (Thermo Scientific) were used to prevent RNA degradation during RNA purification. Pellet was re-suspended with 500 µl of Cytosol buffer (10 mM Tris-HCl pH 8, 10 mM KCl, 0.5 mM EDTA, 0.1% (v/v) NP40 and supplemented with 1 mM dithiothreitol (DTT) and 1 mM PMSF), which breaks the cytosol membrane, with 1 µl of RNAse inhibitor per p100 mm dish. Solution was centrifuged for 5 min at 3,000 rpm and 4°C (centrifuge Mikron 200R, Hettich Zentrifugen). The supernatant was saved as cytosol sample, and NaCl solution was added until 150 mM NaCl final concentration was reached. Pellet was re-

suspended in Nucleus buffer (50 mM Tris pH 8, 0.4 NaCl, 0.2 mM EDTA, 0.5% (v/v) NP40 and 10% (v/v) glycerol supplemented with 1 mM DTT and 1 mM PMSF) with 1µl of RNAse inhibitors and then incubated for 10 min in ice. The suspension was mixed with gentle vortex intermittently. Samples were centrifuged for 5 min at 3,000 rpm and 4°C (centrifuge Mikron 200R, Hettich Zentrifugen) and the DNA that appeared in mucous form was eliminated with pipette. Cytosol and Nucleus fractions were divided in two, to have RNA and protein samples of each, and then followed with RNA extraction protocol or immunoblot.

3.8 **Polysome profiling.**

Polysome profiling is a method that allows monitoring the translation of mRNAs in cells. Once polysome fractions were collected, the translation activity of each mRNA was analysed by qPCR. Polysome profiling was performed in collaboration with Dr. Encarnación Martínez-Salas´s laboratory with Dr. Rosario Francisco-Velilla from Molecular Biology Centre (CBM) in Madrid, Spain and with Dr. Mehdi Jafarnejad from Goodman Cancer Research Centre in Montreal, Canada. First, we prepared sucrose gradient 10-50% solution, with 60% (w/v) sucrose solution in MilliQ water and 50 mL of 10x sucrose gradient buffer (200 mM HEPES pH 7.6, 1 M KCl, 50 mM MgCl2, 100 µg/ml cycloheximide, 1x protease inhibitor cocktail EDTA-free Roche and 100 units/ml RNase inhibitor). Every solution was filtered through 0.22 µm filter. For sample preparation, cells were seeded for 80-90% confluency that renders the maximum polysomes. The same day of isolation, hypotonic buffer (5mM Tris-HCl pH 7.5, 2.5 mM MgCl2, 1.5 mM KCl, 1x protease inhibitor cocktail EDTA-free and 100 µg/mL cycloheximide) and mix buffer (0.5% (v/v) Triton X-100/sample and 0.5% (w/v) Sodium Deoxycholate/sample, mix by vortex and leave on ice) were prepared. Cells were washed with ice cold PBS containing 100 µg/ml of cycloheximide. MEFs were washed twice,

while Flp-In T-REx HEK293 was only washed once. Cells were scraped and collected in RNAse-free pre-cooled 50 ml tubes and centrifuge for 10 min at 1,200 rpm and 4°C (centrifuge Megafuge 2.0 r, Heraeus). We eliminated the supernatant and resuspend the cells in 430 µl of hypotonic buffer so as to only have cytosolic molecules. We added 1 µl of 1M DTT and 100 units of RNAse inhibitor and vortex for 5 seconds (both for RNAse inactivation), then added 50 µl of the mix solution (detergents to dissolve cytoplasmic wall) and vortex again for 5 seconds. Finally, were centrifuged at maximum speed for 10 min at 4°C (centrifuge Mikron 200R, Hettich Zentrifugen) and the supernatant was transferred to a new pre-chilled RNAse-free 1.5 ml tube. $OD_{260\ nm}$ was measured in nanodrop for each of the samples to load 10-30 $OD_{260\ nm}$ in each of the gradients and at least 50 µl were saved as input. Gradients were carefully weighted and then centrifuged for 2 hours at 35,000 rpm and 4°C using SW40Ti rotor in a Beckman Coulter (Optima L100 XP ultra-centrifuge) with the brake off. While the samples were centrifuging, the fraction collector was cleaned with MilliQ water and RNase ZAP. Once centrifugation was complete the tubes were removed from the rotor and placed them at 4°C. Samples were ran with a chasing solution 60% (w/v) sucrose with bromophenol blue through UV detector and fraction collector (Tledyne ISCO) that had a TracerDAQ software (MicroDAQ). Samples were collected in RNAse-free 2 ml tubes and after each sample fractions were taken, 1 ml of TRI reagent for RNA isolation was added and placed on dry ice to store afterwards at -80°C.

3.9 **Statistical analysis.**

For statistical analysis Excel, Graph Prism and R software were used. For the survival curve Kaplan-Meier test was performed and for the comparison of the curves the Log-Rank method was used. For treatment comparison, two-way ANOVA was applied.

3.10 **RNA-sequencing experiment.**

This experiment was performed in collaboration with Dr. Steve Ley´s laboratory at the Francis Crick Institute in London, England. We used 1 x 10^6 BMDM cells from 6 different WT and $p38\gamma^{171A/171A}$/$p38\delta^{-/-}$ male mice and sequenced non-stimulated samples and samples stimulated with LPS (100ng/ml) for 30- and 60-min (Fig. M-2).

3.11 **Bioinformatical analysis.**

Deep sequencing bioinformatic analysis was performed with data obtained from RNA-sequencing experiment samples performed in Illumina HiSeq 2500, obtaining unstranded single-end reads. These reads were obtained from an unknown strand and it was only sequenced from one end. Quality control of the reads was done with FASTQC (Andrews S., 2010a) finding reads to be 101 nucleotide lengths and each sample rendered 15 x 10^6 reads (Andrews S., 2010a). Reads (FASTQ) were aligned with Bioconductor's Rbowtie2 1.0.1 package (Zhang W, 2017) in R studio 1.1.383 against mouse genome (GRCm38.p5) obtained from ENSEMBL. Aligned reads were inspected with SeqMonk version 1.40.0 browser (Andrews S., 2010b) and then raw counts were obtained (Fig. M-2).

R studio 1.1.383 software with DESeq2 1.18.1 package was used for the analysis of the raw counts and $\log_2$FC (with *p*-value calculation (Love et al., 2014; Quackenbush, 2002). To increase the speed of the programme raw counts were subjected to a minimal pre-clearing where any genes with no reads or nearly no reads added across all the samples were eliminated. Raw counts where then adjusted to a negative binomial distribution for normalization. For the diagnosis test of outliers, DESeq2 calculates for every gene and sample a function called Cook´s distance. To check for sample outliers by clustering the samples, we used regularized log-

transformation (rlog), which transforms the count data into log2 scale in a way that minimized the differences between the samples (Love et al., 2014). After rlog transformation, data was represented as principal component analysis (PCA) calculated with the Euclidian distance between samples. This analysis showed "WT_30_8" very different from the rest of its replicates and in consequence it was not considered for the rest of the analysis.

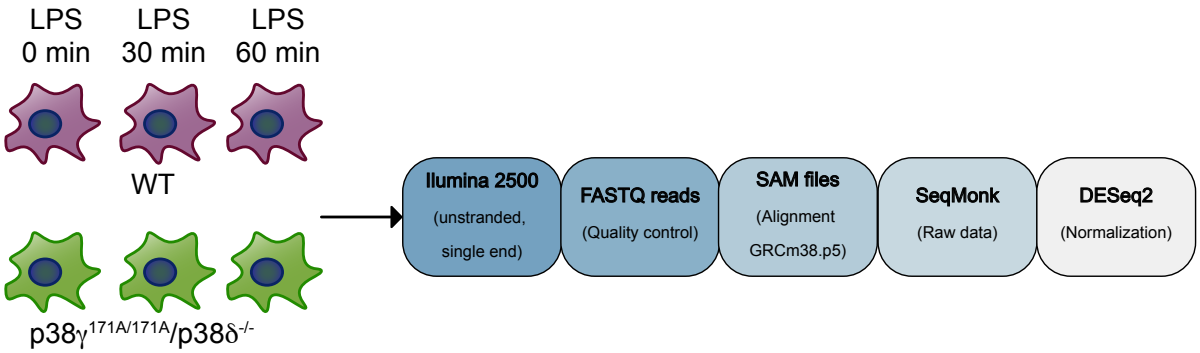

Figure M-2. RNA-sequencing pipeline. BMDM from 6 WT or p38$\gamma^{171A/171A}$/p38$\delta^{-/-}$ male mice were non-stimulated or stimulated with LPS for 30- or 60- min. Using R with Bioconductor packages (DESeq2 1.18.1 package) (Love et al., 2014) logFC and adjusted p-value was calculated. **A)** Graph of the number of genes filtered with *p*-value adjusted <0.05 and -1.5<logFC<1.5 comparing p38$\gamma^{171A/171A}$/p38$\delta^{-/-}$ control vs WT control, p38$\gamma^{171A/171A}$/p38$\delta^{-/-}$ 30 min vs WT 30 min stimulation with LPS and p38$\gamma^{171A/171A}$/p38$\delta^{-/-}$ 60 min vs WT 60 min stimulation with LPS.

Results

4 Results

4.1 Chapter 1. *C. albicans* signalling pathway in BMDM.

C. albicans activates different receptor families, such as TLR and lectin-type receptors, inducing the transcription of cytokines. We have reported that, when stimulating with *C. albicans* or TLR agonists the loss of p38γ/p38δ in BMDM impairs the phosphorylation of ERK1/2 and the transcription of cytokines (Alsina-Beauchamp et al., 2018; Risco et al., 2012). It has been described that Dectin-1 receptor is the main lectin-type receptor activated in macrophages in response to *C. albicans* infection (Netea et al., 2015). Here we investigate if p38γ/p38δ are essential for the signal transduction mediated by Dectin-1 receptor.

4.1.1 Dectin-1-Syk signalling is impaired in p38γ/δ$^{-/-}$ BMDM.

We studied the role of p38γ/p38δ in Dectin-1 receptor signalling pathway that leads to cytokine production. For this, we stimulated BMDM from WT and p38γ/δ$^{-/-}$ mice with two different β-glucan molecules: Zymosan that activates Dectin-1 and TLR2 and Curdlan that only activates Dectin-1 receptor (Brown et al., 2003).

We first confirmed the specificity of Curdlan as a Dectin-1 ligand by examining ERK1/2 activation in MyD88$^{-/-}$ and Dectin1$^{-/-}$ BMDM, and by using the Syk inhibitor, the compound PRT062607 (Spurgeon et al., 2013), in WT BMDM (Fig. R-1A). TLRs signalling is activated via adaptor molecule MyD88, whereas Dectin-1 signalling is mediated by the recruitment of the tyrosine kinase Syk (Reid et al., 2009; Takeuchi and Akira, 2010; Underhill, 2007). We stimulated BMDM with Curdlan or Zymosan and used heat-killed *C. albicans* (HK-Ca) and LPS as controls. We then examined the phosphorylation of ERK1/2 by inmunoblot. LPS is a well-known TLR4 ligand that induces the activation of NF-κB1 and MAPKs

(Cohen, 2014), whereas in macrophages, HK-Ca binds mainly to Dectin-1, TLR4 and TLR2 (Netea et al., 2015).

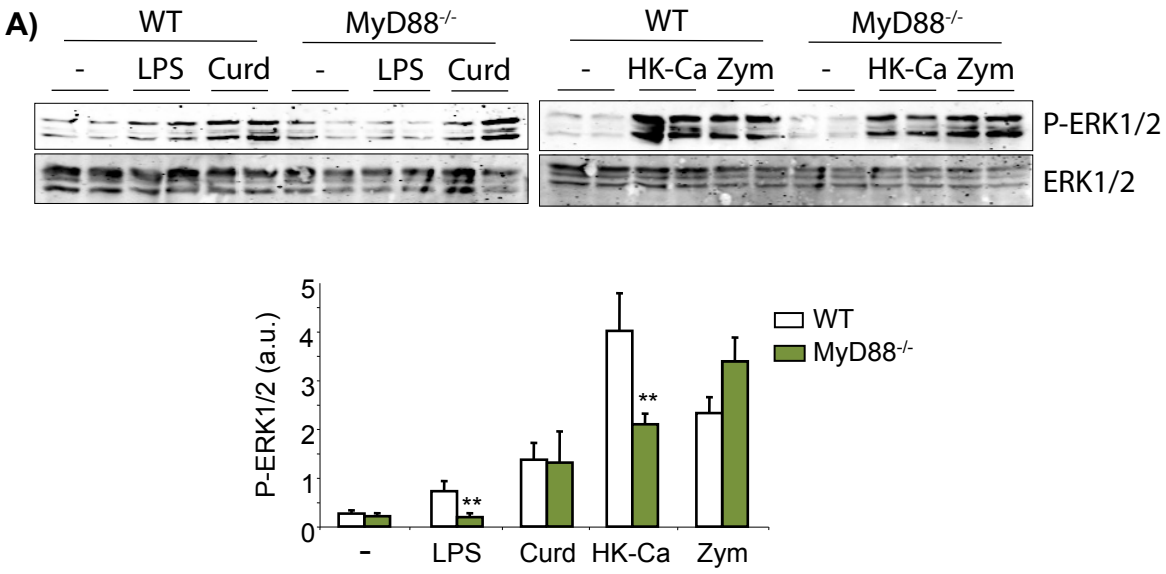

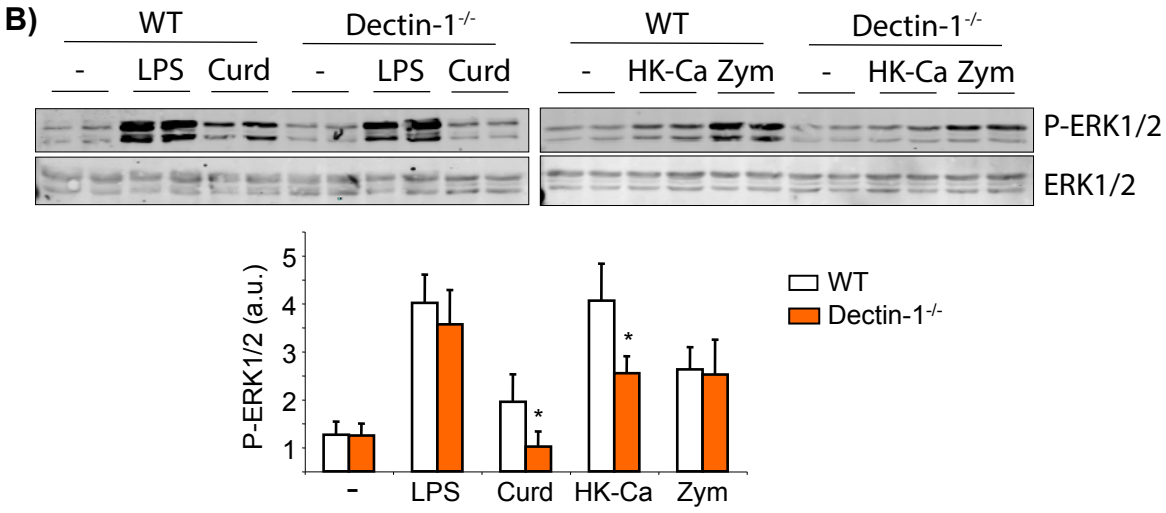

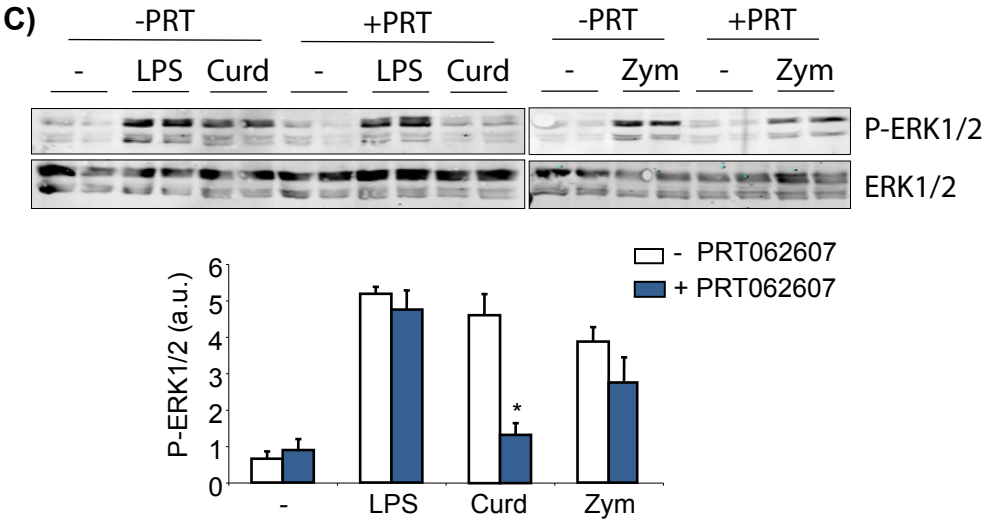

Figure R-1. Curdlan specifically activates Dectin-1 signalling in BMDM. A) BMDM from WT and MyD88$^{-/-}$ or **B)** Dectin1$^{-/-}$ mice or **C)** BMDM from WT mice incubated for 1 h with DMSO or PRT062607, were stimulated with 100 ng/ml of LPS for 30 min, 10 µg/ml of Curdlan for 1 h, 10^6 CFU/ml of HK-Ca for 1 h or 50 µg/ml Zymosan for 1h. Cell lysates (30 µg) were immunoblotted using the indicated antibodies. All immunoblots were quantified by densitometry. Graphs below immunoblots show data mean ± SEM from one representative experiment from two experiments with similar results. *$P \leq 0.05$ and **$P \leq 0.01$ relative to WT control. Parametric, unpaired t-test.

In WT and MyD88$^{-/-}$ BMDM, we found that the activation of ERK1/2 was not affected by the lack of MyD88 in response to Curdlan or Zymosan while in response to HK-Ca this was partially impaired (Fig. R-1A). On the other hand, ERK1/2 phosphorylation was blocked when MyD88$^{-/-}$ BMDM were stimulated with LPS (Fig. R-1A). When using Dectin-1$^{-/-}$ BMDM, we found that in response to Curdlan, the activation of ERK1/2 was inhibited, while ERK1/2 phosphorylation was only partially affected in response to HK-Ca compared to WT BMDM. In contrast, LPS and Zymosan activate ERK1/2 to a similar extent in both WT and Dectin-1$^{-/-}$ BMDM, indicating that these stimuli were ligands of TLR receptors (Fig. R-1B). When we incubated WT BMDM with the compound PRT062607 before stimulation, we observed that in response to Curdlan, ERK1/2 phosphorylation was blocked; however, ERK1/2 phosphorylation in response to Zymosan and LPS was not affected by the incubation with the Syk inhibitor (Fig. R-1C).

In MyD88$^{-/-}$ cells the TLR signalling is blocked, whereas in Dectin-1$^{-/-}$ BMDM and in WT BMDM treated with compound PRT062607 the CLR pathways are blocked. Therefore, these experiments confirm the specificity of Curdlan activating the Dectin-1-Syk-ERK1/2 signalling, and show that Zymosan can cause ERK1/2 activation via both TLR and Detin-1 receptor. We then proceeded to study Dectin-1 signalling pathway in more detail in BMDM stimulated with Curdlan.

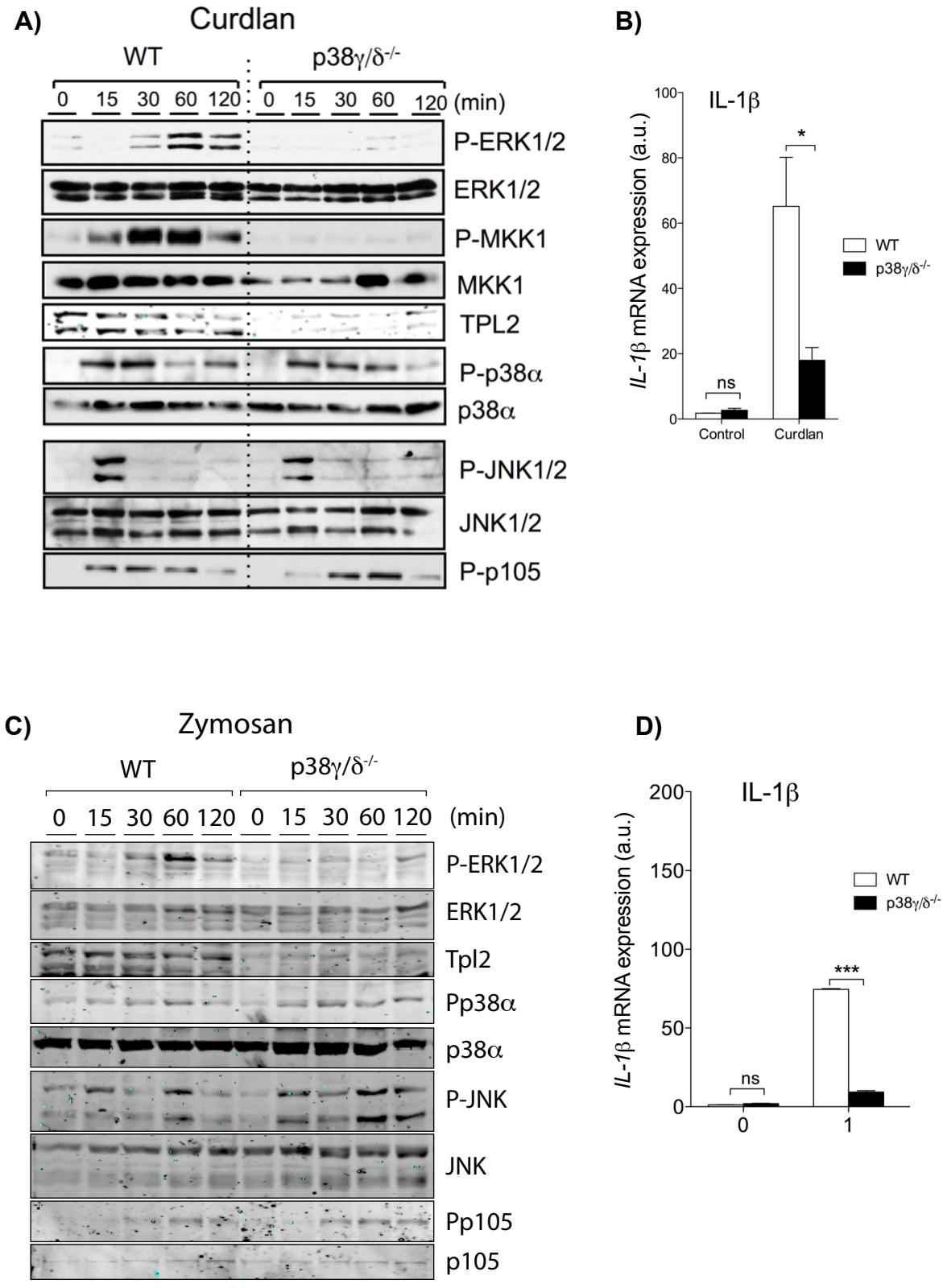

Figure R-2. p38γ/p38δ deletion blocks Dectin-1 signalling in BMDM.

A, B) BMDM from WT and p38γ/δ$^{-/-}$ mice were stimulated with 10 µg/ml of Curdlan for the indicated times. **A)** Cell lysates (30 µg) were immunoblotted with the indicated antibodies. Representative immunoblot from three independent experiments are shown.

B) Relative mRNA expression was determined by qPCR for *IL1β* at 0 or 1 h post-stimulation. Results were normalized to *β-actin* and fold induction was calculated relative to WT expression at 0 h. Data shows mean ± SEM from one representative experiment with similar results of two in triplicate. ns = non-significant, **P*≤0.05 relative to WT control. Parametric, unpaired t-test. **C, D)** BMDM from WT and p38γ/δ$^{-/-}$ mice were stimulated with 50 μg/ml of Zymosan for the indicated times. **C)** Cell lysates (30 μg) were immunoblotted with the indicated antibodies. Representative immunoblot from three independent experiments are shown. **D)** Relative mRNA expression was determined by qPCR for *IL1β* at 0 or 1 h post-stimulation. Results were normalized to *β-actin* and fold induction was calculated relative to WT expression at 0 h. Data shows mean ± SEM from one representative experiment with similar results of two in triplicate. ns = non-significant, **P*≤0.05 relative to WT control. Parametric, unpaired t-test.

ERK1/2 phosphorylation and *IL1β* mRNA expression was markedly reduced in p38γ/δ$^{-/-}$ BMDM as compared to WT after either Curdlan or Zymosan stimulation (Fig. R-2). Zymosan was used in these experiments as control. We observed that the activation of MKK1, which phosphorylates ERK1/2, was also blocked after Curdlan stimulation; moreover, Tpl2 that is an upstream activator of MKK1, had lower protein levels in p38γ/δ$^{-/-}$ compared to WT BMDM. In contrast, loss of p38γ/p38δ did not have a significant effect in the transient levels of JNK, p105 phosphorylation (NF-κB) or p38α after Curdlan stimulation (Fig. R-2A). When stimulating WT and p38γ/δ$^{-/-}$ BMDM with Zymosan we observed similar results to Curdlan (Fig. R-2A). ERK1/2 phosphorylation was blocked in p38γ/δ$^{-/-}$ BMDM, observing again lower protein levels of its activator Tpl2. Also, transient phosphorylation of p105 and p38α remained unaffected by the absence of p38γ/p38δ. In contrast, JNK phosphorylation was found increased in the absence of p38γ/p38δ with Zymosan stimulated BMDM, which was not observed in p38γ/δ$^{-/-}$ BMDM stimulated with Curdlan (Fig. R-2A and C). These results show that Curdlan activates Dectin-1-Syk-Tpl2-ERK1/2 signalling pathway inducing *IL-1β* mRNA production and the absence of p38γ/p38δ blocks this signalling pathway.

4.1.2 TAK1-IKKβ-TPL2 are essential for Dectin-1 signalling in macrophages

We have previously reported that p38γ/δ$^{-/-}$ BMDM did not express the upstream ERK1/2 activator Tpl2 (Risco et al., 2012). Our results suggest that ERK1/2 activation after Dectin-1 stimulation could be mediated by Tpl2.

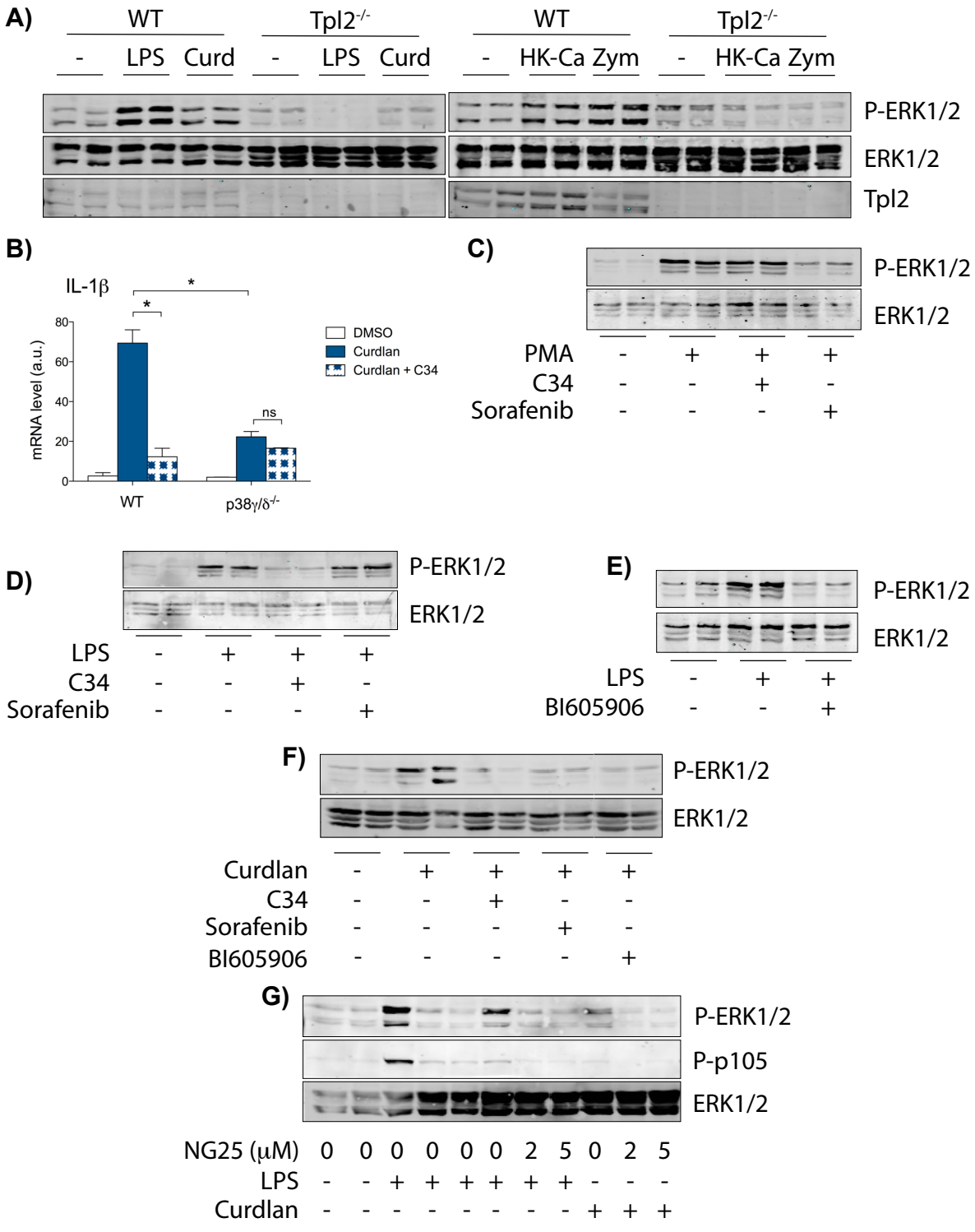

Figure R-3. Dectin-1 signalling pathway in BMDM. A) BMDM from WT and Tpl2$^{-/-}$ mice were stimulated with 100 ng/ml of LPS for 30 min, 10 µg/ml of Curdlan for 1 h, 10^6 CFU/ml of HK-Ca for 1 h or 50 µg/ml Zymosan for 1h. Cell lysates (30 µg) were immunoblotted with the indicated antibodies. Representative immunoblot from two independent experiments are shown. **B)** BMDM from WT mice were incubated for 1 h with DMSO or 5 µM C34 and then stimulated with 10 µg/ml of Curdlan for 1 h. Relative mRNA expression was determined by qPCR for IL1β. Results were normalized to *β-actin* and fold induction was calculated relative to WT expression at 0 h. Data shown mean ± SEM from one representative experiment with similar results. ns = non-significant and $*P \leq 0.05$, relative to WT control. Figure shows the analysis of one representative experiment from two experiments in duplicate. **C, D, E, F, G)** BMDM from WT mice were incubated for 1 h with DMSO, 5 µM C34, 10 µM Sorafenib, 10 µM BI605906 or NG25 at the indicated concentrations and then stimulated with 100 ng/ml of phorbol 12-myristate 13-acetate (PMA) for 10 min, 100 ng/ml of LPS for 30 min or 10 µg/ml of Curdlan for 1 h. Cell lysates (30 µg) were immunoblotted with the indicated antibodies. Representative immunoblot from two independent experiments are shown.

To investigate this in more depth we used Tpl2$^{-/-}$ BMDM. In these cells ERK1/2 activation was blocked in response to Curdlan, HK-Ca, Zymosan and LPS, compare with WT BMDM (Fig. R-3A). This confirmed that Tpl2 mediates ERK1/2 activation downstream of Dectin-1 receptor. Consistently, we found that pharmacological blockade of Tpl2 by the compound C34 (Green et al., 2007; Wu et al., 2009) also significantly reduced *IL-1β* mRNA production in WT BMDM but not in p38γ/δ$^{-/-}$ (Fig. R-3B).

It has been previously described that Raf-1 is activated by Dectin-1 receptor in T cells and that, in macrophages, Dectin-1 activates ERK1/2 through CARD9/RasGRF1/H-Ras complex (Gringhuis et al., 2009; Jia et al., 2014). We confirmed that Raf-1 was involved in the activation of ERK1/2 by Curdlan using the Raf-1 inhibitor Sorafenib (Bay 43-9006) (Lyons et al., 2001) in parallel with C34. We examined if the inhibitors were working accordingly in WT BMDM. We first stimulated WT BMDM with PMA, which is a Raf-dependent (Wellbrock et al., 2004) and Tpl2-independent

stimulus (Beinke and Ley, 2004). We observed that when WT BMDM were stimulated with PMA, ERK1/2 phosphorylation was inhibited by Sorafenib, but not C34 (Fig. R-3C). Secondly, we used LPS which activates ERK1/2 in a Tpl2-depending and Raf-independent manner in WT BMDM. Under LPS stimulation, Sorafenib did not inhibit the activation of ERK1/2, while C34 blocked LPS-induces ERK1/2 phosphorylation (Fig. R-3D). Finally, both inhibitors blocked ERK1/2 activation after stimulation with Curdlan (Fig. R-3F). Our results indicate that in response to Curdlan, ERK1/2 can be activated via Dectin-1-Tpl2 and Dectin-1-Raf-1 signalling.

Tpl2 activation is regulated by IKKβ, which phosphorylates Tpl2 and p105 NF-κB1 in TLR-stimulated macrophages (Ben-Addi et al., 2014; Gantke et al., 2011; Roget et al., 2012). TAK1 is also required for the activation of IKKβ that it is found in the canonical IKK complex leading to Tpl2-MKK1-ERK1/2 activation (Cohen, 2014). Therefore, to investigate whether TAK1-IKK signalling pathway was activated when triggering Dectin-1, we pre-treated WT BMDM with specific TAK1 inhibitor NG25 (Dzamko et al., 2012) or specific IKKβ inhibitor BI605906 (Clark et al., 2011). Both inhibitors were first tested pre-treating WT BMDM with them and then stimulating with the TLR4 ligand, LPS (Cohen, 2014). We observed that LPS-induced ERK1/2 phosphorylation was inhibited by both BI605906 and NG25 (Fig. R-3E and G). Additionally, NG25 blocked p105 NF-κB1 phosphorylation in response to LPS (Fig. R-3G). When we stimulated WT BMDM with Curdlan, after pre-treating the cells with BI605906 or with NG25, we observed that ERK1/2 was not phosphorylated (Fig. R-3F and G). All our data suggest that p38γ/p38δ regulate Dectin-1 pathway by modulating Tpl2 protein levels. We propose a new signalling pathway in which Dectin-1 activates MKK1-ERK1/2 through both, TAK-IKKβ-Tpl2 and Ras-Raf-1.

Our results indicate that Dectin-1 signalling pathway in macrophages activates Bcl10/MALT1/CARD9 and CARD9/RasGRF1/H-Ras complex. The first complex will activate the IRAK family proteins

interacting with TRAF6 and inducing the activation of the TAK1-IKKβ-Tpl2 signalling, while CARD9/RasGRF1/H-Ras complex activates Raf-1 signalling. Both signalling converges in the activation of MAPKs and NF-κB signalling inducing the transcription of cytokines (Fig. R-4).

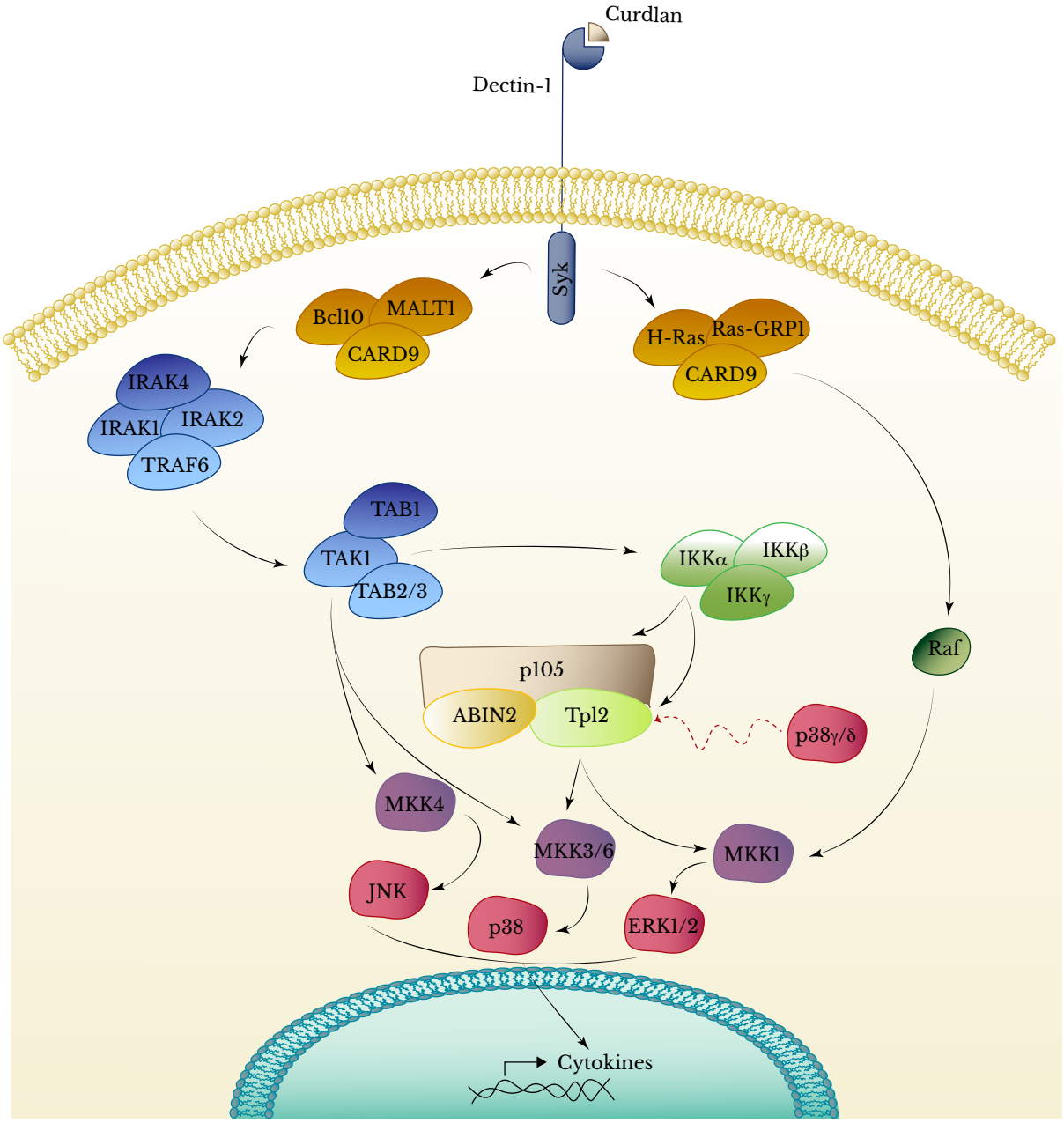

Figure R-4. Schematic representation of Dectin-1 signalling pathway. Dectin-1 when activated, recruits Syk, which induces the recruitment of CARD9/RasGRF1/H-Ras complex for Raf-MKK1-ERK1/2 activation. CARD9/Bcl10/MALT1 complex, is also recruited by Syk, activates IRAK family that interacts with TRAF6 to activate the TAK1/TAB1/2/3 complex. The activation of TAK1 activates IKK-Tpl2-MKK1-ERK1/2 converging with Raf-MKK1-ERK1/2 pathway. p38γ/p38δ regulate the steady-state levels

of Tpl2, which is found forming the Tpl2/ABIN2/p105 complex.

4.2 Chapter 2. Regulation of *Tpl2/ABIN2 protein levels by* p38γ and p38δ.

Tpl2 is a MAP3K that forms a ternary complex with the proteins p105 NF-κB1, an NF-kB inhibitory protein and the precursor of the NF-κB p50 subunit, and ABIN2 (Beinke et al., 2003; Lang et al., 2004). This complex is a key component in the signalling pathway of TLR4. It has been thoroughly studied because its importance in cytokine and chemokine production. This complex is essential in innate immune response and is involved in many autoimmune diseases (Dumitru et al., 2000; Gantke et al., 2011; Xu et al., 2018).

Tpl2 and ABIN2 are very unstable proteins and are continuously degraded by the proteasome. All Tpl2 and ABIN2 in the cell are forming part of the Tpl2/ABIN2/p105 ternary complex at 1:1 stoichiometry, while only a small fraction of total p105 NF-κB1 in the cell is bound to the complex (Lang et al., 2004). We are interested in studying the molecular mechanism by which p38γ and p38δ regulate protein levels of Tpl2 and ABIN2 making this important complex inactive.

4.2.1 p38γ and p38δ regulate protein levels of Tpl2 and ABIN2.

Previous work in our laboratory showed that the absence of p38γ/p38δ reduced the protein levels of Tpl2 and ABIN2 in BMDM (Alsina-Beauchamp et al., 2018; Risco et al., 2012). The consequence is the loss of Tpl2/ABIN2/p105 complex in p38γ/δ$^{-/-}$ BMDM comparing with WT, and a lower production of cytokines. These results lead us to further study the molecular mechanism by which p38γ/p38δ regulate the protein levels of Tpl2 and ABIN2, and how general was this mechanism. We analysed the protein levels of Tpl2 and ABIN2 in different tissue and cells from WT and p38γ/δ$^{-/-}$ mice by inmunoblot. In all tissues, Tpl2 and ABIN2 had lower protein levels in p38γ/δ$^{-/-}$ than in WT mice (Fig. R-5A).

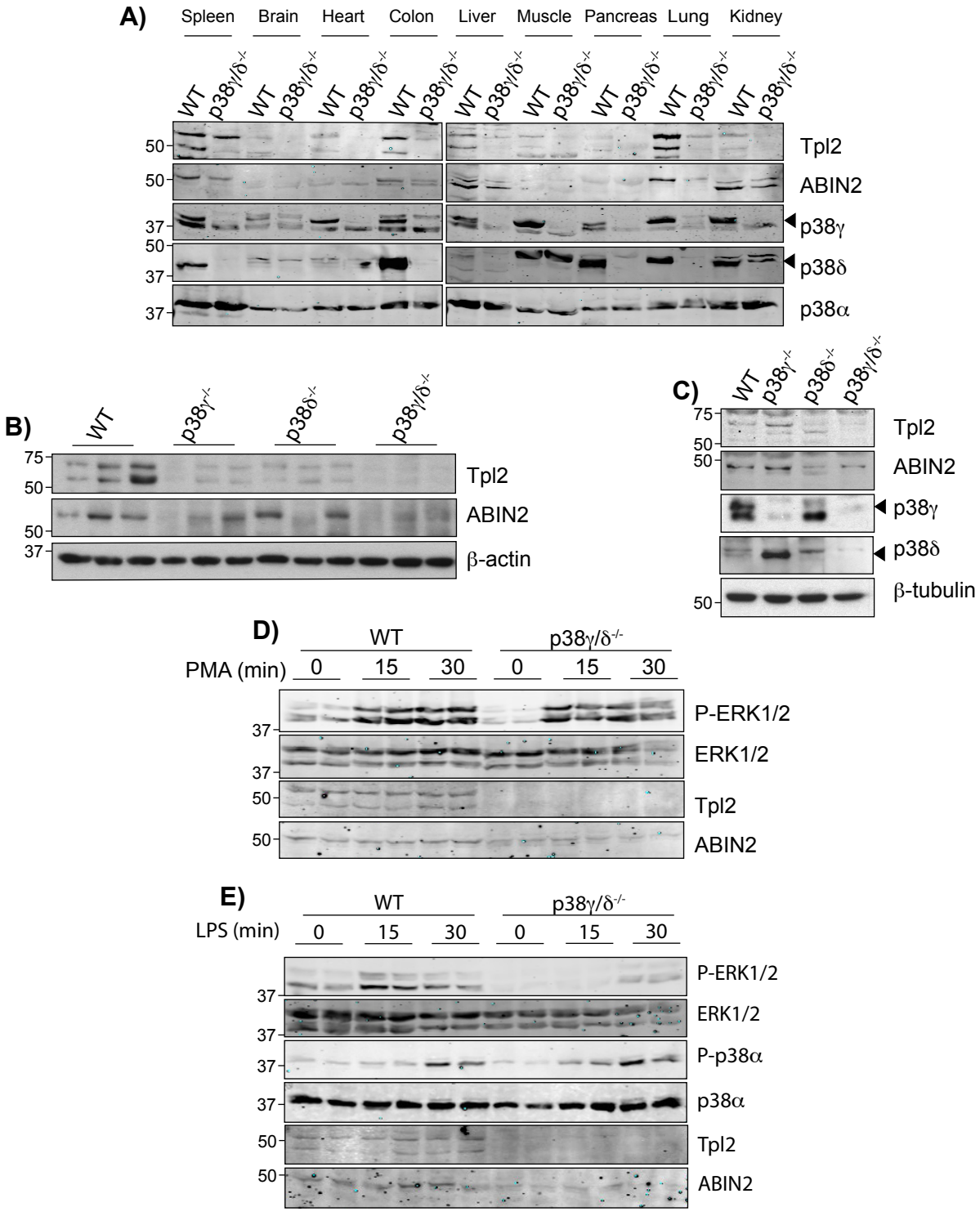

Figure R-5. p38γ and p38δ are needed to maintain Tpl2 and ABIN2 protein levels. A) WT and p38γ/δ$^{-/-}$ tissue lysates (50 µg) from the indicated organs were immunoblotted using the indicated antibodies. **B, C)** WT, p38γ$^{-/-}$, p38δ$^{-/-}$ and p38γ/δ$^{-/-}$ cell lysates (50 µg) from **B)** peritoneal macrophages or **C)** MEFs, were immunoblotted with the indicated antibodies. **D, E)** WT and p38γ/δ$^{-/-}$ MEF were stimulated with **D)** 100 ng/ml of PMA or **E)** 100 ng/ml of LPS for the indicated times and 50 µg of cell lysates were immunoblotted

with the indicated antibodies. The figure shows representative immunoblots.

We examined Tpl2 and ABIN2 protein levels in different cells types like peritoneal macrophages and immortalized MEFs. In peritoneal macrophages, we found that comparing with WT (Fig. R-5B), p38$\gamma^{-/-}$ and p38$\delta^{-/-}$ single knock out macrophages had less protein levels of Tpl2, whereas p38$\gamma/\delta^{-/-}$ macrophages had a severe reduction of Tpl2 and ABIN2 protein levels compared to WT, p38$\gamma^{-/-}$ and p38$\delta^{-/-}$ peritoneal macrophages (Fig. R-5B). In immortalized MEF cells, Tpl2 protein levels were similarly expressed in WT, p38$\gamma^{-/-}$ and p38$\delta^{-/-}$ MEF, while the loss of both p38γ/p38δ, induced a severe reduction of Tpl2 protein levels. On the other hand, ABIN2 showed similar protein levels in WT and p38$\gamma^{-/-}$ MEF and reduced protein levels in p38$\delta^{-/-}$ and p38$\gamma/\delta^{-/-}$ MEF (Fig. R-5C).

Next, we wanted to check if ERK1/2 activation triggered by TLR4 activation was affected in p38$\gamma/\delta^{-/-}$ MEF. WT and p38$\gamma/\delta^{-/-}$ MEF were stimulated with either LPS or PMA, using this second stimuli as control. PMA stimulation leads to the phosphorylation of ERK1/2 in a Raf-dependent and Tpl2-independent manner (Wellbrock et al., 2004). Our results show that ERK1/2 was transiently phosphorylated in both WT and p38$\gamma/\delta^{-/-}$ MEF treated with PMA, indicating that ERK1/2 could be phosphorylated in p38$\gamma/\delta^{-/-}$ cells (Fig. R-5D). LPS is known to activate TLR4 signalling and induce the phosphorylation of ERK1/2 in a Tpl2-dependet and Raf-independent manner (Beinke and Ley, 2004). We stimulated WT and p38$\gamma/\delta^{-/-}$ MEF with TLR4-ligand LPS and observed that ERK1/2 in p38$\gamma/\delta^{-/-}$ MEF was not phosphorylated. In contrast, LPS caused ERK1/2 phosphorylation in WT MEFs (Fig. R-5E). To confirm LPS activation of other MAPKs in p38$\gamma/\delta^{-/-}$ MEF we analysed p38α phosphorylation. p38α was phosphorylated in both WT and p38$\gamma/\delta^{-/-}$ MEF after LPS stimulation (Fig. R-5E). Tpl2 and ABIN2 protein levels were severely reduced in p38$\gamma/\delta^{-/-}$ MEF in comparison to WT MEFs for both experiments (Fig. R-5D and E).

These results show that the absence of p38γ/p38δ, reduces the protein levels of both Tpl2 and ABIN2 in all tissues and cell types of the mice making TLR4-Tpl2-ERK1/2 signalling pathway inactive.

4.2.2 Tpl2 and ABIN2 mRNA levels are not affected by p38γ/δ deletion.

We found that Tpl2 and ABIN2 protein levels were decreased in p38γ/δ$^{-/-}$ mice when compared to WT, and that ERK1/2 phosphorylation was impaired in p38γ/δ$^{-/-}$ cells. We then wanted to elucidate the molecular mechanism by with p38γ/p38δ cause these effects and studied if the lack of p38γ/p38δ decreased *Tpl2* and *ABIN2* mRNA levels.

First, we analysed *Tpl2* and *ABIN2* total mRNA levels in BMDM, peritoneal macrophages and MEF. The lack of p38γ/p38δ did not affect either *Tpl2* or *ABIN2* mRNA levels regardless of cell type (Fig. R-6A to F). mRNAs are transcribed in the nucleus and then translocated to the cytosol. To test if the absence of p38γ/p38δ inhibited specific mRNA transport, we separated WT and p38γ/δ$^{-/-}$ BMDM lysate into cytosol and nucleus fraction and quantified *Tpl2* and *ABIN2* mRNA by qPCR. In the nucleus of p38γ/δ$^{-/-}$ BMDM the levels of *Tpl2* mRNA were higher than in WT BMDM, while *ABIN2* mRNA was similar in both WT and p38γ/δ$^{-/-}$ BMDM (Fig. R-6G and H). In the cytosol fraction *Tpl2* and *ABIN2* mRNA levels were similar in both WT and p38γ/δ$^{-/-}$ BMDM (Fig. R-6G and H). Specific proteins from the cytosol and nucleus fraction were immunoblotted to confirm no cross contamination between the fractions. Lamin-β, which is an inner nuclear membrane protein, was found in the nucleal fractions, while the cytoplasmic cytoskeleton protein, α-tubulin, was in the cytosolic fractions (Fig. R-6E).

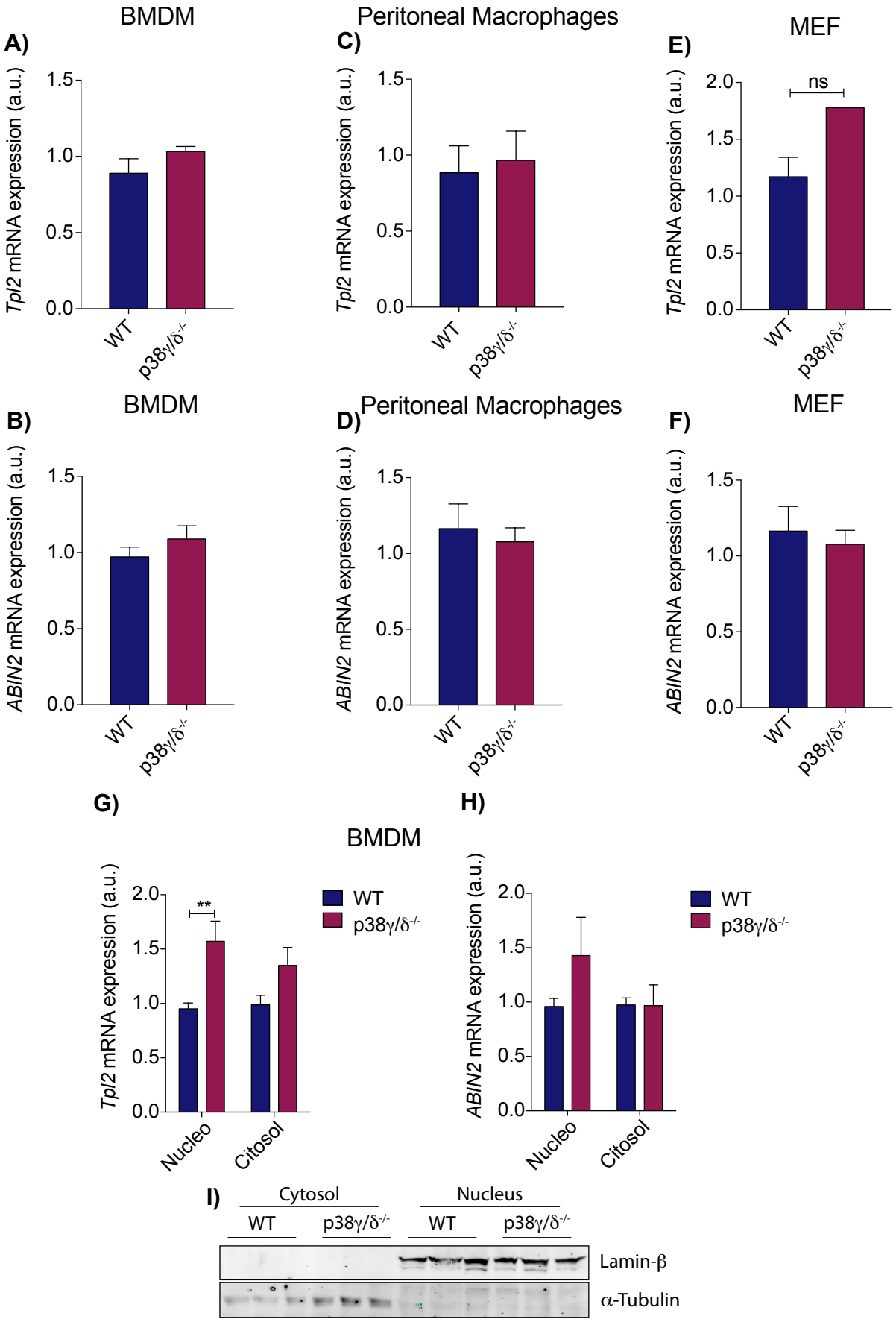
A)
BMDM
Tpl2 mRNA expression (a.u.)
1.5
1.0
0.5
0.0
WT
p38γ/δ-/-
C)
Peritoneal Macrophages
Tpl2 mRNA expression (a.u.)
1.5
1.0
0.5
0.0
WT
p38γ/δ-/-
E)
MEF
Tpl2 mRNA expression (a.u.)
2.0
1.5
1.0
0.5
0.0
ns
WT
p38γ/δ-/-
B)
BMDM
ABIN2 mRNA expression (a.u.)
1.5
1.0
0.5
0.0
WT
p38γ/δ-/-
D)
Peritoneal Macrophages
ABIN2 mRNA expression (a.u.)
1.5
1.0
0.5
0.0
WT
p38γ/δ-/-
F)
MEF
ABIN2 mRNA expression (a.u.)
1.5
1.0
0.5
0.0
WT
p38γ/δ-/-
G)
BMDM
Tpl2 mRNA expression (a.u.)
2.0
1.5
1.0
0.5
0.0
**
WT
p38γ/δ-/-
Nucleo
Citosol
H)
ABIN2 mRNA expression (a.u.)
2.0
1.5
1.0
0.5
0.0
WT
p38γ/δ-/-
Nucleo
Citosol
I)
Cytosol
Nucleus
WT
p38γ/δ-/-
WT
p38γ/δ-/-
Lamin-β
α-Tubulin

Figure R-6. p38γ and p38δ do not regulate Tpl2 and ABIN2 mRNA levels. mRNA expression was determined by qPCR for *Tpl2* and *ABIN2*. Results were normalized to *β-actin* and fold induction was calculated relative to WT expression. Data shown mean ± SEM from one representative experiment of 2 or 3 in triplicate with similar results except for peritoneal macrophages. Total mRNA levels from WT and p38γ/δ$^{-/-}$ **A, B)** BMDM; **C, D)** peritoneal macrophages (n = 3 - 4); **E, F)** MEF. **G, H)** Cytosolic and nuclear mRNA expression levels were determined for *Tpl2* and *ABIN2* as indicated before, from WT and p38γ/δ$^{-/-}$ BMDM. Data shown mean ± SEM from one representative experiment of three with similar results. The *p*-value was determined by two-tailed Student´s t-test: ***P*≤0.01 relative to WT. **I)** Fraction lysates (50 µg) were immunoblotted with the indicated antibodies.

Our results indicate that the decrease of Tpl2 and ABIN2 protein levels in p38γ/δ$^{-/-}$ cells were not due to either a decrease of *Tpl2* or *ABIN2* mRNA levels, indicating that the mRNA synthesis and degradation were similar to those in WT cells, or to a defect in the mRNA transport from the nucleus to the cytosol.

4.2.3 p38γ and p38δ interact with Tpl2.

Tpl2 and ABIN2 are stable proteins in the cell when they are forming the ternary complex Tpl2/ABIN2/p105. It has been described that Tpl2 needs both ABIN2 and p105 to maintain its stability (Beinke and Ley, 2004; Beinke et al., 2003; Lang et al., 2004), while ABIN2 stability has been shown to also depend on Tpl2 (Sriskantharajah et al., 2014). We investigated if p38γ/p38δ were interacting with the Tpl2/ABIN2/p105 complex through Tp2 and/or ABIN2 to maintain their stability. We first used Raw264.7 cell line and separated protein complexes by their molecular weight using a gel filtration chromatography. We observe that Tpl2, ABIN2 and p105 co-elute with p38δ at ~669 kDa, while the band of p38γ was barely detected at ~669 KDa fraction and was mainly found between 29 and 66 KDa, which its near its own molecular weight at 38 KDa

(Fig. R-7).

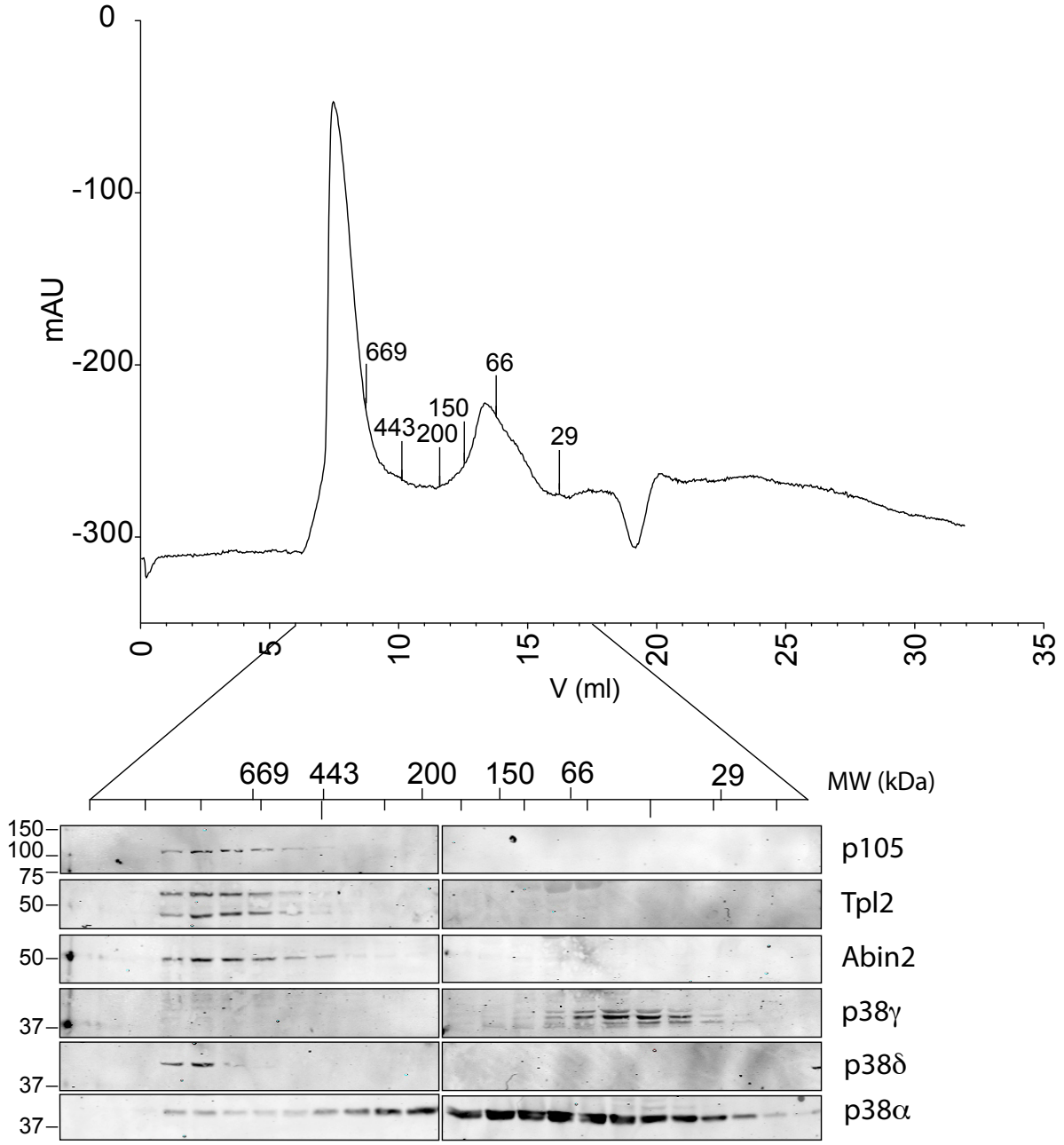

Figure R-7. p38δ co-elutes with Tpl2, ABIN2 and p105. Raw264.7 cell lysates (1 mg) were loaded into the gel filtration chromatography. Upper panel shows the mAU (absorbance unit of UV) of the sample while collecting 0.5 ml/fraction. Graph shows the elution of fixed reference molecular weight markers: 669, 443, 200, 150, 66 and 29 KDa. The lower panel, 50 µl of the indicated fractions were immunoblotted with the indicated antibodies.

We next examined whether p38γ/p38δ were associating to Tpl2/ABIN2/p105 complex. For this, we transfected GST-Tpl2, Flag-

ABIN2 and HA-p105, with HA-p38γ or Myc-p38δ, and then isolated the complex by pull-down assay. We found that pulling-down GST-Tpl2, p38γ or p38δ were bound to the Tpl2/ABIN2/p105 complex (Fig. R-8A and B). Next, to identify which proteins of the Tpl2/ABIN2/p105 complex was directly interacting with either p38γ or p38δ, we transfected GST-tagged versions of Tpl2, ABIN2 or p105 in separate with HA-p38γ and Myc-p38δ. We observed that both p38γ and p38δ interacted with Tpl2 (Fig. R-8A and B), suggesting the binding of the p38MAPKs to the Tpl2/ABIN2/p105 complex was through Tpl2.

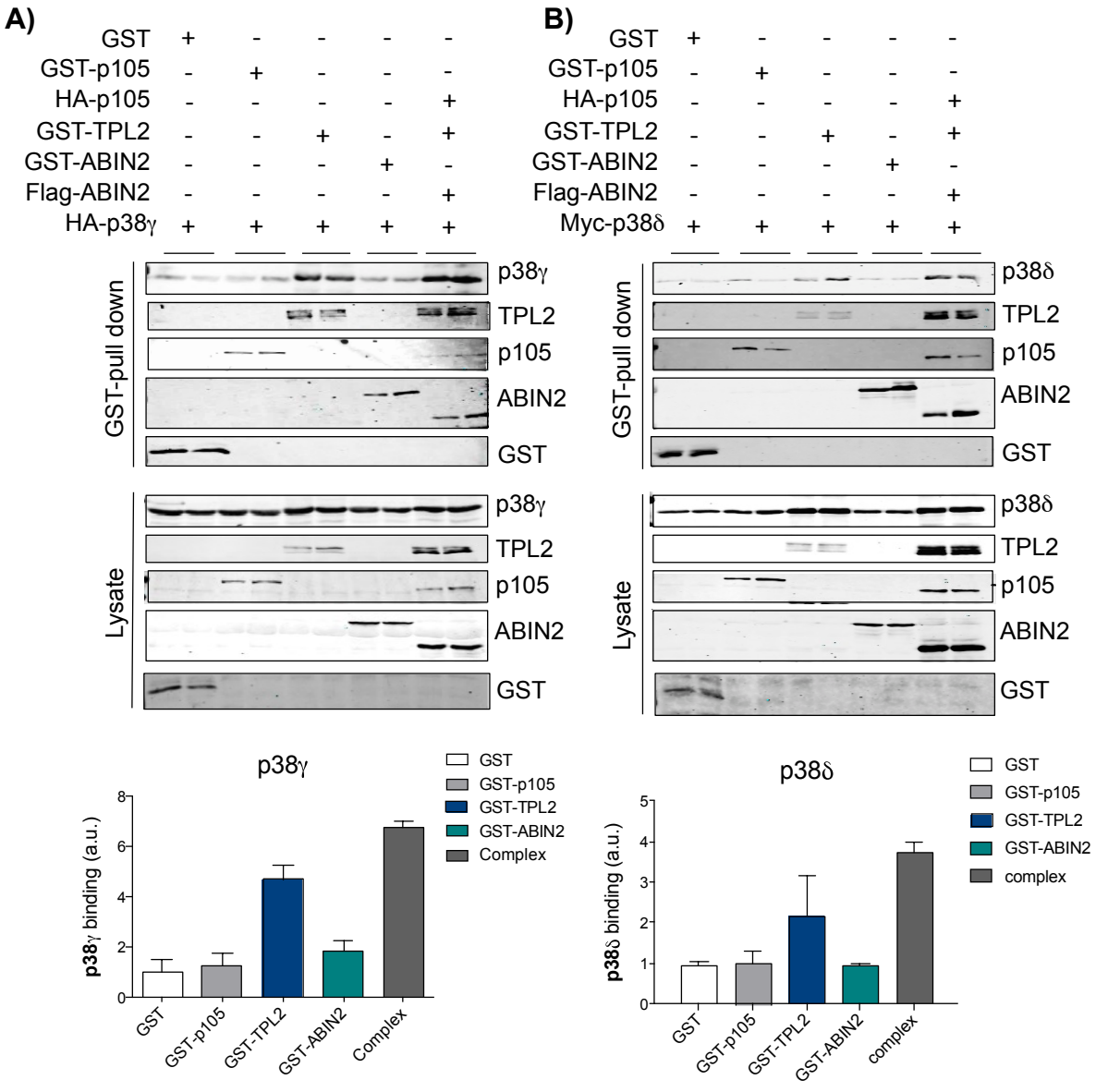

Figure R-8. p38γ and p38δ interact with Tpl2/ABIN2/p105 complex through Tpl2. A, B) HEK293 cells were transfected with plasmids that express the indicated proteins. GST fusion proteins were pulled-down from 500 µg of lysates. The Pellets and 30 µg protein lysates (for loading control) were immunoblotted with the indicated antibodies (upper panel). Representative immunoblots are shown. Bands from 2 experiments were quantified using Odyssey infrared imaging system (bottom panel) data show mean ± SEM from two experiments in duplicate. These experiments were performed in collaboration with Diego González-Romero.

4.2.4 Tpl2 stability depends on p38γ and p38δ.

To study if Tpl2 and ABIN2 stability is regulated by p38γ/p38δ, we analysed the stability of endogenous Tpl2 and ABIN2 from WT and p38γ/δ$^{-/-}$ MEF and BMDM in cycloheximide chased experiment. Although Tpl2 and ABIN2 protein levels were very low in p38γ/δ$^{-/-}$ cells, there was still enough for quantification in MEF; however, in BMDM we were unable to quantify ABIN2 protein. We observed that in MEF and BMDM, Tpl2 was degraded at a higher rate in p38γ/δ$^{-/-}$ than in WT cells (Fig. R-9A, D and E). When measuring ABIN2 stability in MEFs we found no statistical difference between WT and p38γ/δ$^{-/-}$ cell (Fig. R-9B and D). We immunoblotted for p38α as control and observed that its degradation rate in WT and p38γ/δ$^{-/-}$ cells was similar (Fig. R-9C, D and F). These results suggest that p38γ/p38δ were needed to maintain endogenous Tpl2 stability, but not the stability of ABIN2 in MEF.

To study Tpl2 and ABIN2 stability in more depth, we transfected GST-Tpl2 or GST-ABIN2 in WT and p38γ/δ$^{-/-}$ MEFs. First, we performed metabolic labelling with ^{35}S-Met/Cys and pull-chased GST-Tpl2 and GST-ABIN2. We observed that GST-Tpl2 had a faster decreased rate in p38γ/δ$^{-/-}$ than in WT MEF, while GST-ABIN2 had the same decrease in both p38γ/δ$^{-/-}$ than in WT MEF (Fig. R-10A, B). We then analysed the stability of GST-Tpl2 and GST-ABIN2 transfected in WT, p38γ$^{-/-}$, p38δ$^{-/-}$ and p38γ/δ$^{-/-}$ MEF and pull-chased after treatment with cycloheximide (CHX),

which inhibits protein translation. We observed that in p38γ$^{-/-}$, p38δ$^{-/-}$ and p38γ/δ$^{-/-}$ MEF, GST-Tpl2 was degraded at a higher rate than in WT MEF, while GST-ABIN2 was degraded at the same rate in all conditions (Fig. R-11A, B).

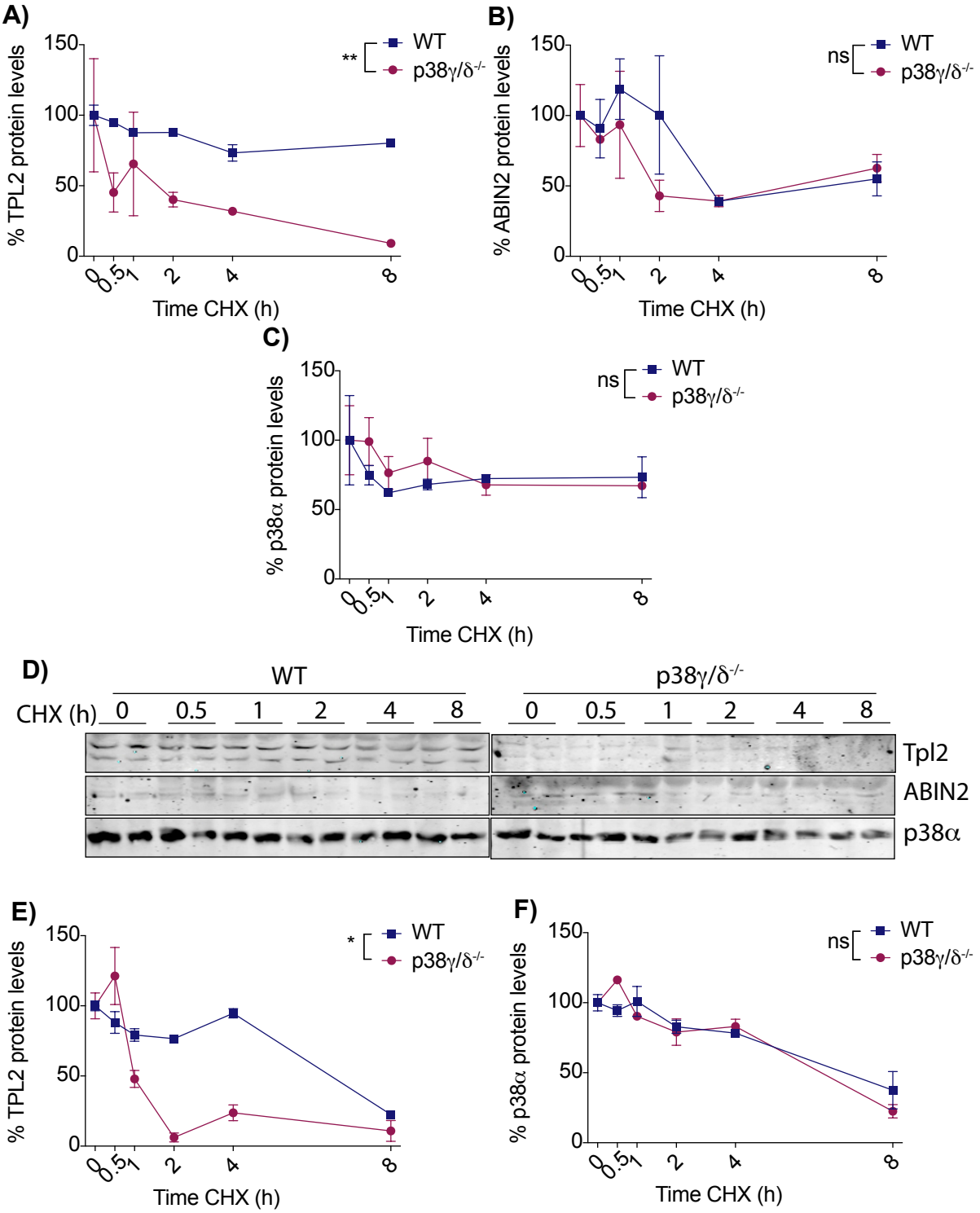

Figure R-9. p38γ and p38δ regulate endogenous Tpl2 protein stability. WT and p38γ/δ$^{-/-}$ cells were incubated with 100 ng/ml of CHX for the indicated time. Cell lysates were immunoblotted and quantified by densitometry. **A, B, C)** Relative protein levels (% relative to protein levels at 0 h) from MEF cells, **D)** Representative immunoblots of the indicated proteins from MEF. **E, F)** Relative protein levels (% relative to protein levels at 0 h) from BMDM. Quantification shows protein levels % relative to protein levels at 0 h lysates. Data show mean ± SEM of one representative experiment of 2 in duplicate. *$P\leq$ 0.05 and **$P\leq$0.01, relative to WT control cells.

Both experiments indicate that the stability of Tpl2 is p38γ- and p38δ-dependent, whereas the stability of ABIN2 protein is p38γ- and p38δ-independent.

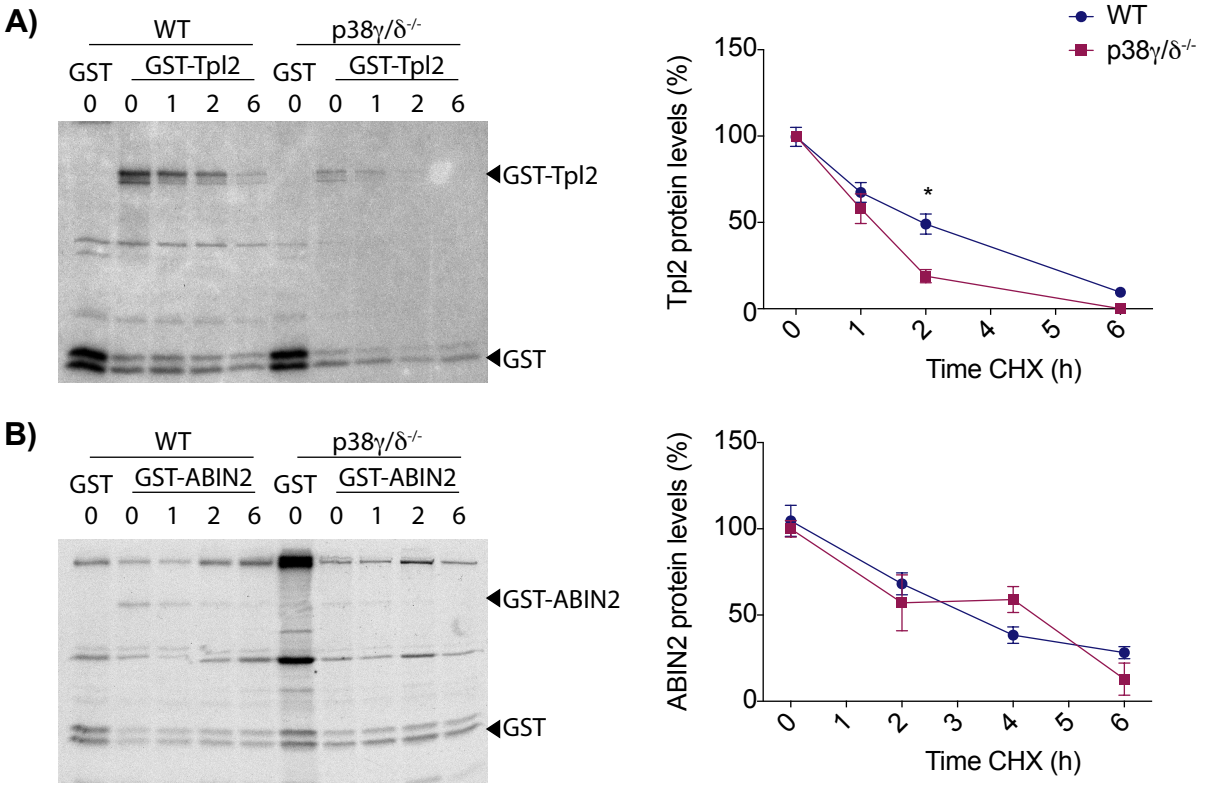

Figure R-10. p38γ and p38δ help to maintain Tpl2 protein stability in transfected cells. WT and p38γ/δ$^{-/-}$ MEF cells were transfected with **A)** GST-Tpl2 or **B)** GST-ABIN2, metabolically labelled with ^{35}S Met/Cys (30 min) and pulse-chase of the GST-proteins was performed at the indicated times. GST proteins were pulled-down, resolved in SDS-PAGE (10% acrylamide) and visualised by radiography. Bands were quantified by densitometry. Panel on the right show the protein levels quantification relative (%) to protein levels at 0 h. Dara show mean ± SEM of one representative experiment of 2 in

duplicate. *$P \leq 0.05$, relative to WT MEF.

Since p38γ/δ$^{-/-}$ cells have low protein levels of both Tpl2 and ABIN2, and previous work suggests that Tpl2 and ABIN2 regulate each other protein stability (Lang et al., 2004; Papoutsopoulou et al., 2006; Sriskantharajah et al., 2014), we investigated if Tpl2 stability was modulated by either p38γ/p38δ, or ABIN2, or both.

We then transfected p38γ/δ$^{-/-}$ MEF with GST-Tpl2 alone or with p38γ/p38δ or with ABIN2 and performed cycloheximide chased experiment. We observed that GST-Tpl2 was more stable when transfected with p38γ/p38δ than when it was transfected alone, although it did not reach those levels that when it was transfected with ABIN2 (Fig. R-11C). We also compared the stability of the over-expressed GST-Tpl2 in MEF WT, p38γ/δ$^{-/-}$, and p38γ/δ$^{-/-}$ transfected with ABIN2. We found that ABIN2 did not restore GST-Tpl2 to the WT levels (Fig. R-11C). Our results show that although ABIN2 stabilized GST-Tpl2 in p38γ/δ$^{-/-}$ cells, it was not enough to achieve the levels of GST-Tpl2 transfected in WT MEF. These results suggest that p38γ/p38δ are required for partial Tpl2 stabilization (Fig. R-11C).

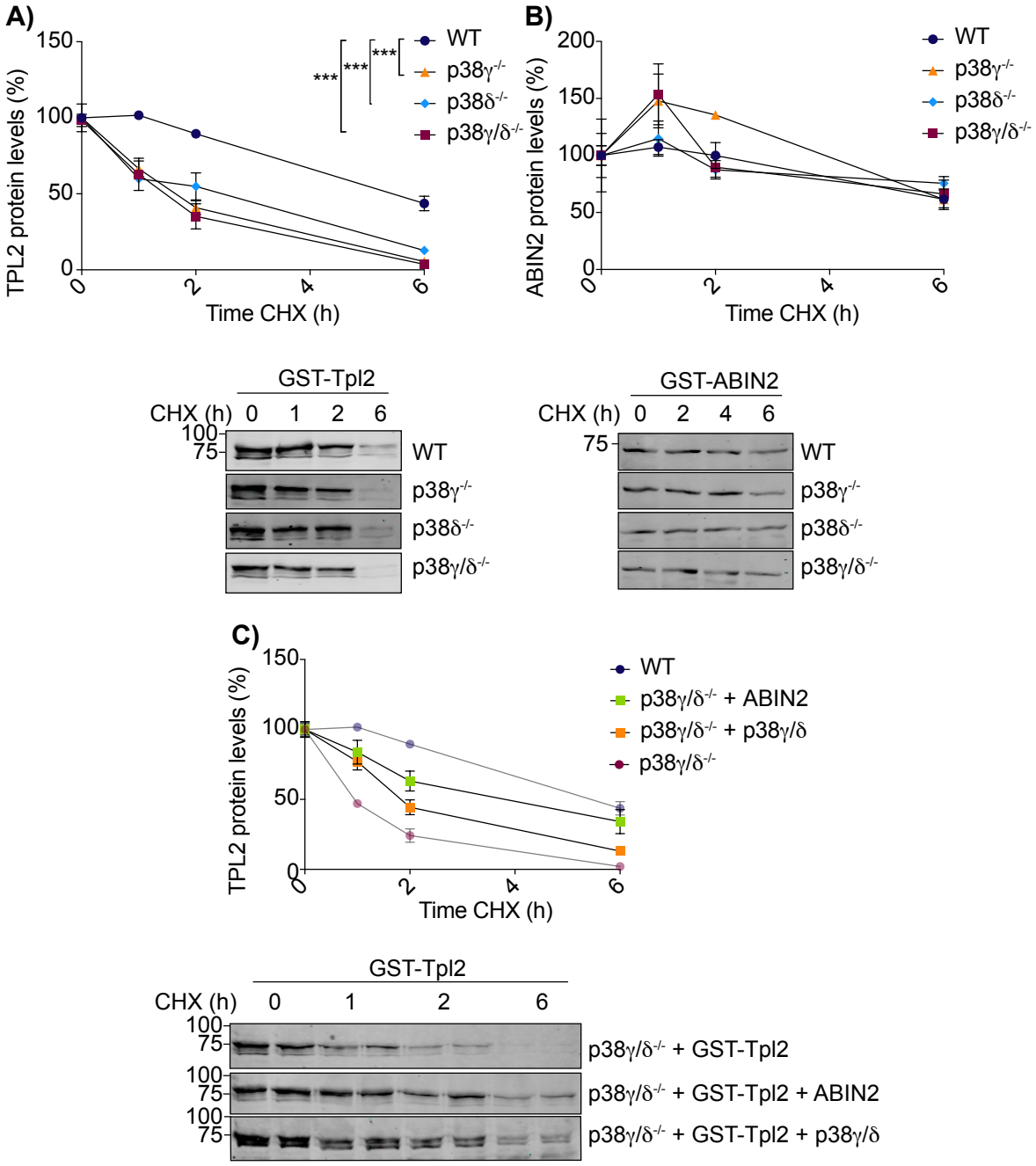

	1 h				2 h				6 h			
	WT	p38γ/δ-/- + ABIN2	p38γ/δ-/- + p38γ/δ	p38γ/δ-/-	WT	p38γ/δ-/- + ABIN2	p38γ/δ-/- + p38γ/δ	p38γ/δ-/-	WT	p38γ/δ-/- + ABIN2	p38γ/δ-/- + p38γ/δ	p38γ/δ-/-
WT		*	**	***		**	***	***		ns	**	***
p38γ/δ-/- + ABIN2			ns	**			ns	**			ns	*
p38γ/δ-/- + p38γ/δ				**				*				**
p38γ/δ-/-												

Figure R-11. p38γ, p38δ and ABIN2 control Tpl2 protein stability in MEF. A, B) WT, p38$\gamma^{-/-}$, p38$\delta^{-/-}$ and p38$\gamma/\delta^{-/-}$ MEF cells were transfected with **A)** GST-Tpl2 or **B)** GST-ABIN2 and then incubated with 100 ng/ml of CHX for the indicated times. Cell lysates were immunoblotted and quantified by densitometry. Upper panels show the quantification of protein levels relative (%) to protein at 0 h. Data are shown as mean ± SEM of one representative experiment of 2 in duplicate. *** $P \leq 0.001$. Representative immunoblots are shown (bottom panels) **C)** WT and p38$\gamma/\delta^{-/-}$ MEF cells were transfected with GST-Tpl2 alone or with the indicated plasmids, and then incubated with 100 ng/ml of cycloheximide for the indicated times. Cell lysates were immunoblotted and quantified by densitometry as indicated before. Data show mean ± SEM of one representative experiment of 2 in duplicate. * $P \leq 0.05$, ** $P \leq 0.01$, *** $P \leq 0.001$.

4.2.5 p38γ and p38δ do not affect Tpl2/ABIN2 degradation by proteasome.

Both Tpl2 and ABIN2, are continuously degraded by the proteasome and translated into the cytosol to maintain total protein levels for signalling (Gándara et al., 2003; Lang et al., 2004). In experiments blocking proteasome activity in ABIN2$^{-/-}$ BMDM it has been shown that the protein level of Tpl2 increases to the same extent than those in WT BMDM, indicating that the lack of ABIN2 in BMDM decreases the steady-state levels of Tpl2 (Papoutsopoulou et al., 2006).

Here we studied if the loss of Tpl2 and ABIN2 in p38$\gamma/\delta^{-/-}$ cells could be due to an increase in proteasome-mediated proteolysis. For this, WT and p38$\gamma/\delta^{-/-}$ BMDM and MEF were treated with the proteasome inhibitor MG132. Tpl2 protein levels increased in WT and p38$\gamma/\delta^{-/-}$ BMDM after 2 and 5 h of incubation with MG132, although the levels of Tpl2 in p38$\gamma/\delta^{-/-}$ BMDM incubated with MG132 did not reach those of WT (Fig. R-12A and D). After incubation for 5 h with the proteasome inhibitor MG132, the level of ABIN2 increases in WT but not in p38$\gamma/\delta^{-/-}$ BMDM (Fig. R-12B and D). As control, we measured p38α protein levels in WT and p38$\gamma/\delta^{-/-}$ BMDM after treatment with the proteasome inhibition and observed no difference between control and MG132-incubated BMDMs (Fig. R-12C

and D). These results show that the lack of p38γ/p38δ do not affect Tpl2 and ABIN2 degradation by proteasome and suggest that p38γ/p38δ might regulate Tpl2 and ABIN2 proteins synthesis.

We then tested if WT and p38γ/δ$^{-/-}$ MEF rendered similar results than those observed in BMDM. We incubated WT and p38γ/δ$^{-/-}$ MEF with MG132 and we observed a small increase of Tpl2 protein levels at 2 h post-incubation in WT MEF but not at 5 h. MG132-incubated p38γ/δ$^{-/-}$ MEF increased Tpl2 in a significantly manner at both 2 and 5 h post-incubation. However, Tpl2 in MG132 treated p38γ/δ$^{-/-}$ MEF never reached the levels of those in WT MEF (Fig. R-12E and H). MG132 treatment did not increase ABIN2 protein in MEF, although there was a small accumulation at 5h post-incubation in p38γ/δ$^{-/-}$ MEF, this never reached the levels of WT MEF (Fig. R-12F and H). We examine p38α protein levels as control and did not observed any difference in all experimental conditions used (Fig. R-12G and H). All our results indicated that p38γ/p38δ regulate protein synthesis of Tpl2 and ABIN2 as well as their stability by interacting with the complex Tpl2/ABIN2/p105.

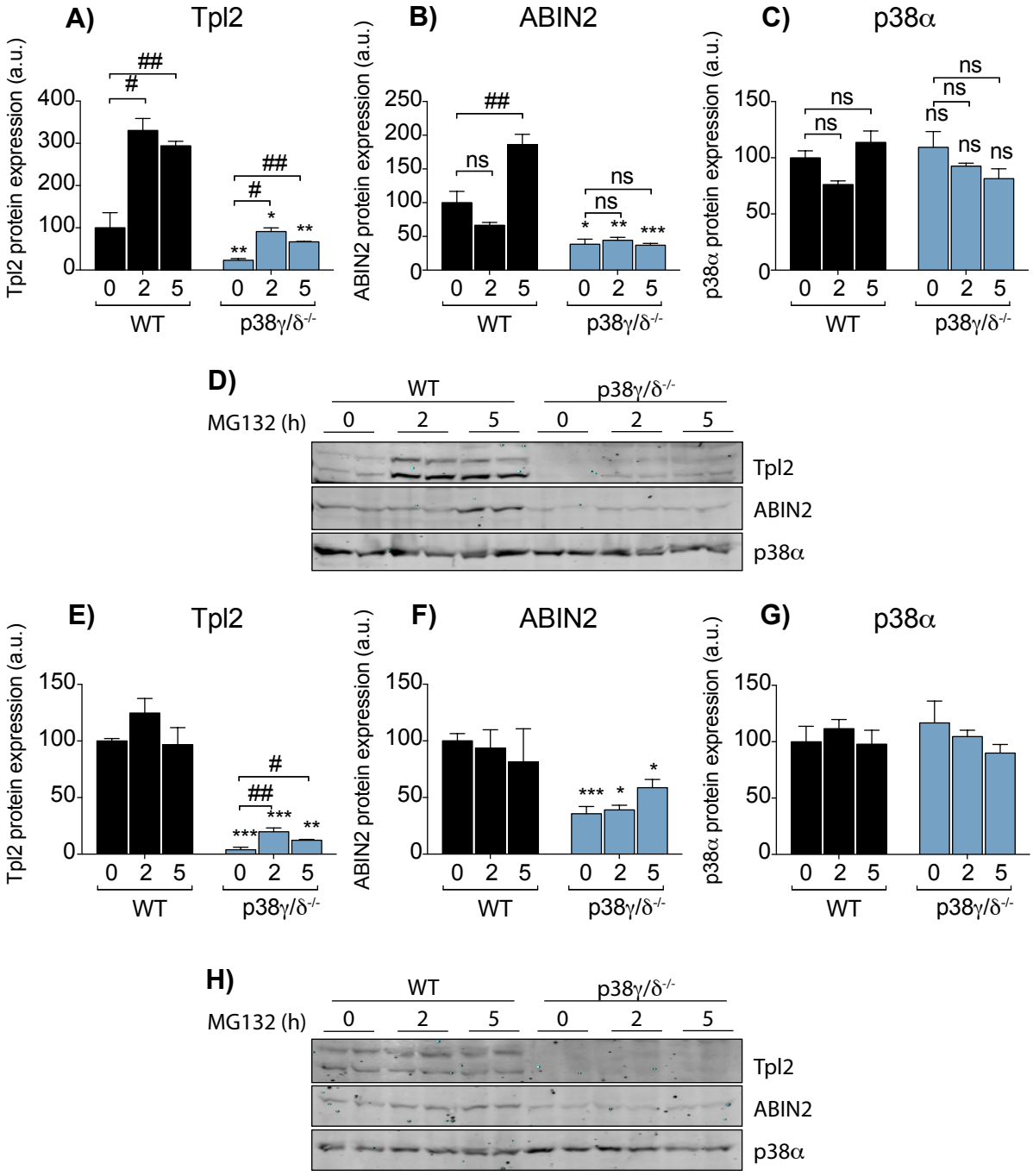

Figure R-12. p38γ and p38δ do not regulate Tpl2 and ABIN2 degradation by proteasome. WT and p38γ/δ$^{-/-}$ **A, B, C, D)** BMDM or **E, F, G, H)** MEF were incubated with DMSO or 40 μM of MG132 for 0, 2 or 5 h. Lysates were immunoblotted for the indicated proteins and they were quantified by densitometry. Quantification shows protein levels relative (%) to 0 h. Data show mean ± SEM of two experiments in duplicate. The *p*-value was determined by two-tailed Student´s t-test: *$P \leq 0.05$, ** $P \leq 0.01$, *** $P \leq 0.001$ relative to control (0 h) or # $P \leq 0.05$ and ## $P \leq 0.01$ relative to WT cells.

4.2.6 p38γ and p38δ regulate protein translation.

Since our results suggest that p38γ and p38δ might regulate Tpl2 and ABIN2 translation in a selective manner, we then analysed polysome profiles of WT and p38γ/δ$^{-/-}$ MEF, which separates RNA-protein complexes. For this, we loaded lysates from WT and p38γ/δ$^{-/-}$ MEF into a 10 – 50% sucrose gradient, separate RNA-protein complexes by centrifugation and while fractions were collected the 254 nm absorbance was measured to obtain the polysome profiles. Figure R-13A, shows the polysome profiles of WT and p38γ/δ$^{-/-}$ MEF in which we can observe the supernatant fraction (free RNAs), then the 40S and 60S ribosomal subunit, the 80S monosome and finally the polysomes (from light to heavy polysomes).

We found that the polysome profile of p38γ/δ$^{-/-}$ MEF had higher 40S and 60S peaks, while the polysome region was decreased compared to WT. This result indicated that in general p38γ/δ$^{-/-}$ MEF had less polysomes than WT and, therefore, less translation (Fig. R-13A). To test the consistency of these results, we generated Flp-In T-REx HEK293 p38γ/δ$^{-/-}$ cells by CRISPR-Cas9 edition. We first confirmed the decrease in p38γ/p38δ protein expression by immunoblot (Fig. R-13B). We analysed the polysome profile of WT and p38γ/δ$^{-/-}$ Flp-In T-REx HEK293 cells in the same conditions described before (Fig. R-13C). We found a similar pattern than in p38γ/δ$^{-/-}$ MEF, in p38γ/δ$^{-/-}$ Flp-In T-REx HEK293, the 40S peak and 80S monosome were increased and the polysome region was decreased when comparing with WT Flp-In T-REx HEK293. This result support the conclusion that p38γ/p38δ are involved in regulating protein translation in general.

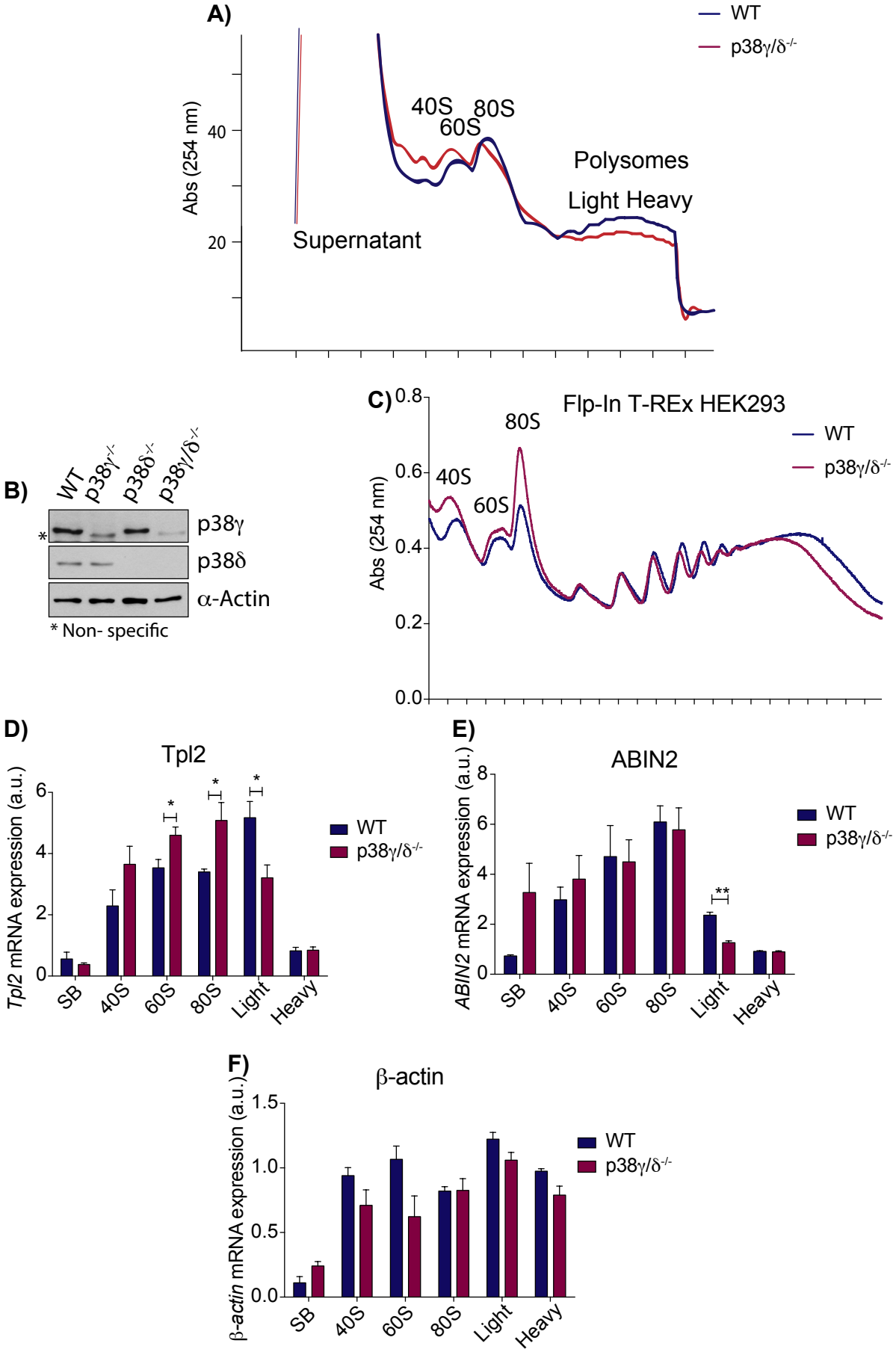
A)
WT
p38γ/δ-/-
Abs (254 nm)
40
20
40S
60S
80S
Polysomes
Light Heavy
Supernatant
B)
WT
p38γ-/-
p38δ-/-
p38γ/δ-/-
p38γ
p38δ
α-Actin
*
* Non- specific
C)
Flp-In T-REx HEK293
Abs (254 nm)
0.8
0.6
0.4
0.2
0.0
40S
60S
80S
WT
p38γ/δ-/-
D)
Tpl2
Tpl2 mRNA expression (a.u.)
6
4
2
0
SB
40S
60S
80S
Light
Heavy
WT
p38γ/δ-/-
E)
ABIN2
ABIN2 mRNA expression (a.u.)
8
6
4
2
0
**
SB
40S
60S
80S
Light
Heavy
WT
p38γ/δ-/-
F)
β-actin
β-actin mRNA expression (a.u.)
1.5
1.0
0.5
0.0
SB
40S
60S
80S
Light
Heavy
WT
p38γ/δ-/-

Figure R-13. Analysis of the polysome profile of WT and p38γ/δ$^{-/-}$ cells. Cytoplasmatic extracts from WT and p38γ/δ$^{-/-}$ cells were fractioned by centrifugation on a 10 – 50 % sucrose gradient. Twelve fractions were collected while 254 nm absorbance was recorded. **A)** Polysome profile of WT and p38γ/δ$^{-/-}$ MEF. Data shows one representative profile (n = 3) of two experiments. **B)** WT, p38γ$^{-/-}$, p38δ$^{-/-}$, p38γ/δ$^{-/-}$ Flp-In T-REx HEK293 cells lysates were immunoblotted for the indicated proteins. * non-specific band appears with p38γ antibody. **C)** Polysome profile of WT and p38γ/δ$^{-/-}$ Flp-In T-REx HEK293 cells. Data show one representative profile (n = 3) of two experiments. **D, E, F)** RNA was extracted for each fraction of WT and p38γ/δ$^{-/-}$ MEF and subjected to qPCR analysis of **D)** *Tpl2*, **E)** *ABIN2* and **F)** *β-actin* mRNAs. Values were normalized to *GAPDH*. Data show mean ± SEM (n = 3). The *p*-value was determined by two-tailed Student´s t-test: **P*>0.05, ***P*≤0.01 relative to WT input.

To analyse if p38γ/p38δ regulate the specific translation of Tpl2 and ABIN2 we extracted mRNA from the polysome profile fractions and quantified the mRNA distribution of *Tpl2* and *ABIN2*, using *β-actin* mRNA as control. When comparing p38γ/δ$^{-/-}$ with WT MEF fractions we observed that *Tpl2* mRNA accumulated in the ribosomal subunit fraction 40S and more significantly in 60S, and this trend remained until 80S monosome. In contrast, *Tpl2* mRNA in the light polysome fraction was significantly decreased (Fig. R-13D). *ABIN2* mRNA in p38γ/δ$^{-/-}$ MEF was more abundant in the supernatant fraction and decreased in the light polysome fractions when compared to WT MEF (Fig. R-13E). We also used *β-actin* mRNA as control for general gene translation, and confirm that *β-actin* mRNA distribution in the fractions did not change between WT and p38γ/δ$^{-/-}$ MEF (Fig. R-13F). These results indicated that p38γ/p38δ are regulating the general process of protein translation and in a specific manner they are regulating the Tpl2 and ABIN2 translation.

4.2.7 p38δ regulates Tpl2 translation through Tpl2 3'UTR mRNA.

mRNAs are highly regulated molecules, whose translation could be altered by many specific and non-specific mechanisms. To study the molecular

mechanism by which p38γ/p38δ might regulate *Tpl2* and *ABIN2* mRNA translation we first identify possible molecules that could be interacting with their mRNA sequence. For this we used a theoretical approach and the ensemble data base (https://www.ensembl.org/index.html) (Fig. R-14). We looked for mouse *Tpl2* and *ABIN2* mRNA binding molecules: RNA binding proteins (RBPs) from RBP Toronto data base (http://rbpdb.ccbr.utoronto.ca), and microRNA from TargetSacnMouse7.1; and also, for open reading frames (uORF). From the RBPs identified we selected the ones that were known to be modulated by p38MAPK (Tiedje et al., 2014): Zinc finger protein 36 (ZFP36), which has been demonstrated to be phosphorylated by p38α/MK2 (Chrestensen et al., 2004); Non-POU Domain Containing Octamer (NONO) that interact with p38γ in data showed afterwards in this thesis; and PABPC1 that promotes ribosome recruitment and translation initiation via p38α/MK2 (Bollig et al., 2003). We found that *Tpl2* 3'UTR mRNA had one binding site for ZFP36, two binding sites for NONO and five binding sites for PABPC1, while *ABIN2* 3'UTR mRNA had only four binding sites for NONO.

In the case of microRNAs, we observed that only *Tpl2* 3'UTR mRNA had microRNA binding sites. We found four different microRNA binding sites. miR-101-3p.2 (binding sequence: UACUGUA), miR-17-5p/20-5p/95-5p/106-5p (binding sequence: GCACUUU), miR-101a-3p.2/101b-3p.1/101b-3p.2 (binding sequence: UACUGUA) and miR-144-3p (binding sequence: AUACUGU, which was the most conserved among species according to the data base). Finally, we searched for uORF, which are located at the 5'UTR of the mRNA. The importance of uORF is that represses normal translation of protein coding sequence (CDS) in situations of integrated stress response where the global control of translation initiation is reduced. Neither *Tpl2* nor *ABIN2* had canonical initiation codons ATG (Fig. R-14).

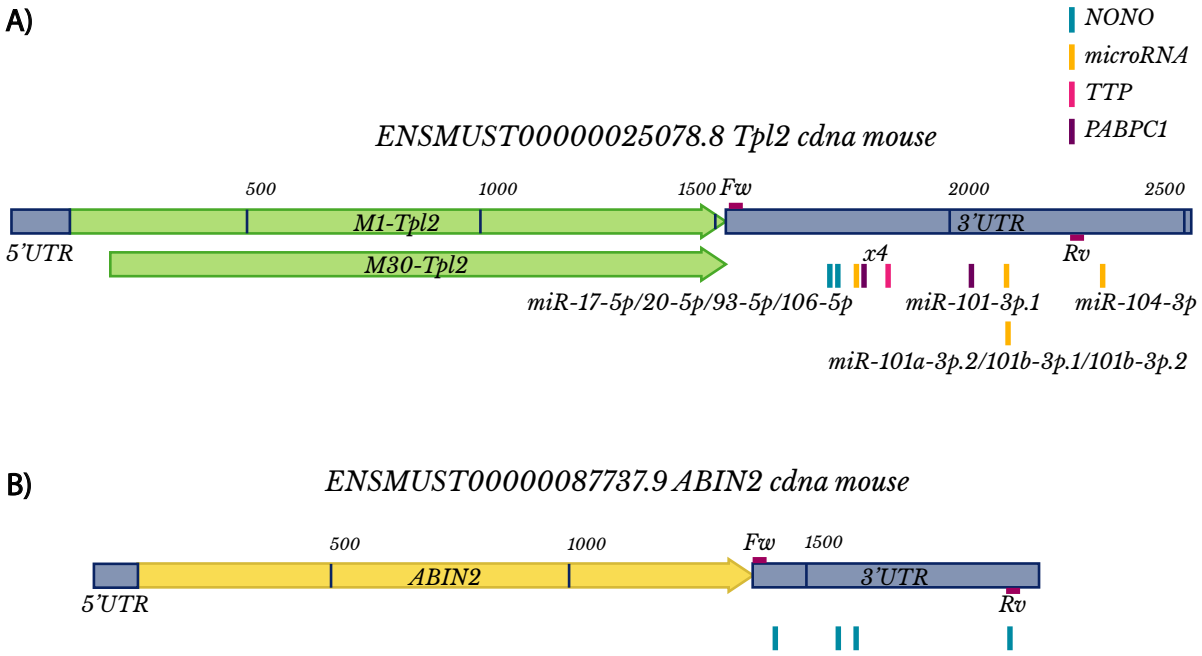

Figure R-14. Schematic representation of mouse mRNA. A) *Tpl2* mRNA and **B)** *ABIN2* mRNA. Representations show 5'UTR, coding regions (M1-Tpl2, M30-Tpl2 and ABIN2) and 3'UTR. In the 3'UTR region, cloning sites for psiCHEK-2 plasmid are showed as forward primer (Fw) and revers primer (Rv) and the binding sites of the RBPs NONO, TTP and PABPC1 or microRNA binding sequences are shown as colour bars.

After this theoretical study we found that most of the possible regulating components were located at the 3'UTR region of the mRNA of *Tpl2* and *ABIN2*. Therefore, we cloned 3'UTR of mouse *Tpl2* mRNA and 3'UTR of mouse *ABIN2* mRNA in psiCHEK2 plasmid (Fig. R-15A).

Both *Tpl2* 3'UTR and *ABIN2* 3'UTR were cloned after *Renilla* CDS to study how *Renilla* expression was modulated by them in WT and p38$\gamma/\delta^{-/-}$ MEF. As described in methods the expression of *firefly*, which is in the same vector, was used as transfection control (Fig. R-15A, Figure M-1). First, we observed that psiCHEK-2 empty vector induced the same expression of *Renilla* in WT and p38$\gamma/\delta^{-/-}$ MEF (Fig. R-15B). When we analyse *Tpl2* 3'UTR plasmid in WT and p38$\gamma/\delta^{-/-}$ MEF, we found that the expression of *Renilla* was significantly more repressed in p38$\gamma/\delta^{-/-}$ MEF than in WT MEF. In contrast, *ABIN2* 3'UTR effect on the expression of *Renilla* was similar in p38$\gamma/\delta^{-/-}$ and WT MEF (Fig. R-15B). These results

indicated that 3'UTR mRNA of *Tpl2*, but not of *ABIN2,* was regulated by p38γ/p38δ.

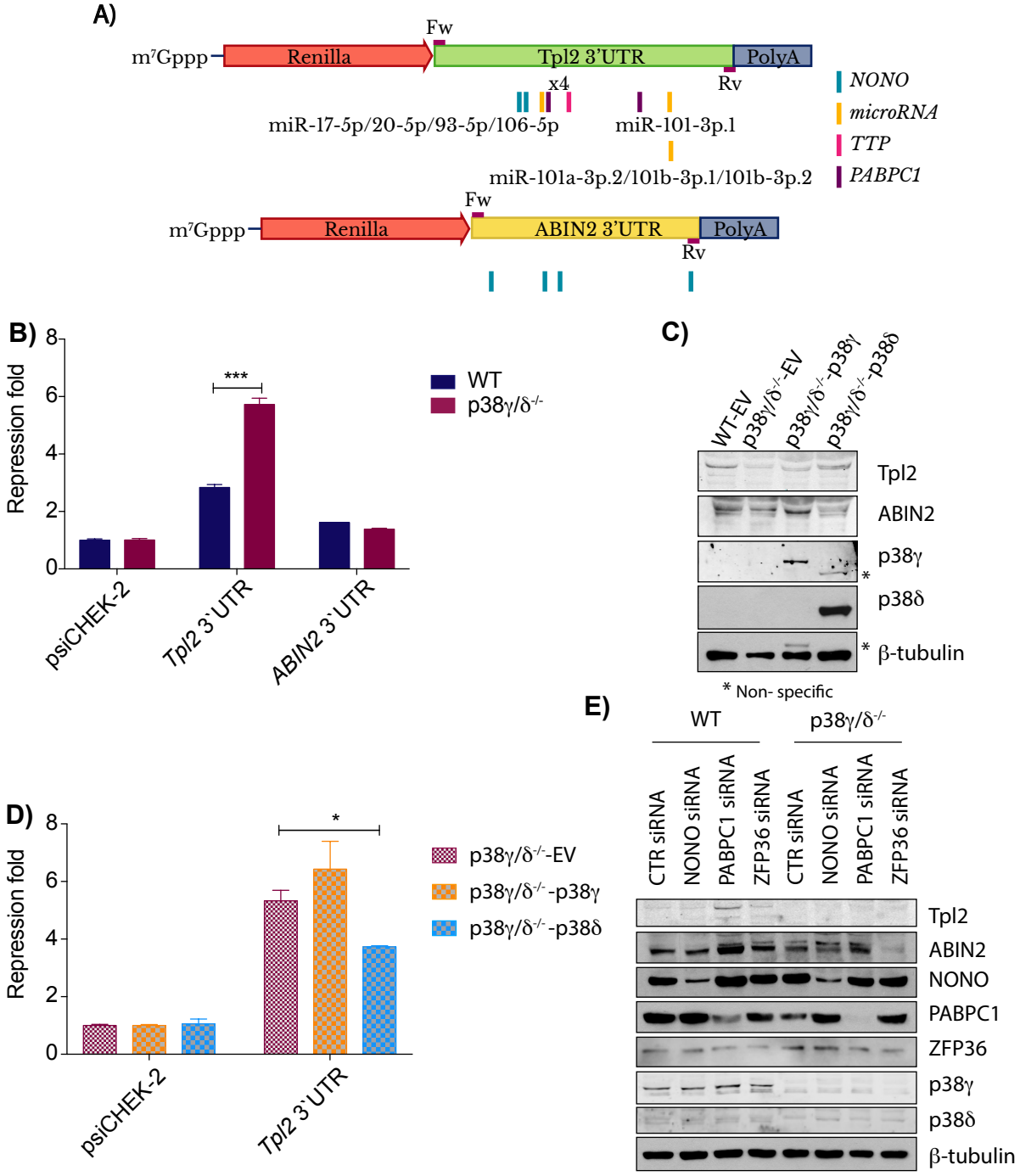

Figure R-15. Effect of p38γ/p38δ on the role of 3'UTR of *Tpl2* and *ABIN2* mRNA in translational repression. A) Schematic representation of the psiCHEK2-*Renilla-Tpl2* 3'UTR (*Tpl2* 3'UTR) and psiCHEK2-*Renilla-ABIN2* 3'UTR (*ABIN2* 3'UTR) reporter. **B)** WT and p38γ/δ$^{-/-}$ MEF were transfected with either luciferase plasmids psiCHEK-2 as empty vector, or *Tpl2* 3'UTR or *ABIN2* 3'UTR. Luciferase activity was measured 24 h after transfection. Renilla values were normalized against Firefly levels and repression fold was

calculated for the *Tpl2* 3'UTR or *ABIN2* 3'UTR reporter relative to psiCHEK-2 empty vector for each condition. Data show mean ± SEM (n = 3). **C)** Stable MEF cell lines were generated as indicated in Methods: WT-EV, p38γ/δ$^{-/-}$-EV, p38γ/δ$^{-/-}$-p38γ or p38γ/δ$^{-/-}$-p38δ MEF were lysed and 50 µg were immunoblotted with the indicated antibodies. **D)** The indicated stable MEF cell lines were transfected with either psiCHEK-2 empty vector, or *Tpl2* 3'UTR, or *ABIN2* 3'UTR. Luciferase activity was measured 24 h after transfection. Renilla values were normalized against Firefly levels and repression fold was calculated for the *Tpl2* 3'UTR or *ABIN2* 3'UTR reporter relative to psiCHEK-2 for each condition. Data show mean ± SEM (n = 3). **E)** WT and p38γ/δ$^{-/-}$ MEF were transfected for gene silencing with the indicated siRNAs for 72 h. Cells were lysed and 30 µg were immunoblotted with the indicated antibodies. The *p*-value was determined by two-tailed Student´s t-test: **P*≤0.05, ****P*≤0.001.

To confirm that p38γ/p38δ were regulating Tpl2 and ABIN2 total protein levels we performed rescue experiments. We expressed p38γ or p38δ in p38γ/δ$^{-/-}$ MEF by stable lentiviral infection and examined if Tpl2 and/or ABIN2 were expressed. We infected p38γ/δ$^{-/-}$ MEF with either EV (p38γ/δ$^{-/-}$-EV), or p38γ (p38γ/δ$^{-/-}$-p38γ), or p38δ (p38γ/δ$^{-/-}$-p38δ). We also infected WT with either EV alone (WT-EV) to verify the Tpl2 rescue. First, we immunoblotted lysates from infected MEFs and found that in p38γ/δ$^{-/-}$-p38δ MEF the Tpl2 protein expression was rescued, while in p38γ/δ$^{-/-}$-p38γ MEF ABIN2 protein levels were restored (Fig. R-15C). We confirmed that p38γ was expressed in p38γ/δ$^{-/-}$-p38γ MEF and p38δ in p38γ/δ$^{-/-}$-p38δ MEF (Fig. R-15C). Secondly, we studied if the rescued Tpl2 protein levels were due to *Tpl2* 3'UTR regulation. We transfected p38γ/δ$^{-/-}$-EV p38γ/δ$^{-/-}$-p38γ and p38γ/δ$^{-/-}$-p38δ MEFs with psiCHEK-2 or *Tpl2* 3'UTR. We measured *Renilla* and *firefly* luciferase activities and found that *Tpl2* 3'UTR *Renilla* was rescued only in p38γ/δ$^{-/-}$ p38δ MEF (Fig. R-15D), reaching the same repression fold found in WT MEF (Fig. R-15B). *Tpl2* 3'UTR *Renilla* repression fold was similar in p38γ/δ$^{-/-}$ MEF and p38γ/δ$^{-/-}$-EV MEF (Fig. R-15B and D). These two experiments indicate that the main contributor regulating the specific translation of *Tpl2* was p38δ, although for the

regulation of Tpl2 and ABIN2 total protein levels both p38γ/p38δ are needed.

To test if Tpl2 and ABIN2 were translationally repressed by one or more of the identified RBPs we used siRNA technique to silence NONO, PABPC1 or ZFP36 in WT and p38γ/δ$^{-/-}$ MEF. When we examined the RBP protein levels in WT and p38γ/δ$^{-/-}$ MEF, we found that the expression of PABPC1 was reduced in p38γ/δ$^{-/-}$ MEF comparing with WT cells, whereas NONO and ZFP36 were expressed at similar levels (Fig. R-15E). We observed that knockdown of: 1) NONO did not affect Tpl2 nor ABIN2 expression; 2) PABPC1 increased Tpl2 and ABIN2 expression in WT MEF, but not in p38γ/δ$^{-/-}$ MEF; finally, 3) ZFP36 was not silenced in our experimental conditions and therefore we could not reach a conclusion (Fig. R-15E).

4.2.8 p38γ and p38δ interactome and phosphorylation profiles in macrophages.

p38γ can regulate complexes independently of its kinase activity. This characteristic is in part due to its C-terminal sequence that binds to PDZ domains (Hasegawa et al., 1999). Our data from the gel filtration chromatography experiment using Raw264.7 lysates, also indicated that p38δ in macrophages is forming complexes (Fig. R-7). To study the possible targets of p38γ/p38δ that could be regulating translation, we performed two different experiments in unstimulated macrophages: 1) we determine the p38γ/p38δ interactome, and 2) we study phospho-proteome profile of WT, p38γ$^{-/-}$, p38δ$^{-/-}$ and p38γ/δ$^{-/-}$ macrophages.

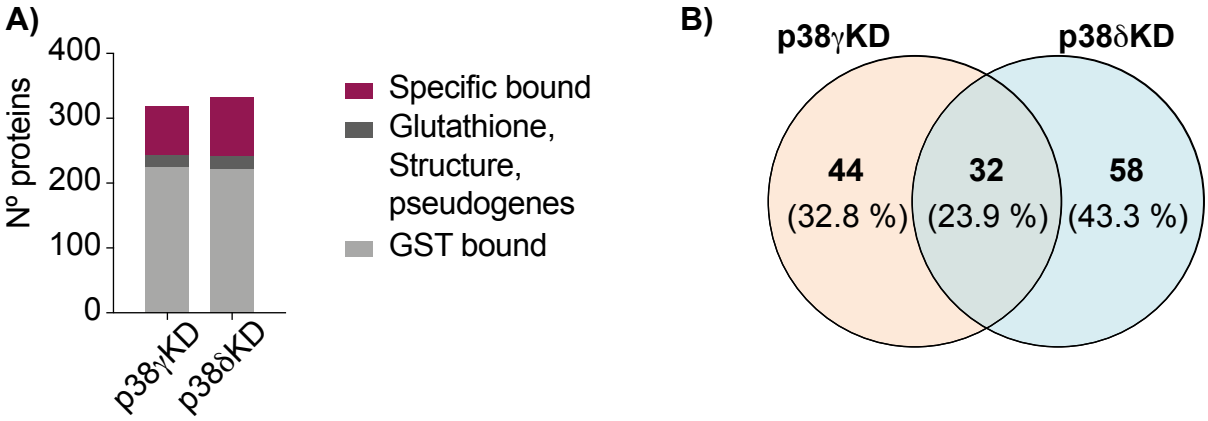

Figure R-16. p38γ and p38δ interactome analysis in BMDM. BMDM from WT mice were lysate and 4.5 mg of protein were incubated with purified proteins GST, GST-p38γKD or GST-p38δKD. Pellets containing the p38MAPK protein complexes were electrophoresed, digested and analysed by LC-MS. **A)** Graph indicating the number of proteins that specifically bind to GST-p38γKD or GST-p38δKD, after filtering the data as indicated in the text. **B)** Venn diagram of GST-p38γKD and/or GST-p38δKD interacting proteins.

To study the interactome of p38γ/p38δ we carried out pull-down assay using lysates from WT BMDM and GST-tagged versions of p38γ/p38δ kinase dead (KD) mutants, which have not kinase activity: GST-p38γKD and GST-p38δKD. We also used GST alone as control. Only peptides with FDR<1% were considered as statistical significance, leaving us with a list of 319 interacting proteins for p38γ and 332 interacting proteins for p38δ. We then search in the lists for proteins that specifically associate to either p38γ or p38δ and could be implicated translation. For this, we first excluded proteins that bind to GST alone (GST bound, 66-70% of the protein), structural proteins (such as actin and keratin), pseudogenes, and glutathione family proteins (~6 % of the proteins) and considered that the rest of the proteins, ~25 %, specifically interacted with p38γ and/or p38δ (Fig. R-16A). Then we examined which of those proteins specifically interacted with either p38γ or p38δ, and found that 32 proteins were common interactors, whereas 44 and 58 of the proteins were specific for p38γ and p38δ, respectively (Fig. R-16B). Using the STRING analysis platform, we determine the enrichment of KEGG-pathways of the

proteins bound to p38γ or p38δ. For p38γKD, the KEGG pathways enrichment with lowest discovery rate was by far the ribosome pathway (Fig. R-17A and Table R-1). Ribosomal proteins that bind to p38γ such as RPS18 and RPL12, indicated that p38γ is implicated in the translational pathway (Fig. R-17A and Table R-1). For p38δKD, the KEGG pathways enrichment with lowest discovery rate was the carbon metabolism pathway indicating that p38δ regulates metabolism in macrophages (Fig. R-17B and Table R-2). In p38δ-interactome we observed that the fourth most enriched pathway was again ribosome pathway and among the proteins interacting with p38δ we found eEF2 and eEF1A1, which are involved in the regulation of the elongation process (Fig. R-17B and Table R-2). eEF2 had already been described to be regulated by p38δ by phosphorylating its kinase eEF2K (Knebel et al., 2001).

To further study the mechanism by which p38γ/p38δ were regulating translation we analysed different steps in mRNA translation by luciferase assay using the following constructs: 1) a bicistronic reporter construct that has *Renilla* luciferase under the simian virus 40 (SV40) promoter that induces cap-dependent translation (Chio et al., 2016); 2) *firefly* luciferase under the control of the internal ribosome entry site (IRES) from the hepatitis C virus (HCV-IRES), which requires only certain canonical initiation factors, such as eIF3 and eIF2α (Otto and Puglisi, 2004); and 3) the cricket paralysis virus IRES (CrPV-IRES) that induces mRNA translation independently of any eIFs and recruiting the ribosomal subunits directly to the mRNA (Wilson et al., 2000) (Fig. R-18). We transfected these plasmids in WT and p38γ/δ$^{-/-}$ MEF and found that both SV40-CAP and specially CrPV-IRES significantly decreased luciferase translation in p38γ/δ$^{-/-}$ comparing with WT MEF (Fig. R-18). This indicated that p38γ and p38δ were regulating both cap-dependent and cap-independent translation; however, we still do not know how these kinases selectively regulated *Tpl2* and *ABIN2* mRNAs translation.

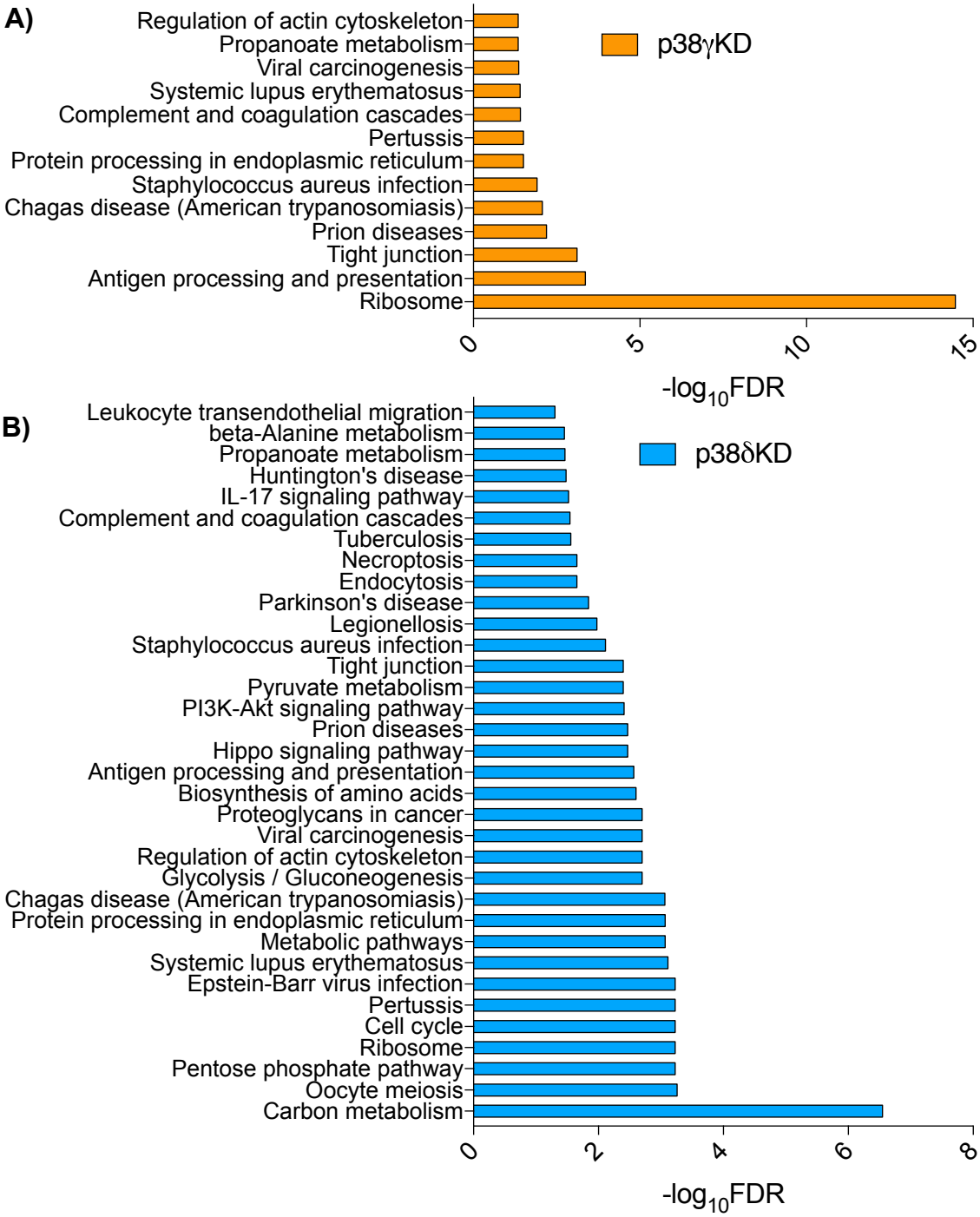

Figure R-17. p38γ and p38δ interactome KEGG-pathways analysis. Enrichment in KEGG pathways analysed using STRING platform with a medium confidence of 0.4. All sources were considered except Gene fusion source. **A)** GST-p38γKD and **B)** GST-p38δKD.

Table R-1. GST-p38γKD interacting proteins involved in translation, in macrophages.

GST-p38γKD		
Protein_Acc	**Description**	**Gene**
Q561N5	40S ribosomal protein S18 OS=Mus musculus GN=Rps18 PE=2 SV=1	RPS18
Q545F8	40S ribosomal protein S4 OS=Mus musculus GN=Rps4x PE=2 SV=1	RPS4X
Q497E9	40S ribosomal protein S8 OS=Mus musculus GN=Rps8 PE=1 SV=1	RPS8
Q3UBI6	Putative uncharacterized protein OS=Mus musculus GN=Rpl7 PE=2 SV=1	RPL7
Q5YLW3	40S ribosomal protein S3 OS=Mus musculus GN=Rps3 PE=1 SV=1	RPS3
O70251	Elongation factor 1-beta OS=Mus musculus GN=Eef1b PE=1 SV=5	EEF1B
Q3TIQ2	Putative uncharacterized protein OS=Mus musculus GN=Rpl12 PE=2 SV=1	RPL12
Q3U5P8	40S ribosomal protein S3a OS=Mus musculus GN=Rps3a1 PE=2 SV=1	RPS3A1
Q5RKP3	60S ribosomal protein L13 OS=Mus musculus GN=Rpl13 PE=2 SV=1	RPL13
A0A0G2JES3	60S ribosomal protein L9 (Fragment) OS=Mus musculus GN=Rpl9 PE=1 SV=1	RPL9
O89072	Ribosomal protein S2 (Fragment) OS=Mus musculus GN=Rps2 PE=2 SV=1	RPS2
Q4VA28	Ribosomal protein L21 OS=Mus musculus GN=Rpl21 PE=2 SV=1	RPL21
Q3U561	Ribosomal protein OS=Mus musculus GN=Rpl10a PE=2 SV=1	RPL10A
Q3TK12	Putative uncharacterized protein OS=Mus musculus GN=Rps17 PE=2 SV=1	RPS17
Q9CWI9	Putative uncharacterized protein OS=Mus musculus GN=Rps23 PE=2 SV=1	RPS23

Table R-2. GST-p38δKD interacting proteins involved in translation, in macrophages.

GST-p38δKD		
Protein_Acc	**Description**	**Gene**
Q3UA81	Elongation factor 1-alpha OS=Mus musculus GN=Eefla1 PE=2 SV=1	EEF1A1
Q3TJZ1	Putative uncharacterized protein OS=Mus musculus GN=Eef2 PE=2 SV=1	EEF2
Q3TIQ2	Putative uncharacterized protein OS=Mus musculus GN=Rpl12 PE=2 SV=1	RPL12
Q3UBI6	Putative uncharacterized protein OS=Mus musculus GN=Rpl7 PE=2 SV=1	RPL7
S4R223	40S ribosomal protein S19 OS=Mus musculus GN=Rps19 PE=1 SV=1	RPS19
Q3UJS0	Putative uncharacterized protein OS=Mus musculus GN=Rpl8 PE=2 SV=1	RPL8
Q497E9	40S ribosomal protein S8 OS=Mus musculus GN=Rps8 PE=1 SV=1	RPS8

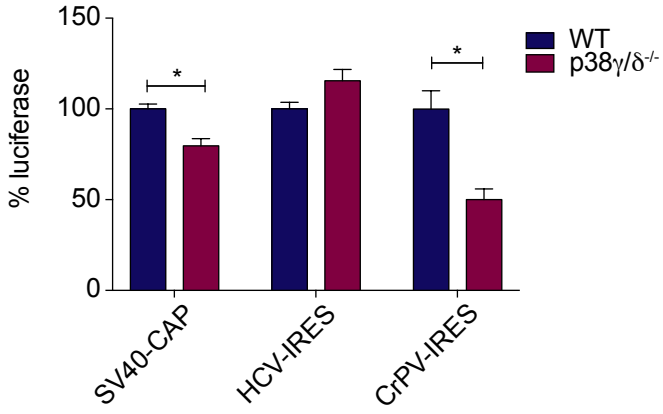

Figure R-18. p38γ and p38δ were regulating both cap-dependent and cap-independent protein translation. WT and p38γ/δ$^{-/-}$ MEF were transfected with bicistronic reporter plasmids SV40-CAP, HCV-IRES or CrPV-IRES. Luciferase activity was measured 24 h after transfection. Data show mean ± SEM (n = 3) and relative to WT luciferase values. The *p*-value was determined by two-tailed Student´s t-test: *$P \leq 0.05$.

To elucidate possible targets of p38γ/p38δ that could be regulating *Tpl2* mRNA specifically we performed comparative phospho-proteomics analysis. The phospho-proteomic experiments were done using peritoneal macrophages from WT, p38$\gamma^{-/-}$, p38$\delta^{-/-}$ and p38$\gamma/\delta^{-/-}$ mice, in triplicate and in basal conditions. This will identify proteins that could be differentially phosphorylated and cause the decrease in the steady-state protein levels of Tpl2 and ABIN2. The phospho-proteomic analysis was performed in collaboration with Dr. Eric Bonneil from the Proteomic Platform in the Institute for research in immunology and cancer in Montreal, Canada and Dr. Mehdi Jafarnejad from Goodman Cancer Research Centre in Montreal, Canada (Fig. R-19). Interestingly the results from these analyses indicate that p38γ is repressing phosphorylation, since we observed a clear increase in phosphorylated proteins when p38γ is deleted in macrophages (Fig. R-19A, D). Contrary, p38δ had the expected opposite effect, p38δ deletion caused a decrease in general protein phosphorylation compared to WT (Fig. R-19B, D).

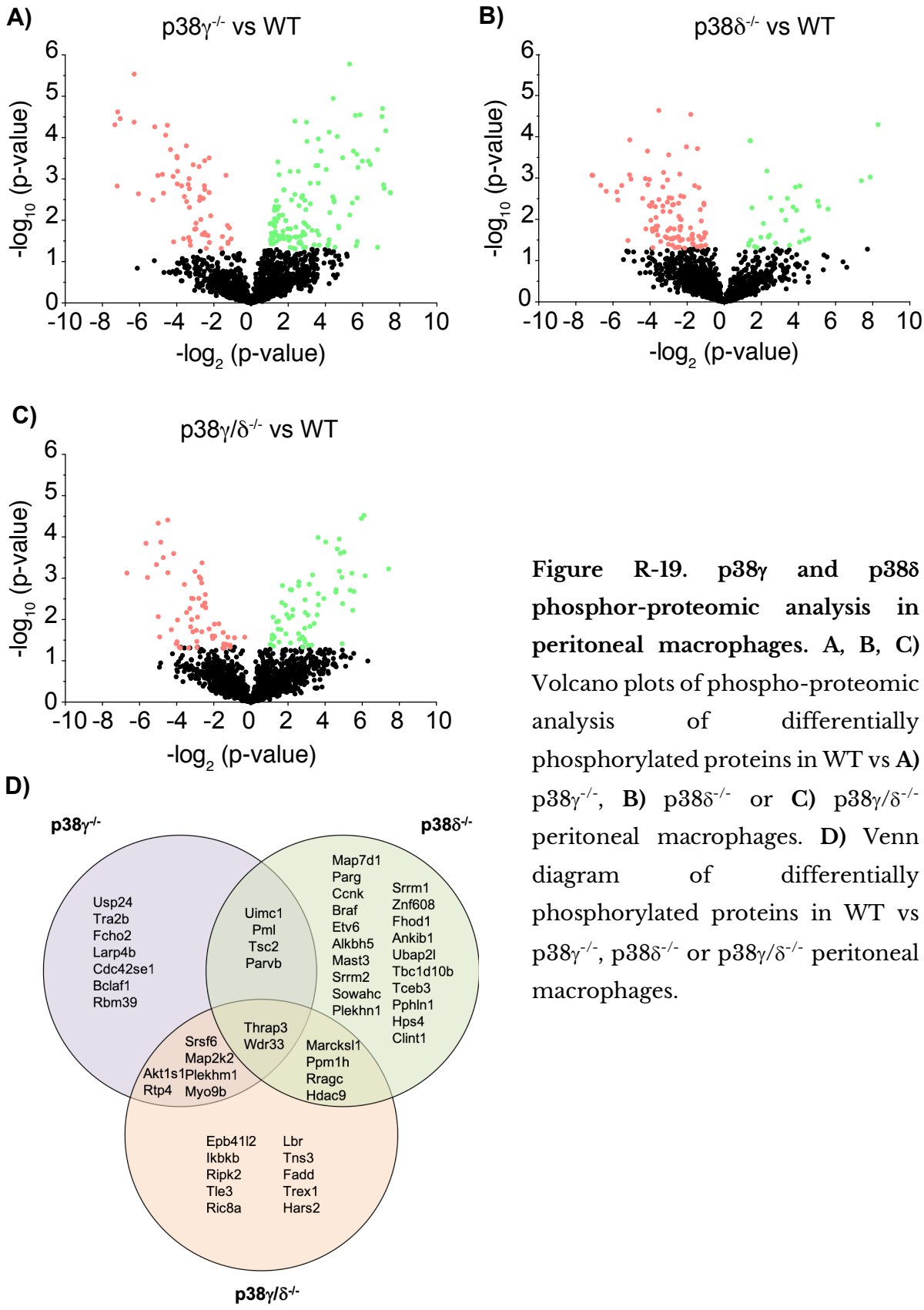

Figure R-19. p38γ and p38δ phosphor-proteomic analysis in peritoneal macrophages. A, B, C) Volcano plots of phospho-proteomic analysis of differentially phosphorylated proteins in WT vs **A)** p38γ$^{-/-}$, **B)** p38δ$^{-/-}$ or **C)** p38γ/δ$^{-/-}$ peritoneal macrophages. **D)** Venn diagram of differentially phosphorylated proteins in WT vs p38γ$^{-/-}$, p38δ$^{-/-}$ or p38γ/δ$^{-/-}$ peritoneal macrophages.

When we analysed p38γ/δ$^{-/-}$ vs WT, the absence of both kinases compensated the effect of either p38γ or p38δ single deletion by reaching an equilibrium in the number of phosphorylated vs unphosphorylated proteins (Fig. R-19C, D). We then selected proteins that were down regulated in WT vs p38γ$^{-/-}$, p38δ$^{-/-}$ or p38γ/δ$^{-/-}$ and among them searched for peptides phosphorylated on Ser or Tyr residues followed with a Pro. This will permit to identify possible direct substrates of p38γ o p38δ (Fig. R-19D). p38δ phosphorylates specifically 20 proteins, whereas p38γ phosphorylates only 7 in agreement with what we observed in the volcano plots (Fig. R-19D). Venn diagram representation show that only the phosphorylation of two proteins was downregulated in all three p38γ$^{-/-}$, p38δ$^{-/-}$ or p38γ/δ$^{-/-}$ macrophages (Fig. R-19D). These two proteins were thyroid hormone receptor-associated protein 3 (Tharp3) and WD repeat domain 33 (Wdr33), and both were involved in mRNA processing. Tharp3 is implicated in pre-mRNA splicing and Wdr33 regulates poly(A) mRNA by binding to the AAUAAA sequence (Chan et al., 2014; Schönemann et al., 2014).

We then combined p38γ or p38δ interactome and phospho-proteomic analysis using the STRING platform to identify the most important functions or biological process in which these kinases are involved in macrophages (Fig. R-20 and R21). The only common protein between the interactome to p38γKD and the phospho-proteomic analysis, Rbm39, which was part of the mRNA processing enrichment group (Fig. R-20 and R21).

p38γ enriched terms with STRING platform provides the following terms: Translation, mRNA processing, Mitochondria inner membrane, Rab subfamily of small GTPase, Myosin complex, Complement family C1q domain, Anexin superfamily, Unfolded protein binding, Short Calmodulin binding motif and 14-3-3 homologues (Fig. R-20). On the other hand, the terms produced by p38δ analysis were: Metabolic pathways, Thioredoxin like superfamily, Unfolded protein

binding, Translation, mRNA processing, Rab family small GTPase, 14-3-3 homologues and DNA binding transcription factor binding (Fig. R-21).

The main groups to identify possible candidates that could be regulating specifically *Tpl2* and *ABIN2* mRNA translation were: Translation and mRNA processing.

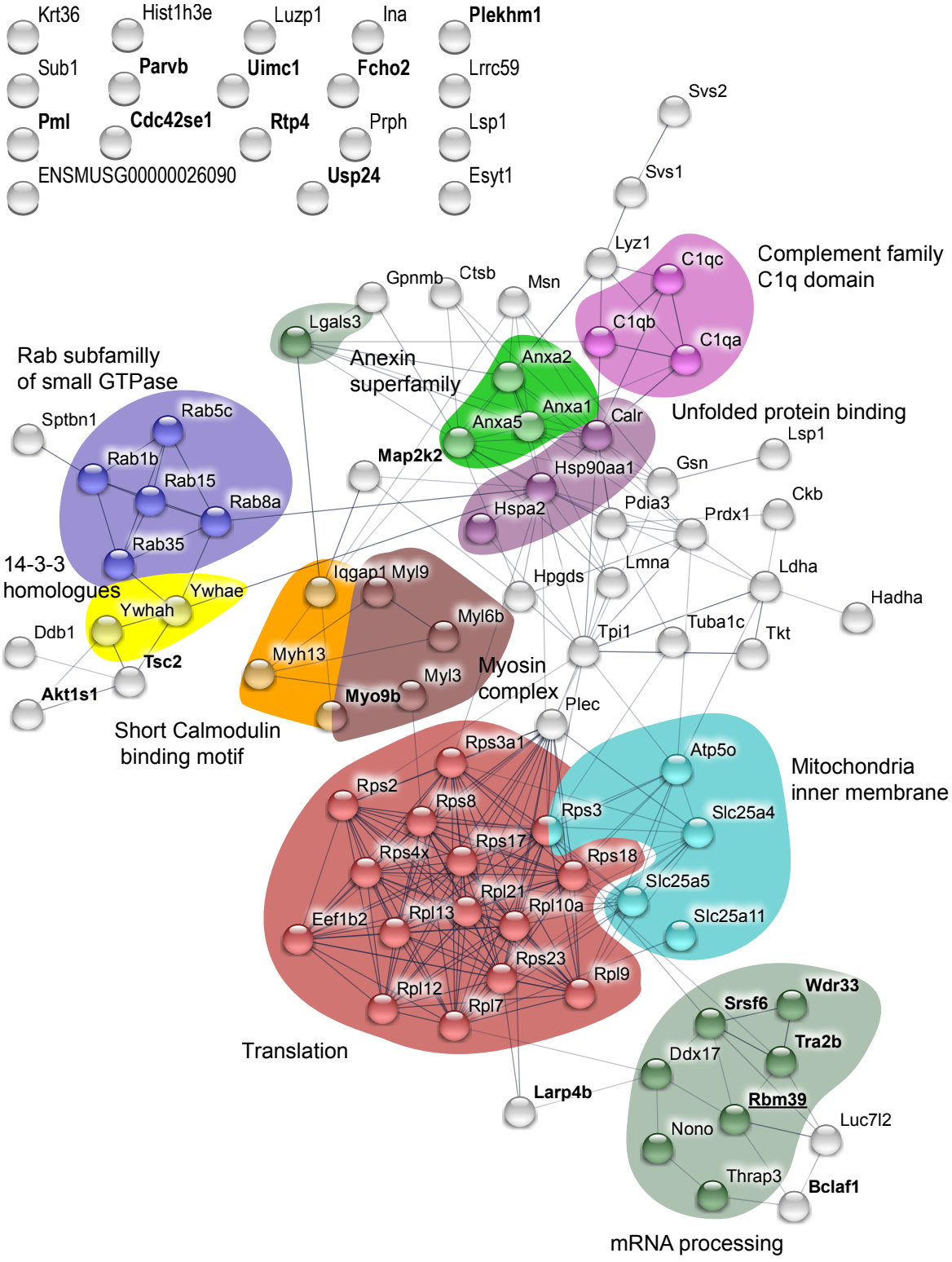

In this chapter we have demonstrated that steady-state protein levels of Tpl2 are specifically regulated by p38γ/p38δ by two possible independent mechanisms, one by regulating Tpl2 stability through interaction and a second mechanism in which p38δ modulates specific *Tpl2* mRNA translation through the regulation of its 3'UTR. Finally, these studies have shown that p38γ/p38δ are regulating general translation in a cap-independent manner (Fig R-22).

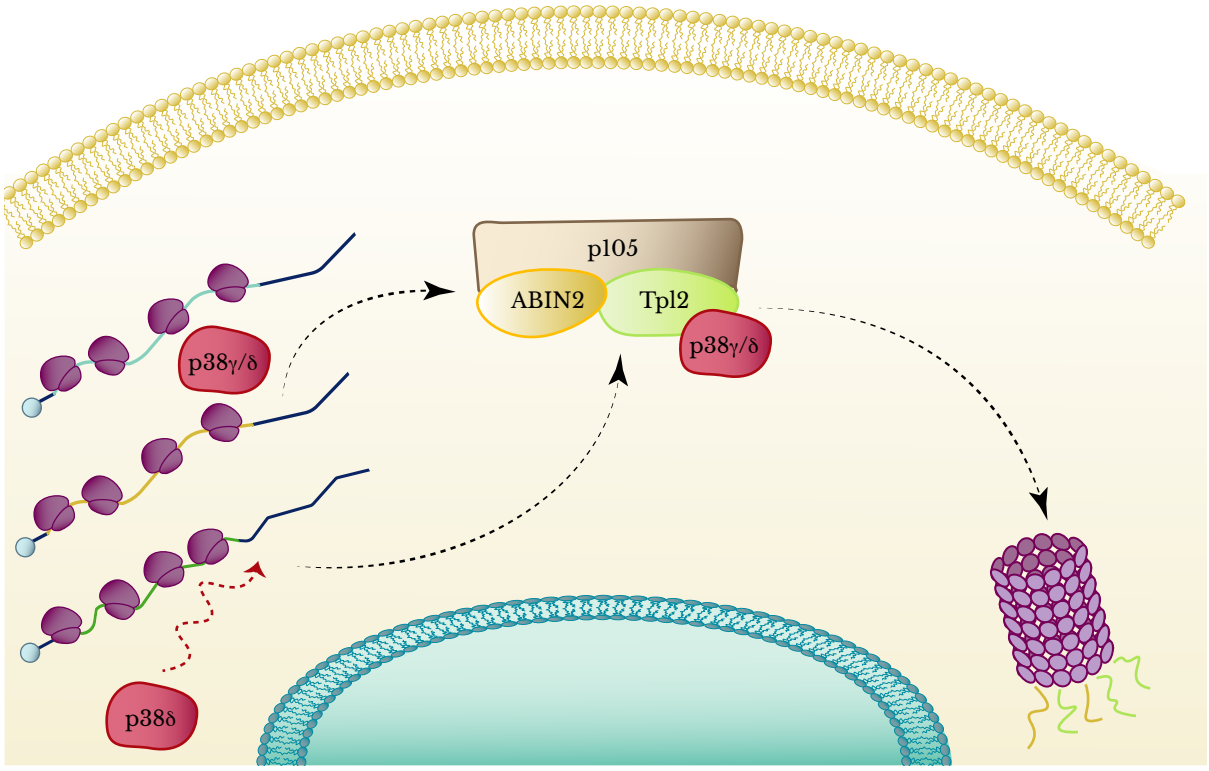

Figure R-22. Schematic representation of p38γ and p38δ biological function in macrophages. p38γ/p38δ regulate Tpl2 by interaction to maintain steady-state protein levels. p38δ modulates *Tpl2* mRNA translation by regulating its 3'UTR. p38γ/p38δ regulates cap-independent general translation probably by binding to the ribosome.

4.3 Chapter 3. New roles of p38γ and p38δ in macrophages.

We next wanted to investigate the roles of p38γ/p38δ in macrophages that were Tpl2-independent. We have demonstrated that loss of p38γ/p38δ decreases Tpl2 protein levels, which is a key protein that modulates cytokine production in macrophages. Tpl2 protein stability depends on Tpl2/ABIN2/p105 complex formation (Lang et al., 2004; Papoutsopoulou et al., 2006). Since we have evidence that p38γ interacts with Tpl2, and p38γ regulates protein complexes composition independently of its kinase activity, we hypothesised that just the expression of p38γ would be enough to maintain Tpl2 protein levels as in WT. We then decided to generate a new mouse line that expressed inactive p38γ ($p38\gamma^{171A/171A}$) and does not express p38δ ($p38\delta^{-/-}$) (Sabio et al., 2005, 2010).

4.4 The generation and characterization of $p38\gamma^{171A/171A}/p38\delta^{-/-}$ mouse.

We generated a new $p38\gamma^{171A/171A}/p38\delta^{-/-}$ mouse line by crossing $p38\gamma^{171A/171A}$ mice, that express inactive kinase p38γ, and $p38\delta^{-/-}$ mice, which does not express p38δ. Both mice have a C57BL/6 genetic background and were generated previously in our laboratory (Sabio et al., 2005, 2010). We genotyped the new $p38\gamma^{171A/171A}/p38\delta^{-/-}$ mouse line by PCR as described in Methods and in (Sabio et al., 2005, 2010), using $p38\gamma/\delta^{-/-}$ and $p38\gamma^{171A/171A}$ mice as positive controls, and WT as a negative control (Fig. R-23A).

To demonstrate that $p38\gamma^{171A/171A}/p38\delta^{-/-}$ mice had inactive p38γ and do not express p38δ, we isolated primary MEFs from WT and $p38\gamma^{171A/171A}/p38\delta^{-/-}$ mice. We first checked p38γ and p38δ expression by immunoblot and we observed that $p38\gamma^{171A/171A}/p38\delta^{-/-}$ MEF expressed p38γ, whereas p38δ was not detectable (Fig. R-23B). The levels of expression of p38α, ERK1/2, ERK5 and JNK, were similar in WT and $p38\gamma^{171A/171A}/p38\delta^{-/-}$ MEF (Fig. R-23B). Next, we confirmed that p38γ in

p38γ$^{171A/171A}$/p38δ$^{-/-}$ mice was inactive. For this we stimulated MEFs primary cells with sorbitol to induce osmotic shock. Under these conditions p38MAPK, JNK and ERK5 are activated. We observed phosphorylation of p38α, p38γ, JNK and ERK5 in both WT and p38γ$^{171A/171A}$/p38δ$^{-/-}$ MEF (Fig. R-23B, C, D). It has been previously described that p38γ is responsible, under osmotic shock, for the phosphorylation of hDlg/SAP97 in phospho-Ser158 (Sabio et al., 2010); we then examined hDlg/SAP97 in p38γ$^{171A/171A}$/p38δ$^{-/-}$ cells. hDlg/SAP97 was not phosphorylated at residue Ser158 in sorbitol stimulated p38γ$^{171A/171A}$/p38δ$^{-/-}$ MEF when comparing with WT MEF, showing that p38γ$^{171A/171A}$/p38δ$^{-/-}$ cells express inactive p38γ (Fig. R-23D).

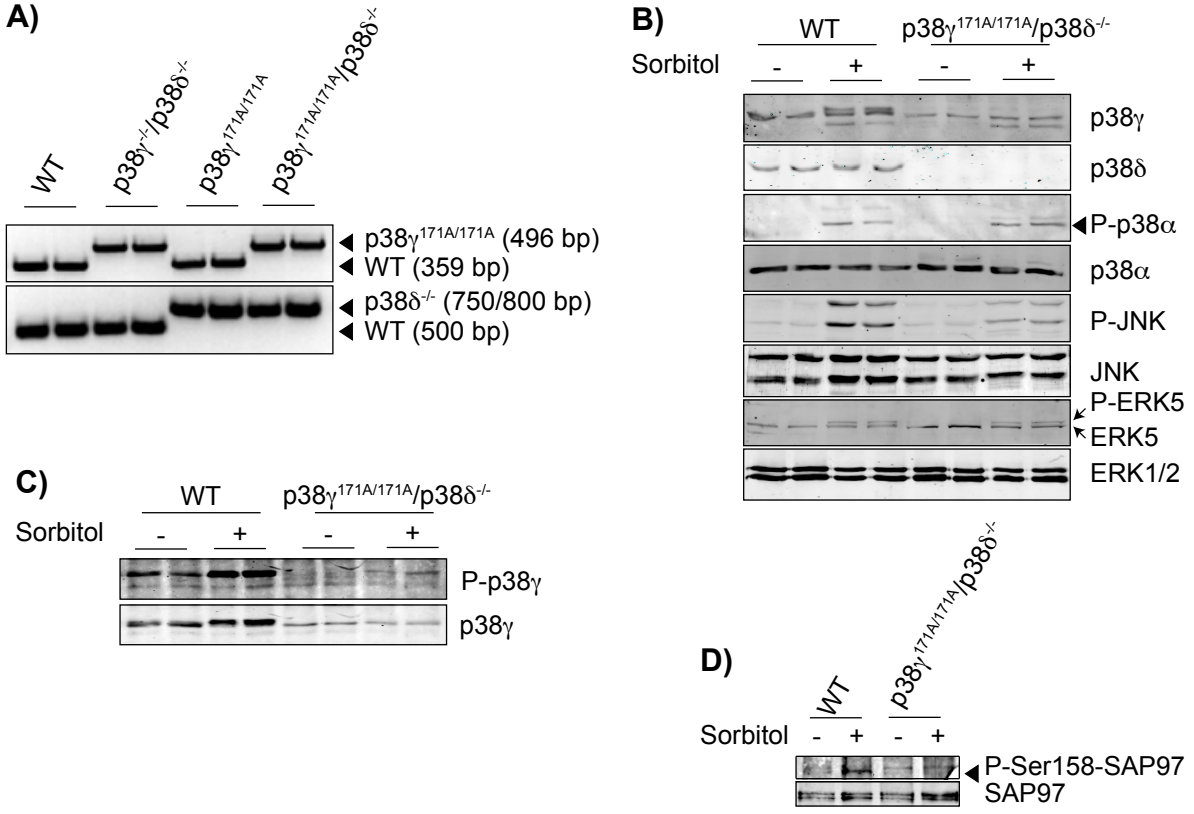

Figure R-23. Generation of p38γ$^{171A/171A}$/p38δ$^{-/-}$ mouse. A) p38γ$^{171A/171A}$ and p38δ$^{-/-}$ genomic DNA purified from tail biopsy sample was used as a template for PCR, electrophoresed on a 1% agarose gel and examined by ethidium bromide staining. **B, C, D)** primary MEFs from WT or p38γ$^{171A/171A}$/p38δ$^{-/-}$ mice in control or osmotic shock conditions (15 min sorbitol at 0.5 M). **B)** MEF lysates (30 µg) were immunoblotted with the indicated antibodies. **C)** p38γ was immunoprecipitated with 2 mg of cell lysates with anti-p38γ coupled to protein G-sepharose and consecutively immunodetected with anti-phospho-

p38γ or anti-p38γ. **D)** hDlg/SAP97 was immunoprecipitated from 1 mg of cell lysates with the anti-SAP97 coupled to protein G-sepharose and immunodetected with anti-P-Ser158-SAP97 or anti-SAP97. Representative blots from two independent experiments are shown.

4.4.1 p38γ expression is necessary for the activation of ERK1/2 in LPS stimulated macrophages.

We first examined Tpl2 and ABIN2 protein levels in $p38\gamma^{171A/171A}/p38\delta^{-/-}$ and found that BMDM express Tpl2 and ABIN2 (Fig. R-24A), indicating that p38γ expression, independently of its kinase activity, was essential to maintain Tpl2 and ABIN2 steady-state levels.

Then we study the role of p38γ and p38δ in innate immune response. We performed an *in vitro* comparative analysis of BMDM activation. For this, we prepared BMDM from WT, $p38\gamma^{171A/171A}$, $p38\gamma^{-/-}$, $p38\gamma^{171A/171A}/p38\delta^{-/-}$ and $p38\gamma/\delta^{-/-}$ mice and stimulated them with LPS to activate TLR4 receptor signalling pathway (Fig. R-24A). We examined Tpl2 and ABIN2 protein levels, and confirmed that WT, $p38\gamma^{171A/171A}$, $p38\gamma^{-/-}$ and $p38\gamma^{171A/171A}/p38\delta^{-/-}$ cells, but not $p38\gamma/\delta^{-/-}$ BMDM expressed normal levels of Tpl2 and ABIN2 (Fig. R-24A). We examined the transient phosphorylation of ERK1/2, finding that this was blocked in the absence of both p38γ/p38δ in LPS stimulated BMDM. In contrast, in $p38\gamma^{171A/171A}$, $p38\gamma^{-/-}$ and $p38\gamma^{171A/171A}/p38\delta^{-/-}$ cells, were found to have the same transient phosphorylation of ERK1/2 than in WT BMDM (Fig. R-24A). JNK phosphorylation in LPS stimulated $p38\gamma/\delta^{-/-}$ BMDM was consistently delayed when comparing with WT, $p38\gamma^{171A/171A}$, $p38\gamma^{-/-}$ and $p38\gamma^{171A/171A}/p38\delta^{-/-}$ BMDM (Fig. R-24A). Finally, we observed that p38α, and p105 transient phosphorylation was similar in all genotypes under LPS stimulation. Our results show that WT, $p38\gamma^{171A/171A}$, $p38\gamma^{-/-}$ and $p38\gamma^{171A/171A}/p38\delta^{-/-}$ BMDM express active Tpl2, while the loss of p38γ and p38δ blocked ERK1/2 phosphorylation because of the significant decrease of Tpl2 and ABIN2 protein levels (Fig. R-24A).

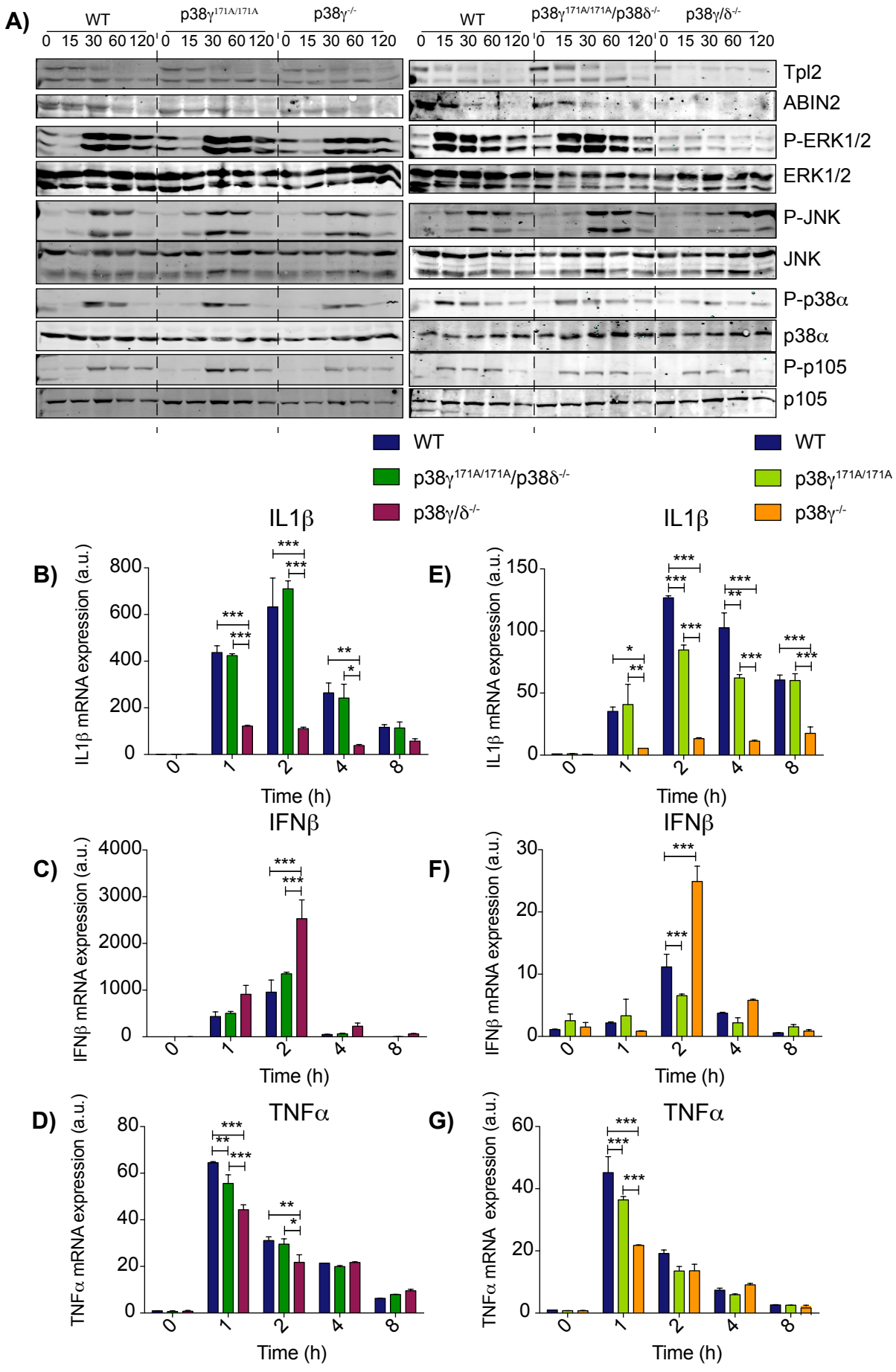
A)
WT
p38γ171A/171A
p38γ-/-
WT
p38γ171A/171A/p38δ-/-
p38γ/δ-/-
0 15 30 60 120
Tpl2
ABIN2
P-ERK1/2
ERK1/2
P-JNK
JNK
P-p38α
p38α
P-p105
p105
WT
p38γ171A/171A/p38δ-/-
p38γ/δ-/-
WT
p38γ171A/171A
p38γ-/-
B)
IL1β
IL1β mRNA expression (a.u.)
Time (h)
E)
IL1β
IL1β mRNA expression (a.u.)
Time (h)
C)
IFNβ
IFNβ mRNA expression (a.u.)
Time (h)
F)
IFNβ
IFNβ mRNA expression (a.u.)
Time (h)
D)
TNFα
TNFα mRNA expression (a.u.)
Time (h)
G)
TNFα
TNFα mRNA expression (a.u.)
Time (h)

Figure R-24. MAPK signalling activation and cytokine production induced by LPS in p38γ$^{171A/171A}$/p38δ$^{-/-}$ BMDM. BMDM from WT, p38γ$^{171A/171A}$, p38γ$^{-/-}$, p38γ$^{171A/171A}$/p38δ$^{-/-}$ and p38γ/δ$^{-/-}$ mice were stimulated with 100 ng/ml of LPS in the indicated times. **A)** Cell lysates (30 µg) were immunoblotted with the indicated antibodies. **B to G)** Total mRNA levels of **B, E)** ILlβ, **C, F)** IFNβ and **D, G)** TNFα were measured by qPCR in BMDM. Data show mean ± SEM from one representative experiment of three with similar results. **P*≤ 0.05, ***P*≤0.01, ****P*≤0.001 relative to WT control.

Quantitative PCR was used to determine the effect of p38γ/p38δ activities in LPS induced cytokine transcription in BMDM. (Fig. R-24B to G). We observed that loss of either p38γ alone or p38γ/p38δ reduced LPS induction of *IL1β* mRNA, whereas *IFNβ* mRNA production was increased (Fig. R-24B, C, E and F). Presence of inactive p38γ in p38γ$^{171A/171A}$ and p38γ$^{171A/171A}$/p38δ$^{-/-}$ cells, was sufficient to maintain normal transcription levels of *IL1β* and *IFNβ* mRNA (Fig. R-24B, C, E and F). Our results indicate that p38γ regulates *IL1β* and *IFNβ* mRNA transcription independently of its kinase activity. On the other hand, the production of *TNFα* mRNA was unaffected by the loss of p38γ (activity or protein) and p38δ (Fig. R-24D and G).

4.4.2 p38γ$^{171A/171A}$/p38δ$^{-/-}$ mice have the same behaviour as the WT mice in the LPS/D-Gal induced sepsis.

LPS/D-Gal induced septic shock is a well-characterized mouse model in which the innate immune response leads to sepsis by the overproduction of cytokines. Bacterial LPS is a TLR4-ligand, while D-Gal is a transcriptional inhibitor that enhances septic shock by inhibiting hepatic transaminase. To study the role of p38γ and p38δ in septic shock induced by LPS/D-Gal intraperitoneal injection, we used sex- and age-matched WT, p38γ$^{171A/171A}$, p38γ$^{-/-}$, p38δ$^{-/-}$, p38γ$^{171A/171A}$/p38δ$^{-/-}$ and p38γ/δ$^{-/-}$ mice. We confirmed that mice with complete loss of both p38γ and p38δ were the most resistant to septic shock and ~10% of the mice survived (Fig. R-24A).

The rest of the mouse line examined behaved similar to WT mice (Fig. R-24B). Surprisingly, p38$\gamma^{171A/171A}$/p38$\delta^{-/-}$ mice died at similar rate than WT indicating that just p38γ expression was sufficient to revert the effect caused by the lack of p38γ and p38δ in p38γ/p38$\delta^{-/-}$ mice (Fig. R-24B).

To examine if p38γ and p38δ deficiency affected cytokine release *in vivo*, we measured, by Luminex, proinflammatory (TNFα and IL6) and anti-inflammatory (IL10) cytokines from mouse serum at 2 h post-injection. We observed that TNFα was substantially reduced in p38$\gamma^{-/-}$, p38$\gamma^{171A/171A}$/p38$\delta^{-/-}$ and p38$\gamma/\delta^{-/-}$ mice, indicating that this cytokine production is dependent on the kinase activity of p38γ (Fig. R-25C). IL6 was severely decreased in p38$\gamma/\delta^{-/-}$ mice, while p38$\gamma^{171A/171A}$, p38$\gamma^{-/-}$, p38$\delta^{-/-}$ and p38$\gamma^{171A/171A}$/p38$\delta^{-/-}$ had similar results to WT (Fig. R-25D). These results suggested that Tpl2/ABIN2/p105 complex is essential for the induction of IL6 production. The last cytokine we measured was the anti-inflammatory cytokine IL10 (Fig. R-25E), which significantly increases in p38$\delta^{-/-}$ and decreases in p38$\gamma/\delta^{-/-}$ mice. In contrast, IL10 production in p38$\gamma^{171A/171A}$, p38$\gamma^{-/-}$, and p38$\gamma^{171A/171A}$/p38$\delta^{-/-}$ mice were not significantly different from WT mice.

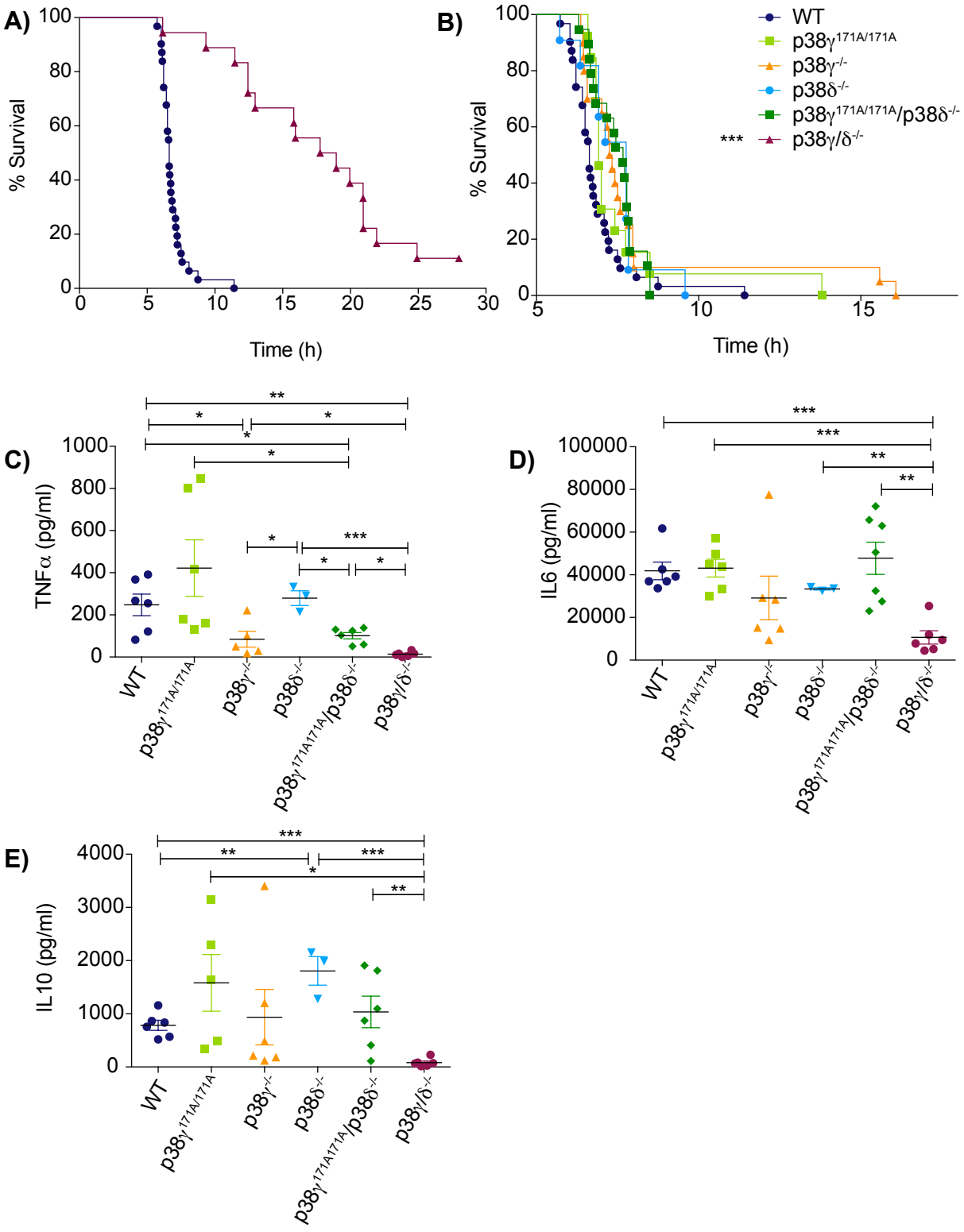

Figure R-25. LPS/D-Gal septic shock induces the same mortality in p38γ$^{171A/171A}$/p38δ$^{-/-}$ as in WT mice. A) and **B)** Mice were injected with LPS (50 µg/kg of mouse) and D-Gal (1 g/kg of mouse) and survival was monitored until 36 h. **A)** WT (n = 31) and p38γ/δ$^{-/-}$ (n = 18). **B)** WT (n = 31), p38γ$^{171A/171A}$ (n = 13), p38γ$^{-/-}$ (n= 20), p38δ$^{-/-}$ (n = 11) and p38γ$^{171A/171A}$/p38δ$^{-/-}$ (n = 19). Results were shown as % of the initial mouse number. *P≤0.05 or ***P≤0.001

relative to WT by Kaplan-Meier test and Log-rank curve comparison. **C, D, E)** Mice were bled at 2 h post- LPS/D-Gal injection and **C)** TNFα, **D)** IL6 and **E)** IL10 were measured by Luminex assay (n = 3 – 6) from the serum. Data show mean ± SEM from one representative experiment of two with similar results. *$P \leq 0.05$, **$P \leq 0.01$, ***$P \leq 0.001$ relative to WT control. Each symbol represents a mouse.

In the LPS/D-Gal septic shock model, D-Gal enhances the response promoting liver damage by inhibiting hepatic transaminase. We extracted the liver at 6 h post-injection to evaluate the damage caused by LPS/D-Gal. We evaluated haemorrhage and measured the apoptotic levels as markers of hepatic damage. First, we analysed the bleeding of the liver by haematoxylin and eosin staining (Fig. R-26A). We observed that $p38\gamma^{171A/171A}$ and $p38\gamma^{171A/171A}/p38\delta^{-/-}$ mice had more haemorrhage that the other genotype (Fig. R-26A). Secondly, we quantified the apoptosis in the liver using TUNEL staining. The level of apoptosis in $p38\gamma^{171A/171A}$ mice was higher than in the rest of the mouse line, although this was not statistically different from WT mice (Fig. R-26B, C).

TNFα production levels correlated with the apoptotic state of the liver, but this result did not entirely correlate with the survival curves of the different mouse lines.

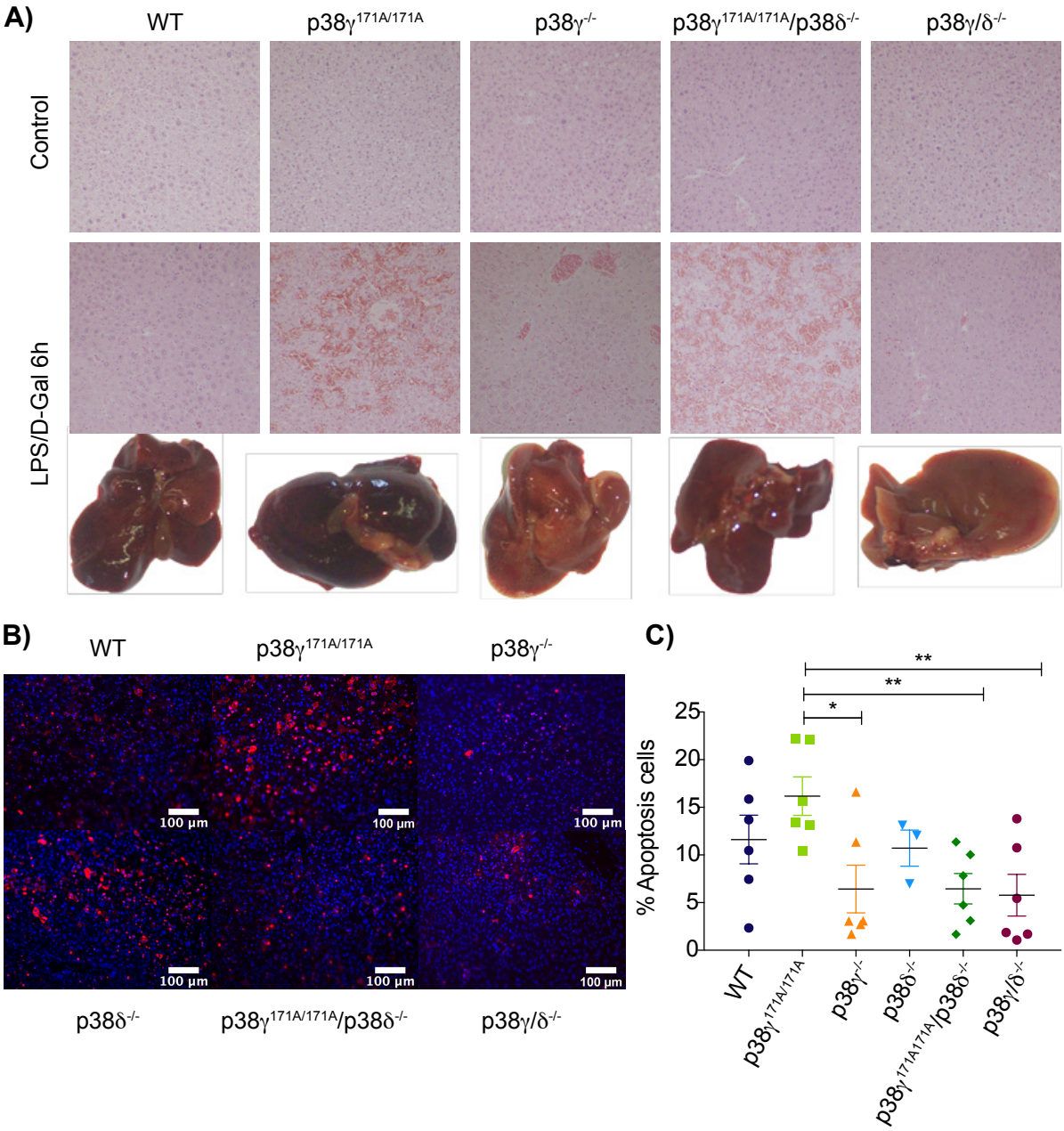

Figure R-26. p38γ affects liver damage caused by LPS/D-Gal induced septic shock. Mice were injected with LPS (50 µg/kg of mouse) and D-Gal (1 g/kg of mouse) and liver was analysed at 6 h post-injection. **A)** The liver of WT, p38γ$^{171A/171A}$, p38γ$^{-/-}$, p38γ$^{171A/171A}$/p38δ$^{-/-}$ and p38γ/δ$^{-/-}$ was extracted and liver sections stained with Haematoxylin/eosin (n= 3). **B, C)** Livers from WT, p38γ$^{171A/171A}$, p38γ$^{-/-}$, p38δ$^{-/-}$, p38γ$^{171A/171A}$/p38δ$^{-/-}$ and p38γ/δ$^{-/-}$ mice (n = 6) were extracted at 6 h post-injection. Liver sections were stained with TUNEL and positive/negative cells were quantified with image j programme and the % of apoptotic cells per section calculated. Cells from 25 sections were counted per mouse. Data show mean ± SEM from one representative experiment with similar results. *P≤0.05 and **P≤0.01. Each symbol represents data from one mouse.

4.4.3 Analysis of the TLR4-induced gene expression in p38γ$^{171A/171A}$/p38δ$^{-/-}$ BMDM.

We next examined gene expression regulated by p38γ/p38δ, but not by Tpl2, in macrophages. For this, we performed RNA-sequencing of BMDM from WT and p38γ$^{171A/171A}$/p38δ$^{-/-}$ mice, stimulated or not with LPS for 30 or 60 min.

To study TLR4 signalling pathway in more depth, we designed an experiment for RNA-sequencing analysis. This experiment was performed in BMDM stimulated with LPS for 0, 30 and 60 min from 6 different male mice that were age-matched for WT and p38γ$^{171A/171A}$/p38δ$^{-/-}$ cells (Fig. R-27A).

Difference between p38γ$^{171A/171A}$/p38δ$^{-/-}$ vs WT for each of the time points were calculated obtaining *p*-value and log_2FC for each gene. The selected genes were statistically significant, *p*-value <0.05, and with a selected expression level, -1.5<logFC<1.5. Basal transcript level 0 and 30 min had ~30 genes, while at 60 min samples increased to ~70 genes (Fig. R-27A). As expected, LPS induced the expression of more genes with time and the difference between WT and p38γ$^{171A/171A}$/p38δ$^{-/-}$ mice was more significant. To assess the overall similarities between the selected gene we plotted the Euclidean distance between principal components analysis (PCA), it indicates that WT 0 and 60 min have very similar behaviour and it is 30 min that has a more differentiated behaviour (Fig. R-27B). For p38γ$^{171A/171A}$/p38δ$^{-/-}$ macrophages we observed that all three conditions differ and the ellipse represented the variability of a broad type of response. We represented the 78 differentially expressed genes in a heatmap representation, here we observed that many of the genes are overexpressed mostly in p38γ$^{171A/171A}$/p38δ$^{-/-}$ BMDM after 60 min LPS stimulation (Fig. R-27C).

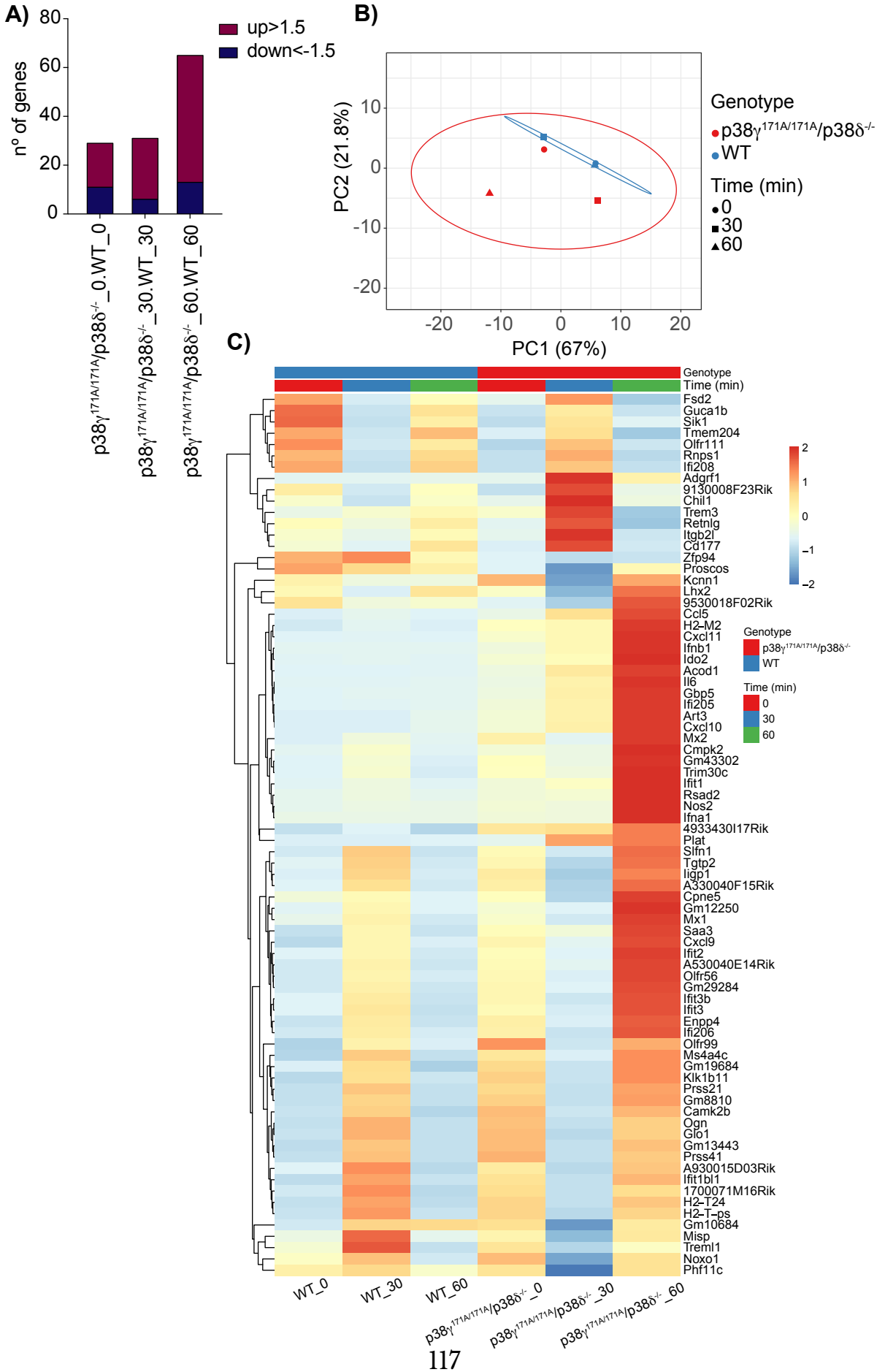
A)
nº of genes
up>1.5
down<-1.5
p38γ171A/171A/p38δ-/- _0.WT_0
p38γ171A/171A/p38δ-/- _30.WT_30
p38γ171A/171A/p38δ-/- _60.WT_60
B)
PC2 (21.8%)
PC1 (67%)
Genotype
p38γ171A/171A/p38δ-/-
WT
Time (min)
0
30
60
C)
Genotype
Time (min)
Fsd2
Guca1b
Sik1
Tmem204
Olfr111
Rnps1
Ifi208
Adgrf1
9130008F23Rik
Chil1
Trem3
Retnlg
Itgb2l
Cd177
Zfp94
Proscos
Kcnn1
Lhx2
9530018F02Rik
Ccl5
H2-M2
Cxcl11
Ifnb1
Ido2
Acod1
Il6
Gbp5
Ifi205
Art3
Cxcl10
Mx2
Cmpk2
Gm43302
Trim30c
Ifit1
Rsad2
Nos2
Ifna1
4933430I17Rik
Plat
Slfn1
Tgtp2
Iigp1
A330040F15Rik
Cpne5
Gm12250
Mx1
Saa3
Cxcl9
Ifit2
A530040E14Rik
Olfr56
Gm29284
Ifit3b
Ifit3
Enpp4
Ifi206
Olfr99
Ms4a4c
Gm19684
Klk1b11
Prss21
Gm8810
Camk2b
Ogn
Glo1
Gm13443
Prss41
A930015D03Rik
Ifit1bl1
1700071M16Rik
H2-T24
H2-T-ps
Gm10684
Misp
Treml1
Noxo1
Phf11c
WT_0
WT_30
WT_60
p38γ171A/171A/p38δ-/- _0
p38γ171A/171A/p38δ-/- _30
p38γ171A/171A/p38δ-/- _60

Figure R-27. Bioinformatical differential analysis of RNA-sequencing data from p38γ$^{171A/171A}$/p38δ$^{-/-}$ LPS stimulated BMDM. BMDM from 6 WT or p38γ$^{171A/171A}$/p38δ$^{-/-}$ male mice were non-stimulated or stimulated with LPS for 30- or 60- min. Using R with Bioconductor packages (DESeq2 1.18.1 package) (Love et al., 2014) logFC and adjusted *p*-value was calculated. **A)** Number of filtered up- and down-genes, with adjusted *p*-value <0.05 and -1.5<logFC<1.5 comparing p38γ$^{171A/171A}$/p38δ$^{-/-}$ control vs WT control, p38γ$^{171A/171A}$/p38δ$^{-/-}$ 30 min vs WT 30 min stimulation with LPS and p38γ$^{171A/171A}$/p38δ$^{-/-}$ 60 min vs WT 60 min stimulation with LPS. **B)** PCA plot of the Euclidian distance between the selected list of 78 genes obtained and visualized with the web tool 'clustvis'. **C)** Heatmap representation with the web tool 'clustvis'.

To validate the RNA-sequencing analysis we selected a few genes (*nos2*, *sik1* and *camk2b*) and performed quantitative PCR analysis. We observed that *nos2* (nitric oxide synthesis), *sik1* (salt-induced kinase) and *camk2b* (Calcium/Calmodulin Dependent protein kinase II beta) are altered by the loss of p38δ. *nos2* mRNA is induced by LPS stimuli, while *sik1* mRNA is decreased at basal state levels and does not change with LPS stimulation (Fig. R-28A and B). On the other hand, *camk2b* was blocked by p38δ from basal state and could not decrease with LPS stimulation. At the same time, *camk2b* was also regulated by the kinase activity of p38γ blocking the reduction induced by LPS stimulation (Fig. R-28C).

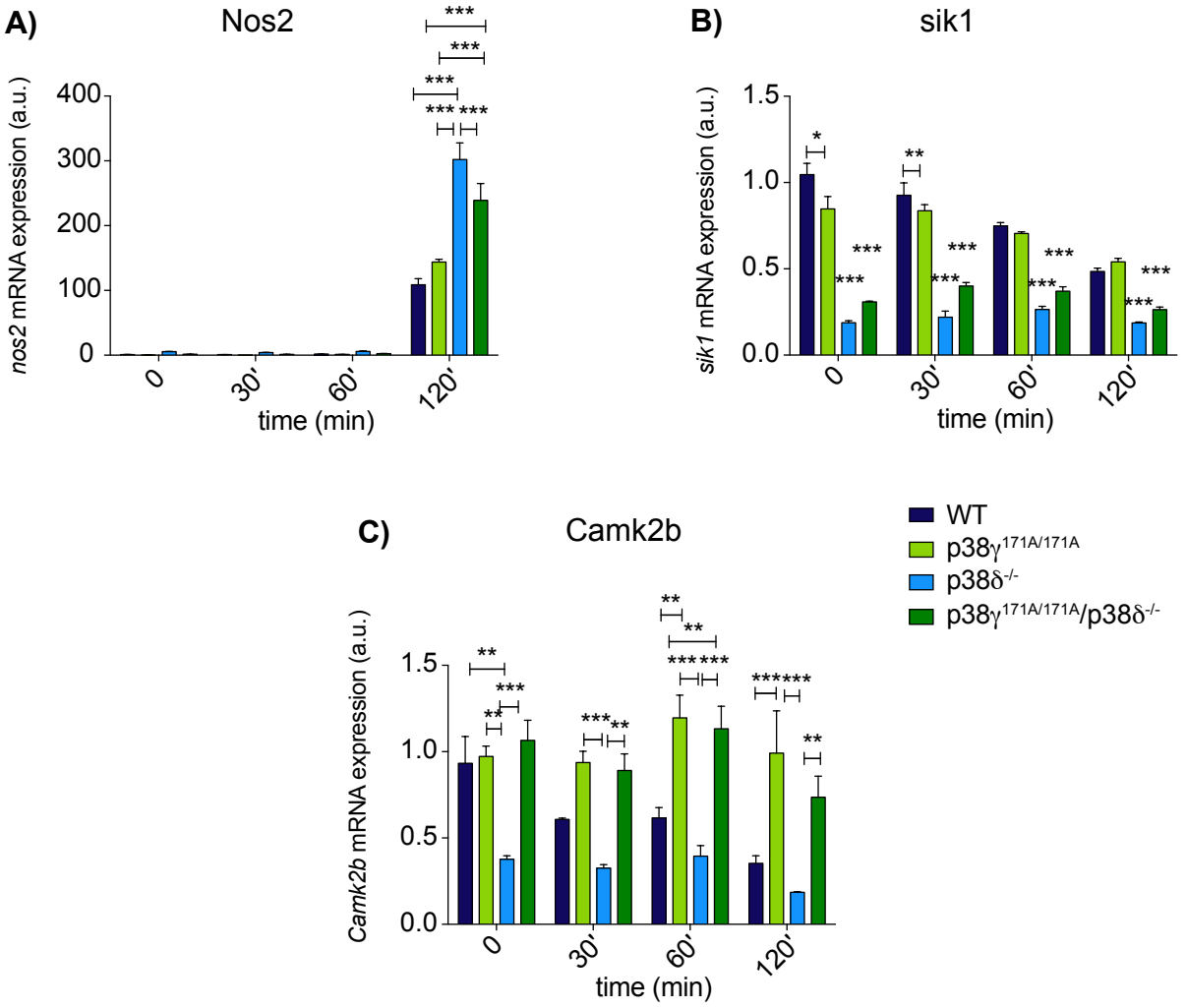

Figure R-28. Validation of p38γ$^{171A/171A}$/p38δ$^{-/-}$ BMDM RNA-sequencing analysis. BMDM from WT, p38γ$^{171A/171A}$, p38δ$^{-/-}$ and p38γ$^{171A/171A}$/p38δ$^{-/-}$ mice were stimulated with 100 ng/ml of LPS for the indicated times. Relative mRNA expression was determined by qPCR for **A)** *nos2*, **B)** *sik1* and **C)** *Camk2b*. Results were normalized to *β-actin* mRNA expression and x-fold induction was calculated relative to WT expression at 0 h. Data show mean ± SEM from one representative experiment of two in triplicate, with similar results. **P*≤0.05, ***P*≤0.01, ****P*≤0.001 relative to WT control.

We next performed functional classification analysis of the 78 selected genes using the Database of Annotation, Visualization and Integrated Discovery (DAVID) Bioinformatic resources through classification into Gene ontology (GO) categories as well as KEGG, and found that the genes are related with innate immune response to virus and to IFN-β production (Fig. R-29A).

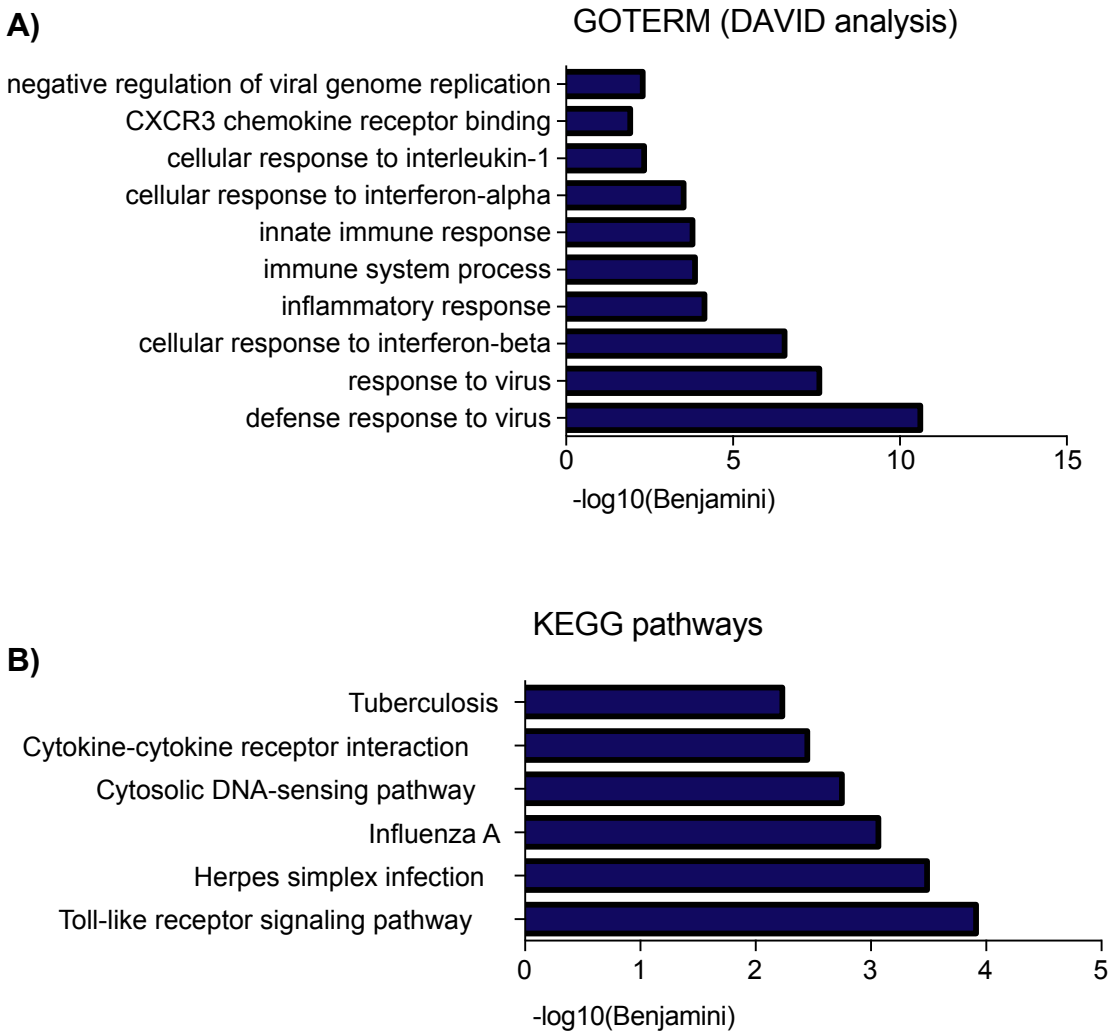

Figure R-29. DAVID enrichment analysis of the selected genes from WT and p38γ$^{171A/171A}$/p38δ$^{-/-}$ LPS stimulated BMDM. BMDM from 6 WT or p38γ$^{171A/171A}$/p38δ$^{-/-}$ male mice were non-stimulated or stimulated with LPS for 30- or 60-min. Selection of differentially expressed genes were analysed for enrichment with DAVID for **A)** GO terms and **B)** KEGG pathways.

In KEGG pathway enrichment analysis Herpes simplex infection, influenza A and Tuberculosis were the most enriched terms (Fig. R-29B). This analysis indicated that p38γ and p38δ deficiency affects TLR4 signalling and that they are involved in virus defence, while p38δ in particular regulates IFN type I transcription (Fig. R-30).

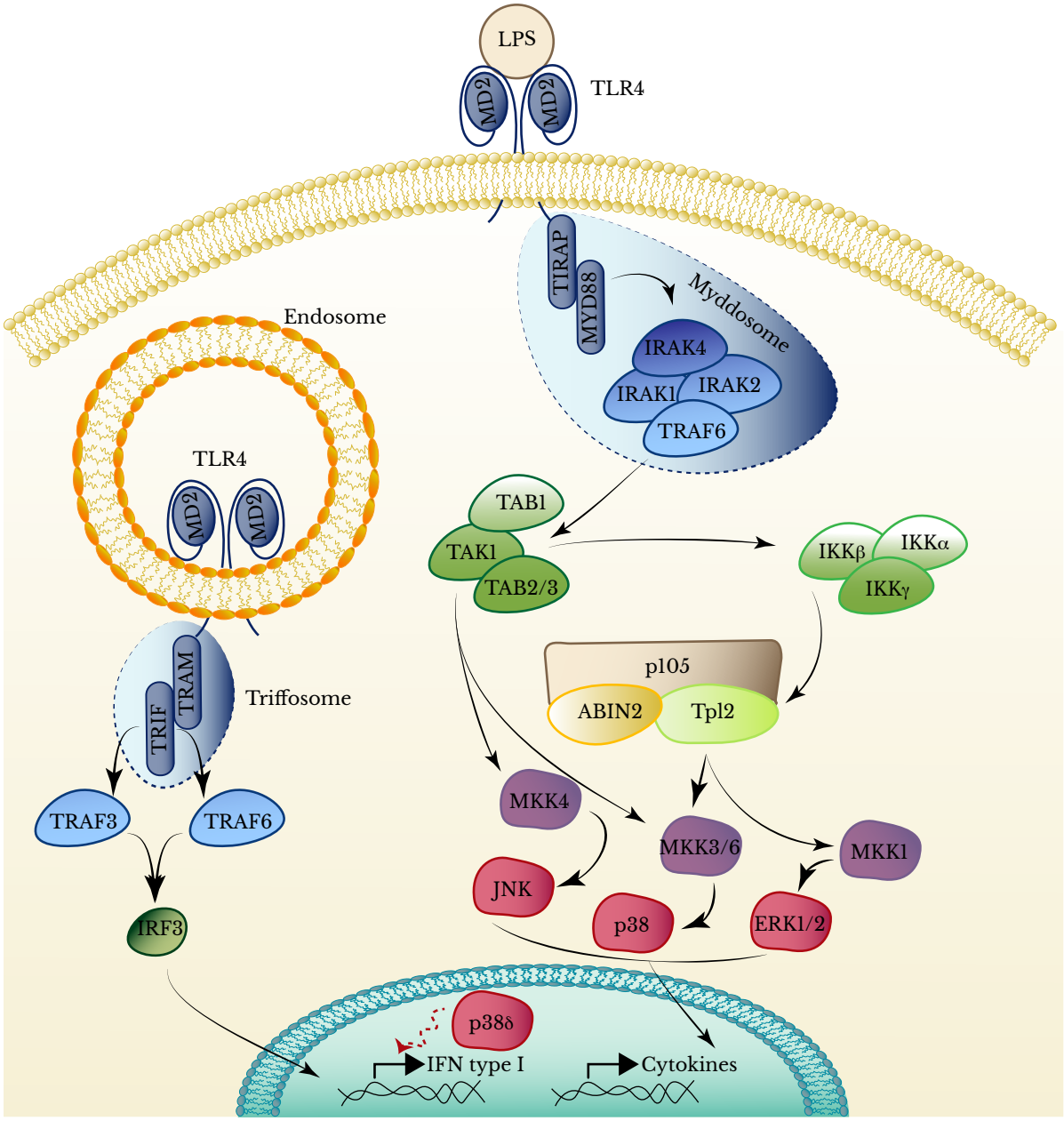

Figure R-29. Schematic representation of TLR4 signalling in macrophages. TLR4-MD2 activation recruits IRAK family proteins activations TRAF6 and forming the Myddosome supramolecular complex. TRAF6 activates MAP3K TAK1 that activates IKKβ-Tpl2-MKKs while activating at the same time MKKs. MAPKs are then activated and cytokine production is induced. Once LPS-TLR4-MD2 is activated it is also internalised where through the early endosome interacts with TRAM/TRIF for Triffosome formation. This complex activates TRAF3 and 6 for IRF3 translocation to induce IFN type I production, where p38δ seems to be involved in regulating their transcription.

Discussion

5 Discussion

5.1 Chapter 1. *C. albicans* signalling pathway in BMDM.

Our research shows that p38γ/p38δ are essential for the cytokine production in macrophages in response to Dectin-1 receptor activation. Using BMDM from different knock out mice in combination with kinase inhibitors, we have been able to amplify the knowledge of Dectin-1 signalling pathway in macrophages. Dectin-1 receptor is one of the main CLR in macrophages and is activated by *C. albicans* infection. The absence of p38γ/p38δ in macrophages infected with *C. albicans* induces a decrease in the production of cytokine and chemokine that play an important role during fungal infection (Alsina-Beauchamp et al., 2018; Brown, 2011; Swamydas et al., 2015). We have previously described that in p38γ/δ$^{-/-}$ BMDM cytokine and chemokine production is disrupted due to the regulation of steady-state levels of Tpl2 by p38γ/p38δ (Risco et al., 2012). In this thesis, we have demonstrated that Tpl2-MKK1-ERK1/2 signalling is downstream of Dectin-1 receptor in BMDM, therefore the absence of p38γ/p38δ blocks Dectin-1 signalling and cytokine production. It was previously known that Dectin-1 receptor activated ERK1/2 and NF-κB canonical pathways (Geijtenbeek and Gringhuis, 2009; Netea et al., 2015; Reid et al., 2009), nevertheless the intermediate steps to achieve this activation were not known. After the specific stimulation with Curdlan, the Syk adaptor molecule is recruited to Dectin-1 receptor, this is required for the assembly of two protein complexes: CARD9/RasGRF1/H-Ras (Jia et al., 2014) and CARD9/BCL-10/MALT1 (Cohen, 2014; Geijtenbeek and Gringhuis, 2009). The first complex CARD9/RasGRF1/H-Ras, has been shown to activate Raf-1 in BMDM. The Raf-1 inhibitor, Sorafenib, blocked ERK1/2 phosphorylation in response to the specific Dectin-1 agonist, curdlan, concluding that Raf-1 was the kinase responsible for MKK1-ERK1/2 activation downstream of CARD9/RasGRF1/H-Ras. Regarding the

second complex, CARD9/BCL-10/MALT1, we describe in this thesis that activates the TAK1-IKKβ-Tpl2-MKK1-ERK1/2 signalling. It has been shown that the SMOC formation is essential for TAK1 activation and signalling of IKK complex (Cohen, 2014; Geijtenbeek and Gringhuis, 2009; Gorjestani et al., 2012; Kieser and Kagan, 2017). Therefore, we propose that Dectin-1 receptor induces Syk-SMOC-TRAF6-TAK1-IKKβ-Tpl2-MKK1-ERK1/2 signalling in macrophages. In consequence, the absence of p38γ/p38δ disrupts this signalling pathway by regulating the steady state levels of Tpl2 (Fig. D-1).

5.2 Chapter 2. Regulation of *Tpl2/ABIN2 protein levels by* p38γ and p38δ.

Tpl2/ABIN2/p105 complex is essential to induce cytokines and chemokines production in the inflammatory process. The absence of p38γ/p38δ decreases Tpl2 and ABIN2 steady-state protein levels of by an unknown mechanism, and therefore blocks TLR4 signalling pathway. This chapter was dedicated to unravel the mechanism by which p38γ/p38δ regulate Tpl2/ABIN2 protein levels (Risco et al., 2012).

First, we established that the absence of p38γ/p38δ induced the decrease of Tpl2 and ABIN2 protein levels in the whole mice. We analysed by immunoblot Tpl2 and ABIN2 in different tissues comparing WT with p38γ/δ$^{-/-}$ mice, and found that Tpl2 and ABIN2 protein levels in different mouse tissues were lower in p38γ/δ$^{-/-}$ compared to WT. One of the processes regulated by Tpl2 and ABIN2 in macrophages is the production of cytokines after TLR activation (Gantke et al., 2011; Xu et al., 2018). We observed that peritoneal macrophages from p38γ$^{-/-}$ and p38δ$^{-/-}$ mice had less Tpl2 than WT, while ABIN2 proteins levels were similar to WT. In contrast, p38γ/δ$^{-/-}$ peritoneal macrophages had lower protein level of both Tpl2 and ABIN2 than p38γ$^{-/-}$, p38δ$^{-/-}$ or with WT cells. These results indicated that the regulation of the steady-state levels of Tpl2 by p38γ/p38δ was stronger than the regulation of ABIN2.

We also have used MEF, among others, to study how p38γ/p38δ regulate Tpl2 and ABIN2 steady-state protein levels. MEF cells have been widely used by other laboratories to study Tpl2 signalling pathway, in parallel to primary cells studies (Xiao et al., 2014). It has been shown that in MEF, TNFα and IL1β activate Tpl2 signalling (Das et al., 2005), and that TAK1 activates Tpl2 (Xiao et al., 2014). We checked if p38γ/δ$^{-/-}$ MEF had the same levels of Tpl2 and ABIN2 than WT, and, examining phospho-ERK1/2, if the LPS stimulated signalling pathway was blocked by the absence of p38γ/p38δ. We confirmed that p38γ/δ$^{-/-}$ MEF behave similar to

p38γ/δ$^{-/-}$ BMDM, they have lower Tpl2 and ABIN2 protein levels than WT cells and ERK1/2 phosphorylation was blocked after LPS stimulation.

Tpl2 has been thoroughly studied and it was discovered, by Steve Dr. Steve Ley´s laboratory, to be part of the Tpl2/ABIN2/p105 ternary complex (Lang et al., 2004). Other interactors have been reported for this complex, such as the member of the NF-κB family, the protein RelAP43 with a role in rabies virus infection (Besson et al., 2017) or 14-3-3 proteins that interact with phosphorylated Tpl2 C-terminal domain and are needed for the correct activation of ERK1/2 (Ben-Addi et al., 2014). Tpl2 is found unstable when is not in a protein complex, so our hypothesis was that p38γ and/or p38δ were interacting with Tpl2 and therefore stabilizing it (Lang et al., 2004). Our results from gel filtration experiments indicated that, at least p38δ, could interact with the Tpl2/ABIN2/p105 complex in the mouse macrophage cell line Raw264.7. We found that all the proteins from the ternary complex, Tpl2/ABIN2/p105, co-eluted together above 669 KDa fraction, which correlated with results from other groups (Gantke et al., 2013). We observed that p38δ was predominantly found co-eluting with the complex above 669 KDa fraction. In contrast, p38γ was predominantly eluting at its monomeric molecular weight fraction (~40 KDa). These results suggested a possible interaction of p38δ with Tpl2/ABIN2/p105 complex. Nonetheless, we cannot exclude the possibility that p38γ was also interacting with the Tpl2/ABIN2/p105 complex, since: i) we needed to delete p38γ/p38δ together to completely diminish the protein levels of Tpl2 and ABIN2; and ii) these two p38 isoforms have high sequence homology, of ~70%, and one can substitute the other in certain complexes as it has been shown with their interaction with DEPTOR (González-Terán et al., 2016). Our results from pull-down assays in HEK293 cells overexpressing the Tpl2/ABIN2/p105 complex with p38γ or p38δ, showed that the complex interacted with either p38MAPK. We also discovered that only Tpl2 interacted with p38γ and p38δ.

The function of Tpl2/ABIN2/p105 ternary complex is to maintain the steady-state protein levels of Tpl2 and ABIN2 and prevent them from being proteolyzed by the proteasome (Lang et al., 2004; Sriskantharajah et al., 2014). To determine if the role of p38γ/p38δ was to maintain the complex stability we analysed Tpl2 and ABIN2 stability in p38γ/δ$^{-/-}$ cells and compared with WT. Our results indicated that GST-Tpl2 was less stable when expressed in p38γ/δ$^{-/-}$ than in WT MEF, while GST-ABIN2 was found to have similar stability levels in WT and p38γ/δ$^{-/-}$ MEF. Similar results were observed with endogenous Tpl2 and ABIN2 and BMDM and MEF. When we studied Tpl2 stability in single knock-outs, p38γ$^{-/-}$ and p38δ$^{-/-}$ MEFs, to elucidate which specific p38 isoform is regulating it, we obtained similar results as the ones in p38γ/δ$^{-/-}$ MEF. This indicate that either p38γ or p38δ can stabilise Tpl2, and agrees with: i) the results obtained from the interaction experiments in which both p38γ/p38δ bind to Tpl2; ii) with the observation that Tpl2 protein levels in p38γ$^{-/-}$, p38δ$^{-/-}$ and WT MEF and BMDM are similar, and iii) that to see a complete decrease in Tpl2 levels the deletion of both p38γ/p38δ is necessary. Tpl2 and ABIN2 stability are intricately related, since these two proteins regulate each other (Lang et al., 2004; Sriskantharajah et al., 2014). Therefore, it is possible that p38γ/δ$^{-/-}$ MEF did not express Tpl2 because did not have ABIN2. We observed that ABIN2 and p38γ/p38δ stabilized GST-Tpl2 in p38γ/δ$^{-/-}$ MEF although not to the same extent than in WT MEF.

Both Tpl2 and ABIN2 are continuously proteolyzed by the proteasome (Gándara et al., 2003; Lang et al., 2004). By inhibiting the proteasome in p38γ/δ$^{-/-}$ MEF or BMDM we tested if Tpl2 protein increased and if this increase reached similar levels of that of WT cells in the same conditions. Tpl2 protein levels increase in both WT and p38γ/δ$^{-/-}$ BMDM, and similar results were obtained in MEF, although the effect in these cells was less pronounced than in macrophages. The increase of Tpl2 protein

in p38γ/δ$^{-/-}$ cells incubated with the proteasome inhibitor MG132 never reached the levels of that in WT treated with MG132 suggesting that there was another mechanism (different that of proteolysis) at play to explain the low Tpl2 protein levels in p38γ/δ$^{-/-}$ cells. On the other hand, after MG132 treatment, ABIN2 protein was increased in p38γ/δ$^{-/-}$ cells, but again never to the levels found in WT post-MG132 incubated cells. The same result was observed in MEF and BMDM. Tpl2 and ABIN2 protein levels in p38γ/δ$^{-/-}$ cells were lower than those of WT cells, although mRNA studies showed that *Tpl2* and *ABIN2* mRNA total levels and transport was the same in WT and p38γ/δ$^{-/-}$ cells. These results together indicated that the translation of *Tpl2* and *ABIN2* mRNA to Tpl2 and ABIN2 protein is deceased in p38γ/δ$^{-/-}$ cells, and therefore, p38γ/p38δ might be regulating the specific translation of *Tpl2* and *ABIN2* mRNA.

We first analysed polysome profiles of WT and p38γ/δ$^{-/-}$ MEF to check if p38γ/p38δ were altering the general translation proteins, and then extracted and quantified *Tpl2* and *ABIN2* mRNA from polysome fractions to examine if there were any difference in their fraction distribution between WT and p38γ/δ$^{-/-}$ MEF. Polysome profile analysis was performed to separate free ribosomes and ribosomal subunits (40S, 60S and 80S monosome) from translating ribosomes (polysomes) of WT and p38γ/δ$^{-/-}$ MEF lysates, in sucrose gradient. When comparing p38γ/δ$^{-/-}$ and WT MEF polysome profiles we observed that p38γ/δ$^{-/-}$ cells had higher 256 nm values in the ribosomal subunits 40S and 60S, while 256 nm values were lower in the polysome region indicating less translation. We generated Flp-In T-REx HEK293 p38γ/δ$^{-/-}$ cells to test the consistency of the polysome results in a human cell line, and we found similar results to those in MEFs. These results indicated lower translation in p38γ/δ$^{-/-}$ in comparison with WT Flp-In T-REx HEK293, since we observed higher 256 nm values of 80S monosome fraction and lower in the polysome region. Our results indicate that both p38γ/p38δ are very important not

only regulating Tpl2 and ABIN2 protein levels but also regulating general protein translation in mouse and in human cells. Quantification of *Tpl2* and *ABIN2* mRNA levels from polysome profile fractions show that *Tpl2* mRNA was more abundant in the 40S and 60S ribosomal subunits fractions and in the 80S monosome in p38γ/δ$^{-/-}$ when compared with WT MEF. Opposite results were obtained in the polysome fractions, where *Tpl2* mRNA in p38γ/δ$^{-/-}$ MEF in the polysome fractions was lower than in the WT MEF polysome fractions. Regarding *ABIN2* mRNA we found that it accumulated in the first fractions (supernatant, fractions with ribosomal material) in p38γ/δ$^{-/-}$ compared to WT MEF. With these results we confirmed that both *Tpl2* and *ABIN2* mRNA are regulated at translational level by p38γ and/or p38δ, which would regulate specific mRNA translation of *Tpl2* and *ABIN2*, and general protein translation. The regulation of the general protein translation by p38γ and/or p38δ could be due to their effect on Tpl2 protein levels itself, since p38γ/δ$^{-/-}$ cells do not have Tpl2 and this protein has already been established to be involved in regulating cap-dependent translation (López-Pelaéz et al., 2012).

Analysing *Tpl2* and *ABIN2* mRNA sequences, using several databases and the bibliography, we performed a theoretical study to identify possible regulators of their translation, and we selected RBPs that could be regulated by p38γ/p38δ. These RBPs, ZFP36, NONO and PABPC1, bind to the 3'UTR mRNA sequences of both *Tpl2* and/or *ABIN2* mRNA, and could be regulated by p38MAPK (Tiedje et al., 2016). ZFP36, has been demonstrated to be phosphorylated by p38α/MK2 signalling (Chrestensen et al., 2004); NONO appears interacting with p38γ in our interactome analysis; and PABPC1, induces ribosome recruitment and translation initiation through p38α/MK2 signalling (Bollig et al., 2003). To study if p38γ/p38δ regulate Tpl2 and ABIN2 protein translation by affecting the *Tpl2* and *ABIN2* 3'UTRs, we cloned these sequences in bicistronic luciferase reporter vectors. With this bicistronic reporter system we can monitor the regulation of *Renilla* translation by *Tpl2* and *ABIN2* 3'UTRs,

using an empty vector as control. We found that *Tpl2* 3'UTR repressed *Renilla* expression in p38γ/δ$^{-/-}$ cells, comparing with WT, whereas *ABIN2* 3'UTR did not alter *Renilla* translation. It seems to exist more than one mechanism regulating specific protein translation and we also have to consider that Tpl2 is known to regulate cap-dependent translation (López-Pelaéz et al., 2012), which could be affecting ABIN2 specific translation in p38γ/δ$^{-/-}$ cells that express low levels of Tpl2. With the generation of p38γ/δ$^{-/-}$ MEF that stably express either p38γ or p38δ, we show evidence that p38δ alone rescued Tpl2 protein translation (Renilla-*Tpl2* 3'UTR translation) and expression (immunoblot). We silenced the RBPs, ZFP36, NONO and PABPC1 in WT and p38γ/δ$^{-/-}$ MEF, but we did not reach a definitive conclusion from these experiments due to not observing a decrease in the expression of Tpl2 in silenced WT to the same levels of found in p38γ/δ$^{-/-}$ MEF.

To elucidate the molecular mechanism(s) by which p38γ/p38δ regulate protein translation (the general and specific of *Tpl2* and *ABIN2* mRNA) we determined their interactome and phospho-proteome in macrophages. We found that the group of proteins that bind to p38γ was significantly enriched in ribosomal proteins; therefore, we expected p38γ to play important role in the translation process. p38γ could be modulating translation by affecting the composition of ribosomal protein complex and therefore, regulating mRNAs selectively (Shi et al., 2017). At the same time, p38δ interacts with two eukaryotic elongation factors, eEF2 and eEF1A. It has been already shown that p38δ regulate eEF2 *in vitro* and *in vivo* by controlling phosphorylation of its kinase eEF2K (González-Terán et al., 2013; Knebel et al., 2001). When we analysed different steps of mRNA translation using three bicistronic luciferase reporters, SV40-CAP, HCV-IRES and CrPV-IRES, we observed that the absence of p38γ/p38δ decreased both cap-dependent and -independent translation. Results using the SV40-CAP luciferase reporter suggested a

decrease of cap-dependent translation, in p38γ/δ$^{-/-}$ compared to WT cells; this result could be due two reasons. i) p38γ/p38δ have been reported to regulate mTORC1 and mTORC2 by binding and phosphorylating the mTOR inhibitor DEPTOR (González-Terán et al., 2016); however, we did not find DEPTOR interacting with either p38γ or p38δ in our macrophage interactome analysis; and ii) The absence of Tpl2 in p38γ/δ$^{-/-}$ cells reduced cap-dependent mRNA translation (López-Pelaéz et al., 2012). On the other hand, results using the CrPV-IRES luciferase reporter showed ~50% decrease in cap-independent translation in p38γ/δ$^{-/-}$ compared to WT cells. Translation in these conditions starts directly with the recruitment of the ribosomes (Petrov et al., 2016); this correlates with our interactome data in which p38γ binds mainly to ribosomal proteins. All our results suggest that both p38γ/p38δ are regulating general translation of proteins through ribosomal proteins and elongations factors.

Data from the phospho-proteomic analysis show that in basal conditions p38γ$^{-/-}$ macrophages there are more phosphorylated proteins than in WT cells, indicating that p38γ is either repressing phosphorylation at basal condition or inducing the activity of phosphatase(s) for protein dephosphorylation. In contrast, p38δ$^{-/-}$ macrophages show a down-regulation of the phosphorylated proteins in general. Protein phosphorylation analysis of p38γ/δ$^{-/-}$ macrophages shows an intermediate situation between p38γ$^{-/-}$ and p38δ$^{-/-}$ phospho-proteomic results. According to the phospho-proteomic profile, p38γ/p38δ seem to have very different functions in macrophages; this is evident when examining the common phosphorylation peptides. Only two proteins are commonly phosphorylated in p38γ$^{-/-}$, p38δ$^{-/-}$ and p38γ/δ$^{-/-}$ cells, this could be the result of compensatory pathways that appears when knocking out genes. Tharp3 and Wdr33 were the two common phosphorylated protein. Both are involved in mRNA processing. Tharp3 is implicated in pre-mRNA splicing, which is not a good candidate due to our matured mRNA levels of both

Tpl2 and *ABIN2* are the same in WT and p38γ/δ$^{-/-}$ cells. On the other hand, Wdr33 regulates poly(A) mRNA by binding to the AAUAAA sequence, but the *Tpl2* 3'UTR cloned for the luciferase experiments did not include this sequence, although mouse *Tpl2* 3'UTR was found to have it in its 3'end of the mRNA (Chan et al., 2014; Schönemann et al., 2014).

The combined analysis of p38γ/p38δ phospho-proteomic and interactome analysis suggest a common role for p38γ/p38δ in the mRNA processing, which required both interaction with and phosphorylation by the kinases.

Future experiments studying the regulation of the identified proteins (interactome/phospho-proteome) by p38γ/p38δ will help to elucidate and dissect the molecular mechanism by with these p38MAPK are controlling both general protein translation and the specific Tpl2 and ABIN2 protein levels.

5.3 Chapter 3. p38γ and p38δ kinase function in macrophages.

In this thesis we generated a new mouse line, which expresses inactive p38γ ($p38\gamma^{171A/171A}$) and does not express p38δ ($p38\delta^{-/-}$), with the aim of studying the mechanisms by which p38γ/p38δ regulate innate immunity. In previous works we established that the main mechanism by which p38γ/p38δ were affecting the survival of the mice in a septic shock model was the over production of cytokines. In $p38\gamma/\delta^{-/-}$ macrophages, the main cells involved in the cytokine production after LPS challenge, was impaired due to the absence of the Tpl2/ABIN2/p105 complex. We thought that $p38\gamma^{171A/171A}/p38\delta^{-/-}$ mouse could be a very good tool to study the role for p38γ/p38δ in innate immune response, since this mouse has no active p38γ or p38δ, and the masking effect by the absence of Tpl2/ABIN2/p105 complex in $p38\gamma/\delta^{-/-}$ BMDM would be eliminated. So, we then started to study the role of p38γ/p38δ in sepsis using this new type of mice.

The first analysis was the activation of MAPK signalling pathway in BMDM stimulated with LPS, observing that $p38\gamma^{171A/171A}/p38\delta^{-/-}$ mouse have active Tpl2/ABIN2/p105 complex. This confirmed that the new mouse line was a good tool to study the role of p38γ/p38δ, and eliminates the masking effect produced by the absence of Tpl2/ABIN2/p105 complex in $p38\gamma/\delta^{-/-}$ cells. Ours and other laboratories had showed results indicating that p38γ and p38δ had different roles in innate immunity that were independent on the regulation of Tpl2/ABIN2/p105 complex levels (Alsina-Beauchamp et al., 2018; González-Terán et al., 2013; Linares et al., 2015; Rajamäki Kristiina et al., 2016). We have shown that in response to LPS stimulation the *IL1β* mRNA production was impaired, whereas the *IFNβ* mRNA transcription was enhanced in $p38\gamma/\delta^{-/-}$ BMDM compared to WT cells (Risco et al., 2012); however, we observed that just the expression of $p38\gamma^{171A/171A}$ was enough to induce the production of both ILlβ and IFNβ in $p38\gamma^{171A/171A}/p38\delta^{-/-}$ BMDM to similar levels to those of WT BMDM. This

result indicates that p38γ regulate cytokine production independently of its kinase activity, probably by binding to and regulating proteins or protein complexes implicated in this process.

More evidence of the importance of p38γ activity independent on its canonical kinase activity were obtained from the classical septic shock model by injecting LPS/D-Gal to the different mouse lines. In these experiments we observed that p38γ/δ$^{-/-}$ mice were the ones that survived the most, as it was already described (Risco et al., 2012); however, the survival of p38γ$^{171A/171A}$/p38δ$^{-/-}$ and WT mice was similar, which shows the importance of the p38γ presence in this model. The use of D-Gal in the LPS/D-Gal mouse model causes liver damage and therefore, it affects the haemorrhage and apoptosis in the liver. Qualitative and quantitively analysis showed that liver haemorrhage and apoptosis were higher in p38γ$^{171A/171A}$ than in WT and p38γ$^{-/-}$ mice, suggesting that p38γ has a role in liver damage induced by D-Gal both dependent and independent on its kinase activity.

The RNA-sequencing analysis in WT and p38γ$^{171A/171A}$/p38δ$^{-/-}$ stimulated with LPS has allowed the identification of genes, whose transcription is specifically regulated by either p38δ or p38γ. These results showed an increase in IFN type I in the p38γ$^{171A/171A}$/p38δ$^{-/-}$ mice and the signalling pathways affected were all related to virus infection. The increase in IFN type I could be because p38γ/p38δ are modulating TLR4 signalling through the TLR4 that is internalized after Myddosome activation and so, future experiments will be searching for the activities performed by p38γ/p38δ in this area of the signalling pathway.

We decided then to use another approach to study the role of p38γ/p38δ in innate immunity by using RNA-sequencing to study the mRNA transcription that was affected by p38γ/p38δ in LPS stimulated BMDM. These results indicated a high upregulation of IFN type I in the p38γ$^{171A/171A}$/p38δ$^{-/-}$ mice and the signalling pathways affected were all

related to virus infection.

The results from this thesis on the role of p38γ/p38δ in macrophages has unrevealed several unknown biological functions and signalling pathways. Published data had demonstrated that p38γ/p38δ maintains steady-state protein levels of Tpl2/ABIN2/p105 complex (Risco et al., 2012). We have discovered that Tpl2/ABIN2/p105 complex is a key complex in macrophages that regulates Dectin-1 signalling. We propose that Dectin-1 signalling involves de Mydossome formation and therefore it intertwines with TLR signalling in macrophages. TLR4 signalling had already been described to go through Tpl2/ABIN2/p105 complex and therefore be modulated by p38γ/p38δ. Dectin-1 and TLR4 receptors induce cytokines production in response to fungus or bacterial pathogens, orchestrating innate immune response where p38γ/p38δ are found to be essential. On the other hand, we have observed that $p38\gamma^{171A/171A}/p38\delta^{-/-}$ LPS stimulated macrophages (TLR4 signalling) induce an over-production of IFN type I, associating another biological function to p38γ/p38δ.

Because the regulation of steady-state protein levels of Tpl2/ABIN2/p105 complex is crucial in innate immunity and dependent on p38γ/p38δ, we studied the mechanism by which these two proteins regulated Tpl2/ABIN2/p105 complex. We found that, p38γ/p38δ bind to Tpl2 to maintain its stability and at the same time p38δ modulates Tpl2 translation through it 3'UTR. These studies have also opened a new field where the p38γ/p38δ appear modulating general cap-independent translation (Fig. D-1).

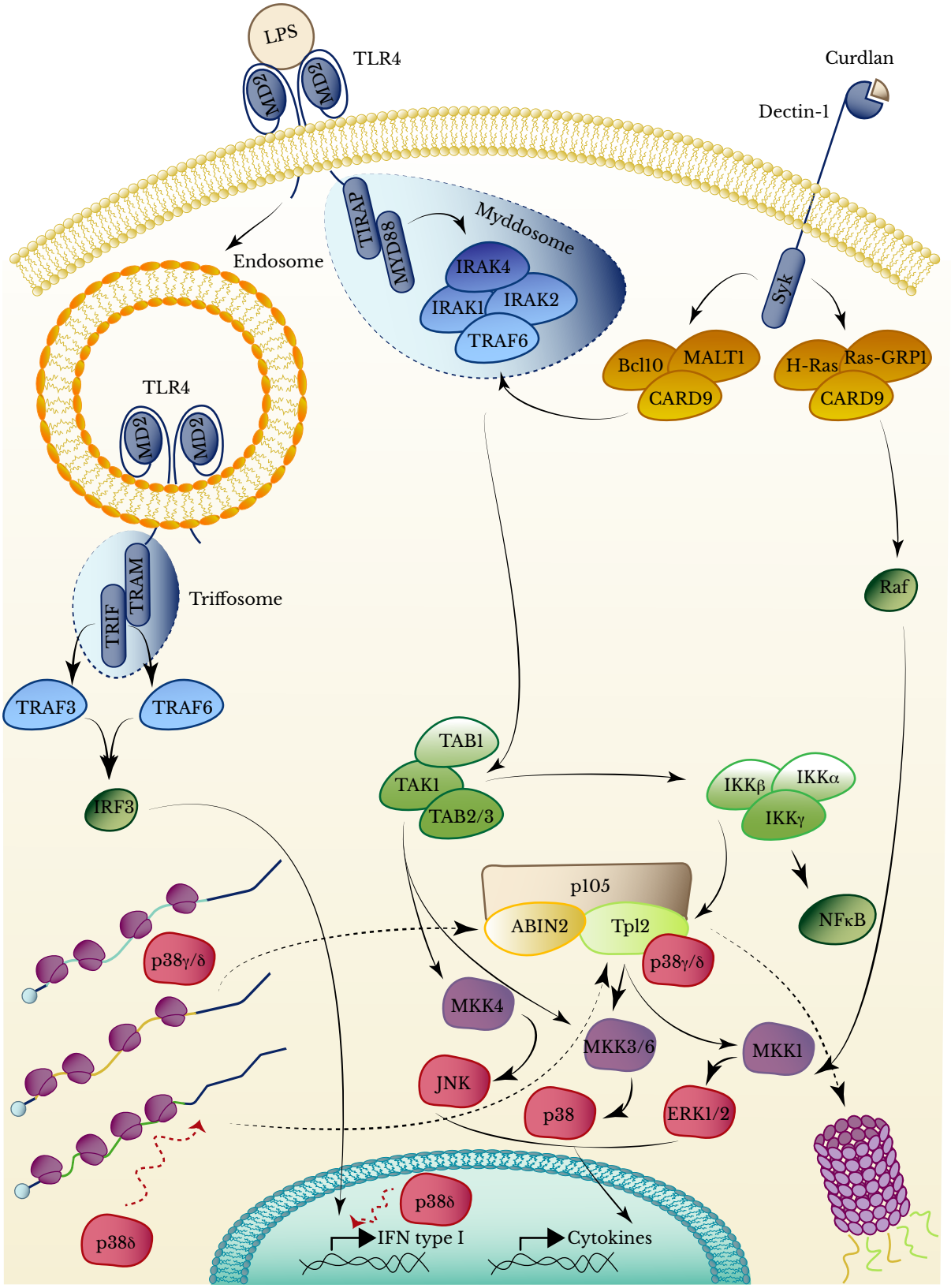

Figure D-1. Schematic representation of possible p38γ/p38δ roles in macrophages. The activation of LPS-TLR4-MD2 and Curdlan-Dectin-1-Syk-CARD9/Bcl10/MAPLT1 triggers TRAF6 activity. TRAF6 activates MAP3K TAK1 that activates IKKβ-Tpl2-MKKs

and MKKs at the same time. MAPKs are then activated and cytokine production is induced. Once TLR4 is activated it is internalised in early endosome where interacts with TRAM/TRIF forming the Triffosome. This complex activates TRAF3 and 6 causing IRF3 translocation to the nucleus and inducing IFN type I production. p38δ seems to be involved in the regulation of IFN transcription. Dectin-1 receptor also activates Raf, that phosphorylated MKK1, via CARD9/RasGRP1/H-Ras. Finally, p38γ/p38δ are stabilizing Tpl2 through interaction. At the same time p38δ induces Tpl2 mRNA translation modulating it 3'UTR. Both p38γ/p38δ are regulating general translation by cap-independent translation.

Conclusions

6 Conclusions

1. Dectin-1 signalling pathway in BMDM activates ERK1/2 through two complexes, CARD9/RasGRF1/H-Ras and CARD9/BCL-10/MALT1. CARD9/RasGRF1/H-Ras complex activates Raf-1-ERK1/2 signalling, whereas CARD9/BCL-10/MALT1 complex activates TAK1-IKKβ-Tpl2-MKK1-ERK1/2 signalling.
2. p38γ and p38δ modulate phosphorylation of ERK1/2 and cytokine production in Dectin-1 signalling pathway in BMDM by regulating proteins levels of Tpl2 and ABIN2.
3. p38γ and p38δ regulate Tpl2 and ABIN2 steady-state protein levels in a wide range of tissues and cell types.
4. p38γ and p38δ regulate Tpl2 stability by interacting with it and so preventing its degradation.
5. p38γ and p38δ control general cap-independent protein translation.
6. The specific translation of *Tpl2* and *ABIN2* mRNA is regulated by p38γ and p38δ.
7. p38δ controls Tpl2 translation through *Tpl2* mRNA 3'UTR.
8. $p38\gamma^{171A/171A}/p38\delta^{-/-}$ mice provides a new tool to study the role of p38γ and p38δ in innate immunity independently of Tpl2/ABIN2/p105 complex.
9. p38γ independent kinase activity is enough to restore the Tpl2/ABIN2 protein levels, activate ERK1/2 and induce cytokine production in LPS stimulated TLR4 in BMDM.

Conclusiones

7 Conclusiones

1. La vía de señalización de Dectin-1 en BMDM activa ERK1/2 a través de dos complejos, CARD9/RasGRF1/H-Ras y CARD9/BCL-10/MALT1. El complejo CARD9/RasGRF1/H-Ras activa la señalización vía Raf-1-ERK1/2, mientras que el complejo CARD9/BCL-10/MALT1 activa la señalización vía TAK1-IKKβ-Tpl2-MKK1-ERK1/2.
2. p38γ y p38δ modulan la fosforilación de ERK1/2 y la producción de citoquinas en la vía de señalización Dectin-1 en BMDM mediante la regulación de los niveles de proteínas de Tpl2 y ABIN2.
3. p38γ y p38δ regulan los niveles de proteína en estado estable de Tpl2 y ABIN2 en una amplia gama de tejidos y tipos de células.
4. p38γ y p38δ regulan la estabilidad de Tpl2 al interactuar con él y evitar así su degradación.
5. p38γ y p38δ regulan la traducción general de proteínas independiente de cap.
6. La traducción específica de mRNA de *Tpl2* y *ABIN2* está regulada por p38γ y p38δ.
7. p38δ controla la traducción de Tpl2 a través de su 3'UTR.
8. Los ratones $p38\gamma^{171A/171A}/p38\delta^{-/-}$ proporcionan una nueva herramienta para estudiar el papel de p38γ y p38δ en la inmunidad innata independientemente del complejo Tpl2/ABIN2/p105.
9. La presencia de p38γ independiente de su actividad quinasa es suficiente para restaurar los niveles de proteína Tpl2/ABIN2, activar ERK1/2 e inducir la producción de citoquinas en BMDM de TLR4 estimulado con LPS.

Bibliography

8 Bibliography

Adams, R.H., Porras, A., Alonso, G., Jones, M., Vintersten, K., Panelli, S., Valladares, A., Perez, L., Klein, R., and Nebreda, A.R. (2000). Essential Role of p38α MAP Kinase in Placental but Not Embryonic Cardiovascular Development. Mol. Cell *6*, 109–116.

Aderem, A., and Ulevitch, R.J. (2000). Toll-like receptors in the induction of the innate immune response. Nature *406*, 782–787.

Akira, S., Uematsu, S., and Takeuchi, O. (2006). Pathogen Recognition and Innate Immunity. Cell *124*, 783–801.

Alsina-Beauchamp, D., Escós, A., Fajardo, P., González-Romero, D., Díaz-Mora, E., Risco, A., Martín-Serrano, M.A., Fresno, C. del, Dominguez-Andrés, J., Aparicio, N., et al. (2018). Myeloid cell deficiency of p38γ/p38δ protects against candidiasis and regulates antifungal immunity. EMBO Mol. Med. *10*, e8485.

Andrews S. (2010a). FastQC: a quality control tool for high throughput sequence data. Available online at: http://www.bioinformatics.babraham.ac.uk/projects/fastqc.

Andrews S. (2010b). SeqMonk: A tool to visualise and analyse high throughput mapped sequence data. Available online at https://www.bioinformatics.babraham.ac.uk/projects/seqmonk/.

Angus, D.C., and van der Poll, T. (2013). Severe Sepsis and Septic Shock. N. Engl. J. Med. *369*, 840–851.

Aoki, M., Hamada, F., Sugimoto, T., Sumida, S., Akiyama, T., and Toyoshima, K. (1993). The human cot proto-oncogene encodes two protein serine/threonine kinases with different transforming activities by alternative initiation of translation. J. Biol. Chem. *268*, 22723–22732.

Arthur, J.S.C., and Ley, S.C. (2013). Mitogen-activated protein kinases in innate immunity. Nat. Rev. Immunol. *13*.

Bain, J., Plater, L., Elliott, M., Shpiro, N., Hastie, C.J., Mclauchlan, H., Klevernic, I., Arthur, J.S.C., Alessi, D.R., and Cohen, P. (2007). The selectivity of protein kinase inhibitors: a further update. Biochem. J. *408*, 297–315.

Barrantes, I. del B., Coya, J.M., Maina, F., Arthur, J.S.C., and Nebreda, A.R. (2011). Genetic analysis of specific and redundant roles for p38α and p38β MAPKs during mouse development. Proc. Natl. Acad. Sci. *108*, 12764–

12769.

Beardmore, V.A., Hinton, H.J., Eftychi, C., Apostolaki, M., Armaka, M., Darragh, J., McIlrath, J., Carr, J.M., Armit, L.J., Clacher, C., et al. (2005). Generation and Characterization of p38β (MAPK11) Gene-Targeted Mice. Mol. Cell. Biol. *25*, 10454–10464.

Beinke, S., and Ley, S.C. (2004). Functions of NF-κB1 and NF-κB2 in immune cell biology. Biochem. J. *382*, 393–409.

Beinke, S., Deka, J., Lang, V., Belich, M.P., Walker, P.A., Howell, S., Smerdon, S.J., Gamblin, S.J., and Ley, S.C. (2003). NF-κB1 p105 Negatively Regulates TPL-2 MEK Kinase Activity. Mol. Cell. Biol. *23*, 4739–4752.

Beinke, S., Robinson, M.J., Hugunin, M., and Ley, S.C. (2004). Lipopolysaccharide Activation of the TPL-2/MEK/Extracellular Signal-Regulated Kinase Mitogen-Activated Protein Kinase Cascade Is Regulated by I?B Kinase-Induced Proteolysis of NF-?B1 p105. Mol. Cell. Biol. *24*, 9658–9667.

Belich, M.P., Salmerón, A., Johnston, L.H., and Ley, S.C. (1999). TPL-2 kinase regulates the proteolysis of the NF-κB-inhibitory protein NF-κB1 p105. Nature *397*, 363–368.

Ben-Addi, A., Mambole-Dema, A., Brender, C., Martin, S.R., Janzen, J., Kjaer, S., Smerdon, S.J., and Ley, S.C. (2014). IκB kinase-induced interaction of TPL-2 kinase with 14-3-3 is essential for Toll-like receptor activation of ERK-1 and -2 MAP kinases. Proc. Natl. Acad. Sci. *111*, E2394–E2403.

Besson, B., Sonthonnax, F., Duchateau, M., Ben Khalifa, Y., Larrous, F., Eun, H., Hourdel, V., Matondo, M., Chamot-Rooke, J., Grailhe, R., et al. (2017). Regulation of NF-κB by the p105-ABIN2-TPL2 complex and RelAp43 during rabies virus infection. PLoS Pathog. *13*.

Bollig, F., Winzen, R., Gaestel, M., Kostka, S., Resch, K., and Holtmann, H. (2003). Affinity purification of ARE-binding proteins identifies poly(A)-binding protein 1 as a potential substrate in MK2-induced mRNA stabilization. Biochem. Biophys. Res. Commun. *301*, 665–670.

Brancho, D., Tanaka, N., Jaeschke, A., Ventura, J.-J., Kelkar, N., Tanaka, Y., Kyuuma, M., Takeshita, T., Flavell, R.A., and Davis, R.J. (2003). Mechanism of p38 MAP kinase activation in vivo. Genes Dev. *17*, 1969–1978.

Brown, G.D. (2011). INNATE ANTIFUNGAL IMMUNITY: THE KEY ROLE OF PHAGOCYTES. Annu. Rev. Immunol. *29*, 1–21.

Brown, G.D., Herre, J., Williams, D.L., Willment, J.A., Marshall, A.S.J., and

Gordon, S. (2003). Dectin-1 Mediates the Biological Effects of β-Glucans. J. Exp. Med. *197*, 1119–1124.

Brown, G.D., Denning, D.W., Gow, N.A.R., Levitz, S.M., Netea, M.G., and White, T.C. (2012). Hidden Killers: Human Fungal Infections. Sci. Transl. Med. *4*, 165rv13-165rv13.

Chan, S.L., Huppertz, I., Yao, C., Weng, L., Moresco, J.J., Yates, J.R., Ule, J., Manley, J.L., and Shi, Y. (2014). CPSF30 and Wdr33 directly bind to AAUAAA in mammalian mRNA 3′ processing. Genes Dev. *28*, 2370–2380.

Cheung, P.C.F., Nebreda, A.R., and Cohen, P. (2004). TAB3, a new binding partner of the protein kinase TAK1. Biochem. J. *378*, 27–34.

Chio, I.I.C., Jafarnejad, S.M., Ponz-Sarvise, M., Park, Y., Rivera, K., Palm, W., Wilson, J., Sangar, V., Hao, Y., Öhlund, D., et al. (2016). NRF2 Promotes Tumor Maintenance by Modulating mRNA Translation in Pancreatic Cancer. Cell *166*, 963–976.

Chrestensen, C.A., Schroeder, M.J., Shabanowitz, J., Hunt, D.F., Pelo, J.W., Worthington, M.T., and Sturgill, T.W. (2004). MAPKAP Kinase 2 Phosphorylates Tristetraprolin on in Vivo Sites Including Ser178, a Site Required for 14-3-3 Binding. J. Biol. Chem. *279*, 10176–10184.

Clark, K., Peggie, M., Plater, L., Sorcek, R.J., Young, E.R.R., Madwed, J.B., Hough, J., McIver, E.G., and Cohen, P. (2011). Novel cross-talk within the IKK family controls innate immunity. Biochem. J. *434*, 93–104.

Cohen, P. (2014). The TLR and IL-1 signalling network at a glance. J Cell Sci *127*, 2383–2390.

Criado, G., Risco, A., Alsina-Beauchamp, D., Pérez-Lorenzo, M.J., Escós, A., and Cuenda, A. (2013). Alternative p38 mitogen-activated protein kinases are essential for collagen-induced arthritis. Arthritis Rheum.

Cuenda, A., and Rousseau, S. (2007). p38 MAP-kinases pathway regulation, function and role in human diseases. Biochim. Biophys. Acta *1773*, 1358–1375.

Cuenda, A., and Sanz-Ezquerro, J.J. (2017). p38γ and p38δ: From Spectators to Key Physiological Players. Trends Biochem. Sci. *42*, 431–442.

Dadar, M., Tiwari, R., Karthik, K., Chakraborty, S., Shahali, Y., and Dhama, K. (2018). Candida albicans - Biology, molecular characterization, pathogenicity, and advances in diagnosis and control – An update. Microb. Pathog. *117*, 128–138.

Das, S., Cho, J., Lambertz, I., Kelliher, M.A., Eliopoulos, A.G., Du, K., and

Tsichlis, P.N. (2005). Tpl2/Cot Signals Activate ERK, JNK, and NF-κB in a Cell-type and Stimulus-specific Manner. J. Biol. Chem. *280*, 23748–23757.

Dayalan Naidu, S., Sutherland, C., Zhang, Y., Risco, A., de la Vega, L., Caunt, C.J., Hastie, C.J., Lamont, D.J., Torrente, L., Chowdhry, S., et al. (2016). Heat Shock Factor 1 Is a Substrate for p38 Mitogen-Activated Protein Kinases. Mol. Cell. Biol. *36*, 2403–2417.

Delaloye, J., and Calandra, T. (2014). Invasive candidiasis as a cause of sepsis in the critically ill patient. Virulence *5*, 161–169.

Delves, P.J., and Roitt, I.M. (2000). The Immune System. N. Engl. J. Med. *343*, 37–49.

Deutschman, C.S., and Tracey, K.J. (2014). Sepsis: Current Dogma and New Perspectives. Immunity *40*, 463–475.

DiDonato, J.A., Hayakawa, M., Rothwarf, D.M., Zandi, E., and Karin, M. (1997). A cytokine-responsive IκB kinase that activates the transcription factor NF-κB. Nature *388*, 548–554.

Dumitru, C.D., Ceci, J.D., Tsatsanis, C., Kontoyiannis, D., Stamatakis, K., Lin, J.-H., Patriotis, C., Jenkins, N.A., Copeland, N.G., Kollias, G., et al. (2000). TNF-α Induction by LPS Is Regulated Posttranscriptionally via a Tpl2/ERK-Dependent Pathway. Cell *103*, 1071–1083.

Dzamko, N., Inesta-Vaquera, F., Zhang, J., Xie, C., Cai, H., Arthur, S., Tan, L., Choi, H., Gray, N., Cohen, P., et al. (2012). The IkappaB Kinase Family Phosphorylates the Parkinson's Disease Kinase LRRK2 at Ser935 and Ser910 during Toll-Like Receptor Signaling. PLoS ONE *7*.

Escós, A., Risco, A., Alsina-Beauchamp, D., and Cuenda, A. (2016). p38γ and p38δ Mitogen Activated Protein Kinases (MAPKs), New Stars in the MAPK Galaxy. Signaling 31.

Feijoo, C., Campbell, D.G., Jakes, R., Goedert, M., and Cuenda, A. (2005). Evidence that phosphorylation of the microtubule-associated protein Tau by SAPK4/p38δ at Thr50 promotes microtubule assembly. J. Cell Sci. *118*, 397–408.

Fitzgerald, K.A., Rowe, D.C., Barnes, B.J., Caffrey, D.R., Visintin, A., Latz, E., Monks, B., Pitha, P.M., and Golenbock, D.T. (2003). LPS-TLR4 Signaling to IRF-3/7 and NF-κB Involves the Toll Adapters TRAM and TRIF. J. Exp. Med. *198*, 1043–1055.

Gándara, M.L., López, P., Hernando, R., Castaño, J.G., and Alemany, S. (2003). The COOH-Terminal Domain of Wild-Type Cot Regulates Its Stability and Kinase Specific Activity. Mol. Cell. Biol. *23*, 7377–7390.

Gantke, T., Sriskantharajah, S., and Ley, S.C. (2011). Regulation and function of TPL-2, an IκB kinase-regulated MAP kinase kinase kinase. Cell Res. *21*, 131–145.

Gantke, T., Boussouf, S., Janzen, J., Morrice, N.A., Howell, S., Mühlberger, E., and Ley, S.C. (2013). Ebola virus VP35 induces high-level production of recombinant TPL-2–ABIN-2–NF-κB1 p105 complex in co-transfected HEK-293 cells. Biochem. J. *452*, 359–365.

Gebauer, F., and Hentze, M.W. (2004). Molecular mechanisms of translational control. Nat. Rev. Mol. Cell Biol. *5*, 827–835.

Geijtenbeek, T.B.H., and Gringhuis, S.I. (2009). Signalling through C-type lectin receptors: shaping immune responses. Nat. Rev. Immunol. *9*, 465–479.

Gillespie, M.A., Le Grand, F., Scimè, A., Kuang, S., von Maltzahn, J., Seale, V., Cuenda, A., Ranish, J.A., and Rudnicki, M.A. (2009). p38-γ–dependent gene silencing restricts entry into the myogenic differentiation program. J. Cell Biol. *187*, 991–1005.

Goedert, M., Cuenda, A., Craxton, M., Jakes, R., and Cohen, P. (1997). Activation of the novel stress-activated protein kinase SAPK4 by cytokines and cellular stresses is mediated by SKK3 (MKK6); comparison of its substrate specificity with that of other SAP kinases. EMBO J. *16*, 3563–3571.

González-Terán, B., Cortés, J.R., Manieri, E., Matesanz, N., Verdugo, ρngeles, Rodríguez, M.E., González-Rodríguez, ρgueda, Valverde, ρngela, Martín, P., Davis, R.J., et al. (2013). Eukaryotic elongation factor 2 controls TNF-α translation in LPS-induced hepatitis. J. Clin. Invest. *123*, 164–178.

González-Terán, B., López, J.A., Rodríguez, E., Leiva, L., Martínez-Martínez, S., Bernal, J.A., Jiménez-Borreguero, L.J., Redondo, J.M., Vazquez, J., and Sabio, G. (2016). p38γ and δ promote heart hypertrophy by targeting the mTOR-inhibitory protein DEPTOR for degradation. Nat. Commun. *7*.

Gorjestani, S., Darnay, B.G., and Lin, X. (2012). Tumor Necrosis Factor Receptor-associated Factor 6 (TRAF6) and TGFβ-activated Kinase 1 (TAK1) Play Essential Roles in the C-type Lectin Receptor Signaling in Response to Candida albicans Infection. J. Biol. Chem. *287*, 44143–44150.

Green, N., Hu, Y., Janz, K., Li, H.-Q., Kaila, N., Guler, S., Thomason, J., Joseph-McCarthy, D., Tam, S.Y., Hotchandani, R., et al. (2007). Inhibitors of Tumor Progression Loci-2 (Tpl2) Kinase and Tumor Necrosis Factor α (TNF-α) Production: Selectivity and in Vivo Antiinflammatory Activity of Novel 8-Substituted-4-anilino-6-aminoquinoline-3-carbonitriles. J. Med. Chem. *50*, 4728–4745.

Gringhuis, S.I., den Dunnen, J., Litjens, M., van der Vlist, M., Wevers, B., Bruijns, S.C.M., and Geijtenbeek, T.B.H. (2009). Dectin-1 directs T helper cell differentiation by controlling noncanonical NF-κB activation through Raf-1 and Syk. Nat. Immunol. *10*, 203–213.

Gross, O., Gewies, A., Finger, K., Schäfer, M., Sparwasser, T., Peschel, C., Förster, I., and Ruland, J. (2006). Card9 controls a non-TLR signalling pathway for innate anti-fungal immunity. Nature *442*, 651–656.

Han, J., Lee, J.D., Bibbs, L., and Ulevitch, R.J. (1994). A MAP kinase targeted by endotoxin and hyperosmolarity in mammalian cells. Science *265*, 808–811.

Hasegawa, M., Cuenda, A., Spillantini, M.G., Thomas, G.M., Buée-Scherrer, V., Cohen, P., and Goedert, M. (1999). Stress-activated Protein Kinase-3 Interacts with the PDZ Domain of α1-Syntrophin A MECHANISM FOR SPECIFIC SUBSTRATE RECOGNITION. J. Biol. Chem. *274*, 12626–12631.

Hershey, J.W.B., Sonenberg, N., and Mathews, M.B. (2012). Principles of Translational Control: An Overview. Cold Spring Harb. Perspect. Biol. *4*, a011528.

Hoebe, K., Du, X., Georgel, P., Janssen, E., Tabeta, K., Kim, S.O., Goode, J., Lin, P., Mann, N., Mudd, S., et al. (2003). Identification of *Lps2* as a key transducer of MyD88-independent TIR signalling. Nature *424*, 743–748.

Hou, S.-W., Zhi, H.-Y., Pohl, N., Loesch, M., Qi, X.-M., Li, R.-S., Basir, Z., and Chen, G. (2010). PTPH1 dephosphorylates and cooperates with p38γ MAPK to increase Ras oncogenesis through PDZ-mediated interaction. Cancer Res. *70*, 2901–2910.

Hoving, J.C., Wilson, G.J., and Brown, G.D. (2014). Signalling C-Type lectin receptors, microbial recognition and immunity. Cell. Microbiol. *16*, 185–194.

Ittner, A., Block, H., Reichel, C.A., Varjosalo, M., Gehart, H., Sumara, G., Gstaiger, M., Krombach, F., Zarbock, A., and Ricci, R. (2012). Regulation of PTEN activity by p38δ-PKD1 signaling in neutrophils confers inflammatory responses in the lung. J. Exp. Med. *209*, 2229–2246.

Ittner, A., Chua, S.W., Bertz, J., Volkerling, A., Hoven, J. van der, Gladbach, A., Przybyla, M., Bi, M., Hummel, A. van, Stevens, C.H., et al. (2016). Site-specific phosphorylation of tau inhibits amyloid-β toxicity in Alzheimer's mice. Science *354*, 904–908.

Jia, X.-M., Tang, B., Zhu, L.-L., Liu, Y.-H., Zhao, X.-Q., Gorjestani, S., Hsu, Y.-M.S., Yang, L., Guan, J.-H., Xu, G.-T., et al. (2014). CARD9 mediates Dectin-1–induced ERK activation by linking Ras-GRF1 to H-Ras for

antifungal immunity. J. Exp. Med. *211*, 2307–2321.

Kagan, J.C., Su, T., Horng, T., Chow, A., Akira, S., and Medzhitov, R. (2008). TRAM couples endocytosis of Toll-like receptor 4 to the induction of interferon-β. Nat. Immunol. *9*, 361–368.

Kang, Y.J., Seit-Nebi, A., Davis, R.J., and Han, J. (2006). Multiple Activation Mechanisms of p38α Mitogen-activated Protein Kinase. J. Biol. Chem. *281*, 26225–26234.

Kieser, K.J., and Kagan, J.C. (2017). Multi-receptor detection of individual bacterial products by the innate immune system. Nat. Rev. Immunol. *17*, 376–390.

Kim, J.-Y. (2016). Human fungal pathogens: Why should we learn? J. Microbiol. *54*, 145–148.

Kindt, T., Goldsby, R., Osborne, B., and Kuby, J. (2007). Kuby Immunology (6th ed.) (New York: W.H. Freeman and Company).

Knebel, A., Morrice, N., and Cohen, P. (2001). A novel method to identify protein kinase substrates: eEF2 kinase is phosphorylated and inhibited by SAPK4/p38δ. EMBO J. *20*, 4360–4369.

Knebel, A., Haydon, C.E., Morrice, N., and Cohen, P. (2002). Stress-induced regulation of eukaryotic elongation factor 2 kinase by SB 203580-sensitive and -insensitive pathways. Biochem. J. *367*, 525–532.

Kullberg, B.J., and Arendrup, M.C. (2015). Invasive Candidiasis. N. Engl. J. Med. *373*, 1445–1456.

Kuma, Y., Sabio, G., Bain, J., Shpiro, N., Márquez, R., and Cuenda, A. (2005). BIRB796 inhibits all p38 MAPK isoforms in vitro and in vivo. J. Biol. Chem. *280*, 19472–19479.

Kumar, S., McDonnell, P.C., Gum, R.J., Hand, A.T., Lee, J.C., and Young, P.R. (1997). Novel Homologues of CSBP/p38 MAP Kinase: Activation, Substrate Specificity and Sensitivity to Inhibition by Pyridinyl Imidazoles. Biochem. Biophys. Res. Commun. *235*, 533–538.

Kyriakis, J.M., and Avruch, J. (2012). Mammalian MAPK Signal Transduction Pathways Activated by Stress and Inflammation: A 10-Year Update. Physiol. Rev. *92*, 689–737.

Lang, V., Symons, A., Watton, S.J., Janzen, J., Soneji, Y., Beinke, S., Howell, S., and Ley, S.C. (2004). ABIN-2 Forms a Ternary Complex with TPL-2 and NF-?B1 p105 and Is Essential for TPL-2 Protein Stability. Mol. Cell. Biol. *24*, 5235–5248.

Lechner, C., Zahalka, M.A., Giot, J.F., Møller, N.P., and Ullrich, A. (1996). ERK6, a mitogen-activated protein kinase involved in C2C12 myoblast differentiation. Proc. Natl. Acad. Sci. *93*, 4355–4359.

Lee, M.S., and Kim, Y.-J. (2007). Signaling Pathways Downstream of Pattern-Recognition Receptors and Their Cross Talk. Annu. Rev. Biochem. *76*, 447–480.

Lee, J.C., Laydon, J.T., McDonnell, P.C., Gallagher, T.F., Kumar, S., Green, D., McNulty, D., Blumenthal, M.J., Keys, J.R., Vatter, S.W.L., et al. (1994). A protein kinase involved in the regulation of inflammatory cytokine biosynthesis. Nature *372*, 739.

Leppek, K., Das, R., and Barna, M. (2018). Functional *5′* UTR mRNA structures in eukaryotic translation regulation and how to find them. Nat. Rev. Mol. Cell Biol. *19*, 158–174.

Li, M.G., Katsura, K., Nomiyama, H., Komaki, K., Ninomiya-Tsuji, J., Matsumoto, K., Kobayashi, T., and Tamura, S. (2003). Regulation of the Interleukin-1-induced Signaling Pathways by a Novel Member of the Protein Phosphatase 2C Family (PP2Cε). J. Biol. Chem. *278*, 12013–12021.

Li, Z., Jiang, Y., Ulevitch, R.J., and Han, J. (1996). The Primary Structure of p38γ: A New Member of p38 Group of MAP Kinases. Biochem. Biophys. Res. Commun. *228*, 334–340.

Lin, S.-C., Lo, Y.-C., and Wu, H. (2010). Helical assembly in the MyD88–IRAK4–IRAK2 complex in TLR/IL-1R signalling. Nature *465*, 885–890.

Linares, J.F., Duran, A., Reina-Campos, M., Aza-Blanc, P., Campos, A., Moscat, J., and Diaz-Meco, M.T. (2015). Amino acid activation of mTORC1 by a PB1-domain-driven kinase complex cascade. Cell Rep. *12*, 1339–1352.

Liu, J., and Cao, X. (2016). Cellular and molecular regulation of innate inflammatory responses. Cell. Mol. Immunol. *13*, 711–721.

Lomaga, M.A., Yeh, W.-C., Sarosi, I., Duncan, G.S., Furlonger, C., Ho, A., Morony, S., Capparelli, C., Van, G., Kaufman, S., et al. (1999). TRAF6 deficiency results in osteopetrosis and defective interleukin-1, CD40, and LPS signaling. Genes Dev. *13*, 1015–1024.

López-Pelaéz, M., Fumagalli, S., Sanz, C., Herrero, C., Guerra, S., Fernandez, M., and Alemany, S. (2012). Cot/tpl2-MKK1/2-Erk1/2 controls mTORC1-mediated mRNA translation in Toll-like receptor–activated macrophages. Mol. Biol. Cell *23*, 2982–2992.

Love, M.I., Huber, W., and Anders, S. (2014). Moderated estimation of fold change and dispersion for RNA-seq data with DESeq2. Genome Biol. *15*.

Lyons, J.F., Wilhelm, S., Hibner, B., and Bollag, G. (2001). Discovery of a novel Raf kinase inhibitor. Endocr. Relat. Cancer *8*, 219–225.

Mercurio, F., Zhu, H., Murray, B.W., Shevchenko, A., Bennett, B.L., Li, J. wu, Young, D.B., Barbosa, M., Mann, M., Manning, A., et al. (1997). IKK-1 and IKK-2: Cytokine-Activated IκB Kinases Essential for NF-κB Activation. Science *278*, 860–866.

Miyoshi, J., Higashi, T., Mukai, H., Ohuchi, T., and Kakunaga, T. (1991). Structure and transforming potential of the human cot oncogene encoding a putative protein kinase. Mol. Cell. Biol. *11*, 4088–4096.

Motshwene, P.G., Moncrieffe, M.C., Grossmann, J.G., Kao, C., Ayaluru, M., Sandercock, A.M., Robinson, C.V., Latz, E., and Gay, N.J. (2009). An Oligomeric Signaling Platform Formed by the Toll-like Receptor Signal Transducers MyD88 and IRAK-4. J. Biol. Chem. *284*, 25404–25411.

Murray, P.J., and Wynn, T.A. (2011). Protective and pathogenic functions of macrophage subsets. Nat. Rev. Immunol. *11*, 723–737.

Netea, M.G., Joosten, L.A.B., van der Meer, J.W.M., Kullberg, B.-J., and van de Veerdonk, F.L. (2015). Immune defence against Candida fungal infections. Nat. Rev. Immunol. *15*, 630–642.

Newton, K., and Dixit, V.M. (2012). Signaling in innate immunity and inflammation. Cold Spring Harb. Perspect. Biol. *4*.

Noseda, R., Guerrero-Valero, M., Alberizzi, V., Previtali, S.C., Sherman, D.L., Palmisano, M., Huganir, R.L., Nave, K.-A., Cuenda, A., Feltri, M.L., et al. (2016). Kif13b Regulates PNS and CNS Myelination through the Dlg1 Scaffold. PLOS Biol. *14*, e1002440.

Oliveros, J.C., Franch, M., Tabas-Madrid, D., San-León, D., Montoliu, L., Cubas, P., and Pazos, F. (2016). Breaking-Cas—interactive design of guide RNAs for CRISPR-Cas experiments for ENSEMBL genomes. Nucleic Acids Res. *44*, W267–W271.

Otto, G.A., and Puglisi, J.D. (2004). The Pathway of HCV IRES-Mediated Translation Initiation. Cell *119*, 369–380.

Papoutsopoulou, S., Symons, A., Tharmalingham, T., Belich, M.P., Kaiser, F., Kioussis, D., O'Garra, A., Tybulewicz, V., and Ley, S.C. (2006). ABIN-2 is required for optimal activation of Erk MAP kinase in innate immune responses. Nat. Immunol. *7*, 606–615.

Pattison, M.J., Mitchell, O., Flynn, H.R., Chen, C.-S., Yang, H.-T., Ben-Addi, H., Boeing, S., Snijders, A.P., and Ley, S.C. (2016). TLR and TNF-R1 activation of the MKK3/MKK6–p38α axis in macrophages is mediated by

TPL-2 kinase. Biochem. J. *473*, 2845–2861.

Petrov, A., Grosely, R., Chen, J., O'Leary, S.E., and Puglisi, J.D. (2016). Multiple Parallel Pathways of Translation Initiation on the CrPV IRES. Mol. Cell *62*, 92–103.

Proud, C.G. (2015). Regulation and roles of elongation factor 2 kinase. Biochem. Soc. Trans. *43*, 328–332.

Quackenbush, J. (2002). Microarray data normalization and transformation. Nat. Genet. *32*, 496–501.

Rajamäki Kristiina, Mäyränpää Mikko I., Risco Ana, Tuimala Jarno, Nurmi Katariina, Cuenda Ana, Eklund Kari K., Öörni Katariina, and Kovanen Petri T. (2016). p38δ MAPK. Arterioscler. Thromb. Vasc. Biol. *36*, 1937–1946.

Reid, D.M., Gow, N.A., and Brown, G.D. (2009). Pattern recognition: recent insights from Dectin-1. Curr. Opin. Immunol. *21*, 30–37.

Reino, P. del, Alsina-Beauchamp, D., Escós, A., Cerezo-Guisado, M.I., Risco, A., Aparicio, N., Zur, R., Fernandez-Estévez, M., Collantes, E., Montans, J., et al. (2014). Pro-Oncogenic Role of Alternative p38 Mitogen-Activated Protein Kinases p38γ and p38δ, Linking Inflammation and Cancer in Colitis-Associated Colon Cancer. Cancer Res. *74*, 6150–6160.

Remy, G., Risco, A.M., Iñesta-Vaquera, F.A., González-Terán, B., Sabio, G., Davis, R.J., and Cuenda, A. (2010). Differential activation of p38MAPK isoforms by MKK6 and MKK3. Cell. Signal. *22*, 660–667.

Risco, A., and Cuenda, A. (2012). New Insights into the p38γ and p38δ MAPK Pathways. J. Signal Transduct. *2012*.

Risco, A., del Fresno, C., Mambol, A., Alsina-Beauchamp, D., MacKenzie, K.F., Yang, H.-T., Barber, D.F., Morcelle, C., Arthur, J.S.C., Ley, S.C., et al. (2012). p38γ and p38δ kinases regulate the Toll-like receptor 4 (TLR4)-induced cytokine production by controlling ERK1/2 protein kinase pathway activation. Proc. Natl. Acad. Sci. U. S. A. *109*, 11200–11205.

Rogers, N.C., Slack, E.C., Edwards, A.D., Nolte, M.A., Schulz, O., Schweighoffer, E., Williams, D.L., Gordon, S., Tybulewicz, V.L., Brown, G.D., et al. (2005). Syk-Dependent Cytokine Induction by Dectin-1 Reveals a Novel Pattern Recognition Pathway for C Type Lectins. Immunity *22*, 507–517.

Roget, K., Ben-Addi, A., Mambole-Dema, A., Gantke, T., Yang, H.-T., Janzen, J., Morrice, N., Abbott, D., and Ley, S.C. (2012). IκB Kinase 2 Regulates TPL-2 Activation of Extracellular Signal-Regulated Kinases 1 and 2 by Direct Phosphorylation of TPL-2 Serine 400. Mol. Cell. Biol. *32*,

4684–4690.

Roskoski, R. (2012). ERK1/2 MAP kinases: Structure, function, and regulation. Pharmacol. Res. *66*, 105–143.

Rothwarf, D.M., Zandi, E., Natoli, G., and Karin, M. (1998). IKK-γ is an essential regulatory subunit of the IκB kinase complex. Nature *395*, 297–300.

Rouse, J., Cohen, P., Trigon, S., Morange, M., Alonso-Llamazares, A., Zamanillo, D., Hunt, T., and Nebreda, A.R. (1994). A novel kinase cascade triggered by stress and heat shock that stimulates MAPKAP kinase-2 and phosphorylation of the small heat shock proteins. Cell *78*, 1027–1037.

Rousseau, S., Papoutsopoulou, M., Symons, A., Cook, D., Lucocq, J.M., Prescott, A.R., O'Garra, A., Ley, S.C., and Cohen, P. (2008). TPL2-mediated activation of ERK1 and ERK2 regulates the processing of pre-TNFα in LPS-stimulated macrophages. J. Cell Sci. *121*, 149–154.

Roux, P.P., and Topisirovic, I. (2018). Signaling Pathways Involved in the Regulation of mRNA Translation. Mol. Cell. Biol. *38*, e00070-18.

Sabio, G., Reuver, S., Feijoo, C., Hasegawa, M., Thomas, G.M., Centeno, F., Kuhlendahl, S., Leal-Ortiz, S., Goedert, M., Garner, C., et al. (2004). Stress- and mitogen-induced phosphorylation of the synapse-associated protein SAP90/PSD-95 by activation of SAPK3/p38gamma and ERK1/ERK2. Biochem. J. *380*, 19–30.

Sabio, G., Arthur, J.S.C., Kuma, Y., Peggie, M., Carr, J., Murray-Tait, V., Centeno, F., Goedert, M., Morrice, N.A., and Cuenda, A. (2005). p38? regulates the localisation of SAP97 in the cytoskeleton by modulating its interaction with GKAP. EMBO J. *24*, 1134–1145.

Sabio, G., Cerezo-Guisado, M.I., Reino, P. del, Iñesta-Vaquera, F.A., Rousseau, S., Arthur, J.S.C., Campbell, D.G., Centeno, F., and Cuenda, A. (2010). p38γ regulates interaction of nuclear PSF and RNA with the tumour-suppressor hDlg in response to osmotic shock. J. Cell Sci. *123*, 2596–2604.

Sato, S., Sanjo, H., Takeda, K., Ninomiya-Tsuji, J., Yamamoto, M., Kawai, T., Matsumoto, K., Takeuchi, O., and Akira, S. (2005). Essential function for the kinase TAK1 in innate and adaptive immune responses. Nat. Immunol. *6*, 1087–1095.

Schönemann, L., Kühn, U., Martin, G., Schäfer, P., Gruber, A.R., Keller, W., Zavolan, M., and Wahle, E. (2014). Reconstitution of CPSF active in polyadenylation: recognition of the polyadenylation signal by WDR33. Genes Dev. *28*, 2381–2393.

Schulze, J., and Sonnenborn, U. (2009). Yeasts in the Gut: From Commensals to Infectious Agents. Dtsch. Ärztebl. Int. *106*, 837–842.

Schwanhäusser, B., Busse, D., Li, N., Dittmar, G., Schuchhardt, J., Wolf, J., Chen, W., and Selbach, M. (2011). Global quantification of mammalian gene expression control. Nature *473*, 337–342.

Shi, Z., Fujii, K., Kovary, K.M., Genuth, N.R., Röst, H.L., Teruel, M.N., and Barna, M. (2017). Heterogeneous Ribosomes Preferentially Translate Distinct Subpools of mRNAs Genome-wide. Mol. Cell *67*, 71-83.e7.

Shim, J.-H., Xiao, C., Paschal, A.E., Bailey, S.T., Rao, P., Hayden, M.S., Lee, K.-Y., Bussey, C., Steckel, M., Tanaka, N., et al. (2005). TAK1, but not TAB1 or TAB2, plays an essential role in multiple signaling pathways in vivo. Genes Dev. *19*, 2668–2681.

Sonenberg, N., and Hinnebusch, A.G. (2009). Regulation of Translation Initiation in Eukaryotes: Mechanisms and Biological Targets. Cell *136*, 731–745.

Spurgeon, S.E., Coffey, G., Fletcher, L.B., Burke, R., Tyner, J.W., Druker, B.J., Betz, A., DeGuzman, F., Pak, Y., Baker, D., et al. (2013). The Selective Syk Inhibitor P505-15 (PRT062607) Inhibits B Cell Signaling and Function In Vitro and In Vivo and Augments the Activity of Fludarabine in Chronic Lymphocytic Leukemia. J. Pharmacol. Exp. Ther. *344*, 378–387.

Sriskantharajah, S., Gückel, E., Tsakiri, N., Kierdorf, K., Brender, C., Ben-Addi, A., Veldhoen, M., Tsichlis, P.N., Stockinger, B., O'Garra, A., et al. (2014). Regulation of experimental autoimmune encephalomyelitis by TPL-2 kinase. J. Immunol. Baltim. Md 1950 *192*, 3518–3529.

Sumara, G., Formentini, I., Collins, S., Sumara, I., Windak, R., Bodenmiller, B., Ramracheya, R., Caille, D., Jiang, H., Platt, K.A., et al. (2009). Regulation of PKD by the MAPK p38δ in Insulin Secretion and Glucose Homeostasis. Cell *136*, 235–248.

Swamydas, M., Break, T.J., and Lionakis, M.S. (2015). Mononuclear Phagocyte-Mediated Antifungal Immunity: The Role of Chemotactic Receptors and Ligands. Cell. Mol. Life Sci. CMLS *72*, 2157–2175.

Takeuchi, O., and Akira, S. (2010). Pattern Recognition Receptors and Inflammation. Cell *140*, 805–820.

Tiedje, C., Holtmann, H., and Gaestel, M. (2014). The Role of Mammalian MAPK Signaling in Regulation of Cytokine mRNA Stability and Translation. J. Interferon Cytokine Res. *34*, 220–232.

Tiedje, C., Diaz-Muñoz, M.D., Trulley, P., Ahlfors, H., Laaß, K., Blackshear,

P.J., Turner, M., and Gaestel, M. (2016). The RNA-binding protein TTP is a global post-transcriptional regulator of feedback control in inflammation. Nucleic Acids Res. *44*, 7418–7440.

Ullah, M.O., Sweet, M.J., Mansell, A., Kellie, S., and Kobe, B. (2016). TRIF-dependent TLR signaling, its functions in host defense and inflammation, and its potential as a therapeutic target. J. Leukoc. Biol. *100*, 27–45.

Underhill, D.M. (2007). Collaboration between the innate immune receptors dectin-1, TLRs, and Nods. Immunol. Rev. *219*, 75–87.

Underhill, D.M., Rossnagle, E., Lowell, C.A., and Simmons, R.M. (2005). Dectin-1 activates Syk tyrosine kinase in a dynamic subset of macrophages for reactive oxygen production. Blood *106*, 2543–2550.

Ventura, S., Cano, F., Kannan, Y., Breyer, F., Pattison, M.J., Wilson, M.S., and Ley, S.C. (2018). A20-binding inhibitor of NF-κB (ABIN) 2 negatively regulates allergic airway inflammation. J. Exp. Med. *215*, 2737–2747.

Verstak, B., Stack, J., Ve, T., Mangan, M., Hjerrild, K., Jeon, J., Stahl, R., Latz, E., Gay, N., Kobe, B., et al. (2014). The TLR signaling adaptor TRAM interacts with TRAF6 to mediate activation of the inflammatory response by TLR4. J. Leukoc. Biol. *96*, 427–436.

Wang, C., Deng, L., Hong, M., Akkaraju, G.R., Inoue, J., and Chen, Z.J. (2001). TAK1 is a ubiquitin-dependent kinase of MKK and IKK. Nature *412*, 346–351.

Wang, X.S., Diener, K., Manthey, C.L., Wang, S., Rosenzweig, B., Bray, J., Delaney, J., Cole, C.N., Chan-Hui, P.-Y., Mantlo, N., et al. (1997). Molecular Cloning and Characterization of a Novel p38 Mitogen-activated Protein Kinase. J. Biol. Chem. *272*, 23668–23674.

Waterfield, M.R., Zhang, M., Norman, L.P., and Sun, S.-C. (2003). NF-κB1/p105 Regulates Lipopolysaccharide-Stimulated MAP Kinase Signaling by Governing the Stability and Function of the Tpl2 Kinase. Mol. Cell *11*, 685–694.

Wellbrock, C., Karasarides, M., and Marais, R. (2004). The RAF proteins take centre stage. Nat. Rev. Mol. Cell Biol. *5*, 875–885.

Wilson, J.E., Pestova, T.V., Hellen, C.U.T., and Sarnow, P. (2000). Initiation of Protein Synthesis from the A Site of the Ribosome. Cell *102*, 511–520.

Wu, J., Green, N., Hotchandani, R., Hu, Y., Condon, J., Huang, A., Kaila, N., Li, H.-Q., Guler, S., Li, W., et al. (2009). Selective inhibitors of tumor progression loci-2 (Tpl2) kinase with potent inhibition of TNF-α production in human whole blood. Bioorg. Med. Chem. Lett. *19*, 3485–

3488.

Xiao, Y., Jin, J., Chang, M., Nakaya, M., Hu, H., Zou, Q., Zhou, X., Brittain, G.C., Cheng, X., and Sun, S.-C. (2014). TPL2 mediates autoimmune inflammation through activation of the TAK1 axis of IL-17 signaling. J. Exp. Med. *211*, 1689–1702.

Xu, D., Matsumoto, M.L., McKenzie, B.S., and Zarrin, A.A. (2018). TPL2 kinase action and control of inflammation. Pharmacol. Res. *129*, 188–193.

Yamamoto, M., Sato, S., Hemmi, H., Hoshino, K., Kaisho, T., Sanjo, H., Takeuchi, O., Sugiyama, M., Okabe, M., Takeda, K., et al. (2003). Role of Adaptor TRIF in the MyD88-Independent Toll-Like Receptor Signaling Pathway. Science *301*, 640–643.

Yamaoka, S., Courtois, G., Bessia, C., Whiteside, S.T., Weil, R., Agou, F., Kirk, H.E., Kay, R.J., and Israël, A. (1998). Complementation Cloning of NEMO, a Component of the IκB Kinase Complex Essential for NF-κB Activation. Cell *93*, 1231–1240.

Zandi, E., Rothwarf, D.M., Delhase, M., Hayakawa, M., and Karin, M. (1997). The IκB Kinase Complex (IKK) Contains Two Kinase Subunits, IKKα and IKKβ, Necessary for IκB Phosphorylation and NF-κB Activation. Cell *91*, 243–252.

Zhang, J., Clark, K., Lawrence, T., Peggie, M.W., and Cohen, P. (2014). An unexpected twist to the activation of IKKβ: TAK1 primes IKKβ for activation by autophosphorylation. Biochem. J. *461*, 531–537.

Zhang W, W.Z. (2017). Rbowtie2: An R Wrapper for Bowtie2 and AdapterRemoval. R package version 1.0.2.

Zur, R., Garcia-Ibanez, L., Nunez-Buiza, A., Aparicio, N., Liappas, G., Escós, A., Risco, A., Page, A., Saiz-Ladera, C., Alsina-Beauchamp, D., et al. (2015). Combined deletion of p38γ and p38δ reduces skin inflammation and protects from carcinogenesis. Oncotarget *6*, 12920–12935.